

Aus dem Bereich Biologie, der Medizinischen Fakultät der Universität des Saarlandes,  
Homburg/Saar und dem  
Institut für Immunologie/Centre de Recherche Public de la Santé, Luxemburg

Genetische und phänotypische Charakterisierung  
verschiedener Masern Viren und ihre  
Interaktion mit der unspezifischen Immunabwehr

*Genetic and phenotypic characterization of different measles  
virus strains and their interaction with the  
innate immune response*

## **DISSERTATION**

**zur Erlangung des Grades eines Doktors der Naturwissenschaften**

der Medizinischen Fakultät  
der UNIVERSITÄT DES SAARLANDES

2010

vorgelegt von

**Julia Kessler**

geb. am: 29. Mai. 1981, in Saarburg

---

## Table of contents

---

<b>Zusammenfassung</b> .....	1
<b>Abstract</b> .....	4
<b>Chapter I: General Introduction</b>	
1. The measles virus.....	8
1.1. History and Classification.....	8
1.2. Morphology.....	9
1.3. Cellular receptors.....	12
1.4. Virus Replication.....	14
2. Molecular Epidemiology.....	16
2.1. Usefulness of Molecular Epidemiology.....	16
2.2. Measles genotyping and surveillance.....	17
3. Measles disease and host defense.....	20
3.1. Clinical features and complications.....	20
3.2. Immune response against measles virus infection.....	23
4. Measles eradication strategies.....	24
4.1. Measles vaccines.....	24
4.2. Eradication efforts.....	27
4.3. Measles today.....	29
5. Objectives of this study.....	30

---

**Chapter II: Materials and Methods****Materials**

1.	Cells and Viruses .....	33
1.1.	Cells.....	33
1.2.	Viruses.....	34
2.	Patients sera for cytokine analysis.....	35
3.	Clinical specimens for virus characterization .....	37
4.	Chemicals, Buffers and Solutions .....	41
4.1.	Chemicals .....	41
4.2.	Buffers and Solutions.....	42
5.	Commercial kits .....	42
6.	2D-DIGE Material .....	43
7.	2D-DIGE Buffers and Solutions .....	44
8.	Enzymes .....	45
9.	Primers .....	46
10.	Bioinformatics .....	47
11.	Additional programs.....	47
12.	Instruments.....	48

**Methods**

13.	Cell cultures .....	49
13.1.	Cell lines .....	49

---

13.2.	Freezing and thawing cells .....	50
13.3.	Mycoplasma test.....	51
14.	Virus cultures .....	52
14.1.	MV isolation and virus propagation.....	52
14.2.	Virus titration (TCID <sub>50</sub> determination).....	53
14.3.	Virus Concentration (Amicon® Ultra filtration).....	53
15.	Enzyme-Linked-Immuno-Sorbent-Assay (ELISA).....	54
16.	Cytometric bead array (CBA).....	55
17.	RNA extraction.....	57
17.1.	QIAamp® Viral RNA Mini kit .....	57
17.2.	MagMAX™-96 AI/ND Viral RNA Isolation kit .....	57
17.3.	RNeasy® Protect Mini kit.....	58
18.	Reverse Transcription.....	59
19.	Polymerase Chain Reaction (PCR) .....	60
19.1.	MV genotyping PCR .....	61
19.2.	MV TaqMan® PCR .....	62
20.	Agarose gel electrophoresis .....	63
21.	Sanger sequencing .....	63
22.	Phylogenetic analysis .....	66
23.	2D-DIGE Proteomics .....	67

**Chapter III: Results and Discussion****Part I: Genetic and Phenotypic characterisation of various MV strains**

1.	Results.....	74
1.1.	MV wt strains are highly variable in their sensitivity to IFN-alpha .....	74
1.2.	No sequence motif in the P/C/V-locus can be associated with the sensitivity to IFN-alpha.....	75
1.3.	MV wt strains are low IFN-beta inducers unless they express diRNA	76
1.4.	MV wt strains induce significantly lower levels of cytokines than clade A strains, provided they are negative for diRNA .....	79
1.5.	DiRNA induce TNF-alpha expression during early MV infection in Vero cells.....	80
1.6.	Multiple passaging induces diRNA in MV culture.....	81
1.7.	Clinical samples do not contain diRNA .....	85
2.	Discussion .....	85

**Part II: Proteome profiling of Measles virus-host interaction in human lung cells comparing wild type and attenuated strains**

1.	Results.....	90
1.1.	Experimental design .....	90
1.2.	2D DIGE analysis .....	91
1.3.	Comparison of MV strains.....	103
2.	Discussion .....	106

**Part III: MV induced cytokine response in humans**

1.	Results.....	110
2.	Discussion .....	113

**Part IV: Investigation of MV outbreaks**

1.	Results.....	117
1.1.	Genotype D6: Germany.....	117
1.2.	Genotype D6: Belarus.....	118
1.3.	Genotype D6: Russia.....	124
1.4.	Genotype B2: Democratic Republic of Congo.....	125
2.	Discussion.....	130

<b>References.....</b>	<b>138</b>
------------------------	------------

**Anexes**

1.	Conference Participations.....	151
2.	Publications.....	153

<b>Acknowledgements.....</b>	<b>154</b>
------------------------------	------------

---

## Index of Figures

---

Figure 1: Schematic diagram of the measles virus particle correlated with the genetic map .....	10
Figure 2: Structure of human MV receptors.....	13
Figure 3: MV replication cycle.....	14
Figure 4: Typical cytopathic effect of syncytia formation associated with MV replication in Vero/hSLAM cells. ....	16
Figure 5: Geographical distribution of MV genotypes. ....	20
Figure 6: Basic pathogenesis of MV infection. ....	22
Figure 7: MV vaccines. ....	26
Figure 8: Overview about global annual reported measles cases and measles vaccine coverage during 1980 to 2008. ....	28
Figure 9: MV production in IFN-alpha treated or un-treated Vero/hSLAM cells. .	75
Figure 10: Effects of MV on host cells.....	78
Figure 11: Detection of RANTES, MCP-I, IL-8, L-6, TNF-alpha and IL-1 beta in MV infected A549/hSLAM cells.....	80
Figure 12: mRNA expression level of TNF-alpha in MV infected Vero/hSLAM cells.....	81
Figure 13: MV genome nt positions 15670 to 15795 of MV strains used in this study. ....	84
Figure 14: Representative 2D gel maps of MV infected A549/hSLAM cells 12h and 32h p.i. and corresponding Venn diagrams. ....	92
Figure 15: Cytokine induction of IL-5, IL-6, IL-8 and IL-10 in sera of patients infected with either MV genotype C2 or B3.....	112
Figure 16: Cytokine induction of IL-6 and IL-8 stratified according to onset of rash.....	113

---

Figure 17: Phylogenetic tree of D6a strains from Russia and D6b strains from Germany and Belarus displaying MV-NP HVR genes. ....	119
Figure 18: Phylogenetic tree of D6a strains from Russia and D6b strains from Germany and Belarus displaying MV-P/H-pseudo-genes.....	121
Figure 19: Phylogenetic tree of D6a strains from Russia and D6b strains from Germany and Belarus displaying MV-P genes. ....	122
Figure 20: Phylogenetic tree of D6a strains from Russia and D6b strains from Germany and Belarus displaying MV-H genes. ....	123
Figure 21: Phylogenetic trees showing MV-NP HVR and MV-P/H-pseudo-genes of B2 strains collected in the DR-Congo. ....	128
Figure 22: Phylogenetic trees showing MV-P and H genes of B2 strains collected in the DR-Congo. ....	129

---

## Index of Tables

---

Table 1: WHO reference strains for measles genotyping 2010.....	19
Table 2: Cell lines used in part I of the Result Section.....	33
Table 3: MV strains used in part I of the Result Section .....	34
Table 4: Patient sera used in part III of the Result Section .....	36
Table 5: Controle sera used in part III of the Result Section.....	37
Table 6: List of clinical specimens analysed in part IV of the Result Section .....	38
Table 7: DiRNA production in MV strains passaged on Vero, Vero/hSLAM and A549/hSLAM cells .....	82
Table 8: Characteristics of MV 5`copy-back diRNAs .....	83
Table 9: Characterization of MV strains used in this study .....	91
Table 10: Differentially expressed protein spots in A549/hSLAM cells 12 h p.i....	94
Table 11: Differentially expressed protein spots in A549/hSLAM cells 32 h p.i....	97
Table 12: Molecular and cellular functions of differentially expressed proteins in A549/hSLAM cell 12 h and 32 h p.i.....	102
Table 13: Unique proteins affected by MV strains and IFNB .....	105

---

## List of Abbreviations

---

aa	amino acid
2-5AS	2-5 oligoadenylate synthetase
BSL	bio safety level
Ca	calcium
cm	centimeter
CPE	cytopathic effect
2D-DIGE	Two-dimensional Difference Gel Electrophoresis
DMEM	Dulbecco's modified Eagle's medium
DMSO	dimethyl sulfoxide
DNA	deoxyribonucleic acid
DR-Congo	Democratic-Republic of Congo
DTT	dithiothreitol
EDTA	ethylenediaminetetraacetic acid
ELISA	enzyme-linked immunosorbent assay
F	fusion protein
FACS	fluorescence-activated cell sorter
FBS	fetal bovine serum
fw	forward
g	gram or gravity
HBV	Hepatitis B Virus
HIV	human immunodeficiency virus
H	haemagglutinin protein
h	hour
IFN	interferon
IgG	immunoglobulin G
IgM	immunoglobulin M
IL	interleukin
IU	international units
L	large protein
LNS	Laboratoire National de Santé
M	matrix protein
Mg	magnesium
MHC	major histocompatibility factor
min	minutes
ml	milli liter
mM	milli Mol
MMR	Measles Mumps Rubella vaccine
MOI	multiplicity of infection

---

MV	measles virus
N	nucleoprotein
NRW	North-Rhine-Westphalia
nt	nucleotide
OD	optical density
ORF	open reading frame
P	phospho protein
PBS	phosphate buffered saline
PCR	polymerase chain reaction
p.i.	post infection
rpm	rounds per minute
P/S	Penicillin/ Streptomycin mix
RANTES	regulated upon activation, normal T cell expressed and secreted
mRNA	messenger RNA
RNA	ribonucleic acid
RT	room temperature
rv	reverse
SLAM	signaling lymphocyte activation molecule
SSPE	subacute sclerosing panencephalitis
TCID <sub>50</sub>	50% tissue culture infective dose
TNF	tumor necrosis factor
TLR	toll like receptor
μl	micro liter
Ultra-Glu	Ultra-Glutamine
UV	ultraviolet
WHO	World Health Organization
w/o	with out
wt	wild type

---

## Index of Amino Acids

---

single letter code	amino acid name
A	Alanine
R	Arginine
N	Asparagine
D	Aspartic acid
C	Cysteine
E	Glutamic acid
Q	Glutamine
G	Glycine
H	Histidine
I	Isoleucine
L	Leucine
K	Lysine
M	Methionine
F	Phenylalanine
P	Proline
S	Serine
T	Threonine
W	Tryptophan
Y	Tyrosine
V	Valine

---

## Zusammenfassung

---

Die angeborene unspezifische Immunabwehr bildet eine erste Verteidigungslinie gegen viele Viren und Mikroorganismen. Cytokine, die nach der Erkennung von Pathogenen freigesetzt werden, spielen hierbei eine Schlüsselrolle. Eine unterschiedliche Beeinflussung der Cytokinsignalwege durch verschiedene Masernviren (MV) könnte die Virusausbreitung und den Schweregrad der Krankheit verändern.

In der vorliegenden Studie wurde der Phänotyp von 22 MV (14 Repräsentanten aus 19 derzeit zirkulierenden Genotypen), hinsichtlich ihres Einflusses auf die angeborene, unspezifische Immunabwehr charakterisiert. Die Virusreplikation verschiedener MV-Wildtypen (wt) in Zellkultur reduzierte sich durch die Zugabe des Cytokins Interferon-alpha (IFN-alpha) um das 2- bis 47-fache, wohingegen die Produktion der Impfviren lediglich um das 2- bis 3-fache abnahm. Zusätzlich wurde die Produktion verschiedener Cytokine und Effektormoleküle (IFN-beta, RANTES, Interleukin-5 (IL-5), IL-6, IL-8, IL-10, TNF-alpha, IL-1 beta, MxA and 2-5AS) als Reaktion auf die MV-Infektion verfolgt. Während die Großzahl der wt Stämme 71 bis 99% weniger IFN-beta als der „Schwarz“-Impfstamm induzierten, wurden bei drei wt Stämmen vergleichbare Konzentrationen nachgewiesen. In diesen drei wt Stämmen wurden sogenannte „defective interfering RNAs“ (diRNA) nachgewiesen. In klinischen Proben von Masernpatienten konnten wir diese diRNAs nicht nachweisen, jedoch nach mehreren Passagen der Viren in Zellkultur.

Andere Studien zeigten bereits, dass Proteine die vom MV-Phosphoprotein Gen (MV-P) codiert werden die Signalkaskaden von IFN-alpha/beta blockieren können. Sequenzanalysen dieser Gene ließen in unserer Studie allerdings keine

Mutationen erkennen, die mit den verschiedenen beobachteten Phänotypen der MV Stämme übereinstimmen.

Diese *in vitro* Studien zeigten, dass besonders wt MV-Stämme sich in Bezug auf ihre Sensitivität zu IFN-alpha und auf ihre Fähigkeit mit der unspezifischen Immunabwehr zu interagieren, stark unterscheiden. Des Weiteren zeigten unsere Proteomanalysen, dass wt Stämme unterschiedliche Effekte auf Proteine der Wirtszelle haben. Dies könnte Unterschiede in der Pathogenität der wt Stämme reflektieren.

Kürzlich wurde gezeigt, dass Makaken, die mit zwei verschiedenen wt Stämmen (zugehörig zu MV Genotyp C2 oder B3) infiziert wurden, deutliche Unterschiede in klinischen Parametern, Virusproduktion und Antikörperproduktion aufwiesen. In unserer *in vitro* Studie gehörte der verwendete Virus vom Genotyp C2 zu den hochsensitiven Stämmen, wohingegen der B3 Virus die geringste Sensitivität aller Stämme gegen IFN-alpha aufwies. Augenscheinlich korrelierten unsere *in vitro* Resultate mit den oben genannten *in vivo* Daten. Um nun die humane Immunantwort zu überprüfen, untersuchten wir die Cytokin-Level von IL-5, IL-6, IL-8 und IL-10 in Patientenseren, die während Ausbrüchen von Genotyp B3 in Nigeria und Spanien oder einem C2-Ausbruch in Luxemburg gesammelt wurden. Da in allen B3-Seren höhere Cytokinkonzentrationen gemessen wurden scheint die Immunantwort in B3-infizierten-Patienten erhöht zu sein. Zusätzlich fanden wir, dass in C2-infizierten-Patienten die Cytokinkonzentrationen während der ersten acht Tage nach Exanthembildung eine abnehmende Tendenz zeigten, während sie in B3-infizierten-Patienten eher anstiegen. Diese Ergebnisse könnten als Hinweis auf Unterschiede in der Pathogenität von verschiedenen MV wt Stämmen gedeutet werden.

Seit 1998 empfiehlt die Welt-Gesundheits-Organisation (WHO) zur Genotypisierung der MV die Sequenzierung der hypervariablen Region des MV-Nukleoprotein Gens (MV-NP HVR). Die Genotypisierung ermöglicht Übertragungswege und Ausbreitung, sowie Fortschritte in der MV-Ausrottung zu

verfolgen. Mit zunehmenden Impffortschritten nimmt jedoch die genetische Variabilität der zirkulierenden Viren ständig ab. Seit mehreren Jahren finden sich immer häufiger Viren mit identischen MV-NP HVR Sequenzen. Als Folge wird es zunehmend schwerer den Ursprung einzelner MV-Ausbrüche zu bestimmen.

Daher untersuchten wir zusätzlich die Variabilität der MV-P und H Gene. Anhand von vier verschiedener Masern-Ausbrüche in Europa und Afrika konnten wir zeigen, dass die zusätzliche Sequenzinformation des MV-P/H-Pseudo-Gens deutlich zur Verbesserung der Charakterisierung von MV und deren Verfolgung beiträgt und neue Verbreitungswege aufzeigt. So konnten wir z.B. zeigen, dass MV-Genotyp D6 Ausbrüche 2006 in Deutschland und Weißrussland, von verschiedenen Viren ausgelöst wurden, obwohl Viren beider Ausbrüche in ihrer MV-NP HVR identisch waren. Am Beispiel Russlands zeigten wir, dass auch hier mehrere MV Varianten während 2003-2007 co-zirkulierten. Im Speziellen fanden wir für Moskau, dass Ausbrüche nicht in direktem Zusammenhang standen, obwohl alle Viren in der MV-NP HVR identisch waren und bis dato eine direkte Verwandtschaft und anhaltende Zirkulation von MV in der Stadt vermutet wurde. Entsprechend zeigte die Untersuchung der MV-P/H-Pseudo-Gene von Proben aus der Demokratischen-Republik-Kongo, dass auch hier verschiedene MV Importe stattfanden.

Somit konnten wir zeigen, dass obwohl die genetische Variabilität der MV-P und H Gene geringer als die der MV-NP HVR ist, die zusätzliche Untersuchung dieser beiden Gene die Sensitivität der genetischen Analyse deutlich erhöht und Zusammenhänge zwischen Masern-Ausbrüchen, Virusverbreitung, Importe und Zirkulation besser nachvollziehen lässt.

## Abstract

---

The innate immunity is critical to control viral infections during the development of the adaptive immune response. Cytokines are key players in the early immune response to viral infections. Therefore phenotypic differences between measles virus (MV) strains, relating to cytokine induction, may influence virus spread and severity of disease.

We investigated how 22 different MV strains of 14 circulating genotypes interfere with the early immune response. Virus proliferation of vaccine and wild-type (wt) strains was compared, after IFN-alpha treatment. Wt production was 2 to 47-fold lower in IFN-treated cells, whereas vaccine production was reduced only 2 to 3-fold. Furthermore, we compared the cytokine induction of IFN-beta, RANTES, interleukin 5 (IL-5), IL-6, IL-8, IL-10, TNF-alpha and IL-1 beta and mRNA quantification of IFN-alpha/beta response genes (MxA, 2-5AS). While most of the wt strains induced 71-99% less cytokines than the Schwarz vaccine strain, three wt strains induced similar levels of cytokines. These three wt strains were positive for defective interfering RNAs (diRNA). DiRNA emerged only in virus cultures during multiple passaging and was not detectable in clinical samples of measles patients.

Previous studies showed that proteins encoded by the MV-P gene inhibit IFN-alpha/beta signaling. However, sequence analysis of those gene of all used strains, did not display specific amino acid mutations that correlated with the different phenotypes.

The present data show that MV wt strains differ in their sensitivity and their ability to temper with the innate immune response. In addition our proteomic analyses highlight variations in the cellular response induced by different wt strains. These phenotypic characteristics may result in differences in virulence.

Recently it was shown that macaques infected with two different wt strains (genotype C2 or B3) display variations in clinical parameters, MV replication and antibody responses. In our *in vitro* study the used C2 strain was one of the most sensitive wt strains, whereas the B3 strain was the least sensitive one to IFN- $\alpha$  treatment. Since our *in vitro* findings correlated with the latter *in vivo* data we compared also the immune response in humans. Thus, we investigated the cytokine levels of IL-5, IL-6, IL-8 and IL-10 in sera collected from patients during MV outbreaks of genotype B3 in Nigeria and Spain and from a C2 outbreak in Luxembourg. In great contrast to B3 infected patients the cytokine response in C2 infected patients seems to be alleviated. Additionally during eight days after onset of rash cytokine levels decreased in C2 patients, whereas they elevated in B3 infected patients. Thus, our findings also force the hypothesis of differences in pathogenicity among various wt strains.

Since 1998 the WHO recommends sequencing the hypervariable region of the MV nucleoprotein (MV-NP HVR) for MV genotyping. Genotyping is an important tool of measles surveillance to document chains of transmission, discriminate between imported or indigenous viruses and monitor elimination programs. However, with the enhanced vaccination control the genetic variability of circulating strains continues to decrease and identical MV-NP HVR sequences have been found for several years.

Analyzing the variability of the MV-P and H genes, we showed for four different outbreaks in Europe and Africa that phylogenetic analysis of the MV-P/H-pseudo-gene sequences provides a more refined picture of MV circulation. Identical MV-NP HVR sequences found in Belarus and Germany in 2006, may have suggested that strains belong to the same outbreak. However, the MV-P/H pseudo-gene sequences clearly identified both cases as part of two distinct outbreaks. For strains collected throughout Russia 2003 to 2007 the MV-P/H pseudo-gene provides more insights into the time course of strains, indicating rather the circulation and importation of independent variants, than a single major outbreak lasting for several years, like suggested by identical MV-NP HVR

sequences. Also in the DR-Congo our findings suggested an independent evolution of variants and multiple independent importations into the country. By extending the sequencing window recommended by the WHO for molecular epidemiology of MV, links between outbreaks and transmission chains became more clearly defined.

## **Chapter I**

---

### **General Introduction**

---

## 1. The measles virus

### 1.1. History and Classification

Despite enhanced vaccination efforts, the measles virus (MV) remains one of the most important causes of childhood mortality and morbidity worldwide with around 165,000 deaths and 20 millions infected annually particularly in the developing countries (WHO, 2008). MV is a member of the *Morbillivirus* genus of the family of *Paramyxoviridae* and phylogenetically most closely related to the Rinderpest virus, a pathogen of cattle. This close phylogenetic relation suggests that MV is an ancestral virus that has evolved during the early stages of civilization with close proximity of humans and cattle approximately 5,000 years ago (Moss & Griffin, 2006, Norrby et al., 1992).

The name “measles” descends from the Latin word “misellus” meaning miserable. Alternatively, “rubeola or morbilli” are also found as names for the disease, traced back to the Latin words “rubeolus” for reddish and “morbus” for disease. Abu Becr (also known as Rhazes of Baghdad), an Arab physician, is generally cited as first precise descriptor of measles in the 9<sup>th</sup> century (Griffin, 2007, Rhazes, 1748). As a childhood disease measles was first mentioned in 1224 (McNeill, 1976). As a consequence of the conquest of the Americas, measles appeared in parts of the Caribbean and Central America in the early 16<sup>th</sup> century, decimating the Native American population and facilitating the colonization (McNeill, 1976). Humans are the only natural reservoir of MV (Griffin, 2007). The basic principles of measles epidemiology and infection, like the high contagion rate, the 14-days incubation period, the life-long immunity and the respiratory route of transmission, were first elucidated by the Danish physician Peter Panum, who investigated a large measles outbreak on the Faroe Islands in 1846 (Panum, 1938). The first attempts with vaccination against measles were based on the principle of variolation done by Dr. Home 1749 in Edinburgh, Scotland. In 1954, MV was finally isolated successfully in tissue

culture, using the blood of an infected child (David Edmonston) by Enders and Peebles (Enders & Peebles, 1954). The development of vaccines against measles soon followed (details about vaccines, please see section 4.1).

## 1.2. Morphology

MV is a pleomorphic virus ranging in diameter from 100 to 200 nm. The lipid bilayer envelope is derived from the plasma membrane of the host cell and carries surface projections (length: 9 to 15 nm), composed of the two viral transmembrane glycoproteins: haemagglutinin (H) and fusion (F) (Griffin, 2007) (Figure 1). The matrix (M) protein lines the inner surface of the virion. The ribonucleoprotein (RNP) complex, packed within the envelope, has a coiled helical structure with a total length of 1.2  $\mu\text{m}$  and a diameter of 21 nm (Lund et al., 1984). It consists of the nucleoprotein (NP), which surrounds the monopartite, single-stranded, negative sense RNA genome, to which the phospho (P) and large (L) proteins are attached. The RNP contains 2,649 NP and approximately 300 P and 50 L proteins (Plumet et al., 2005). The entire measles genome consists of 15,894 nucleotides (nts) and contains six genes, encoding nine proteins: NP, P, M, F, H and L (Figure 1). Each transcription unit is flanked by a short leader and trailer sequence, containing the genomic (minus strand) and antigenomic (plus strand) promoters. In addition to the P protein, the P gene encodes three accessory proteins C, V and R, generated by alternative initiation of protein translation, mRNA editing and protein truncation, respectively (Bellini et al., 1985, Cattaneo et al., 1989, Liston & Briedis, 1995) .

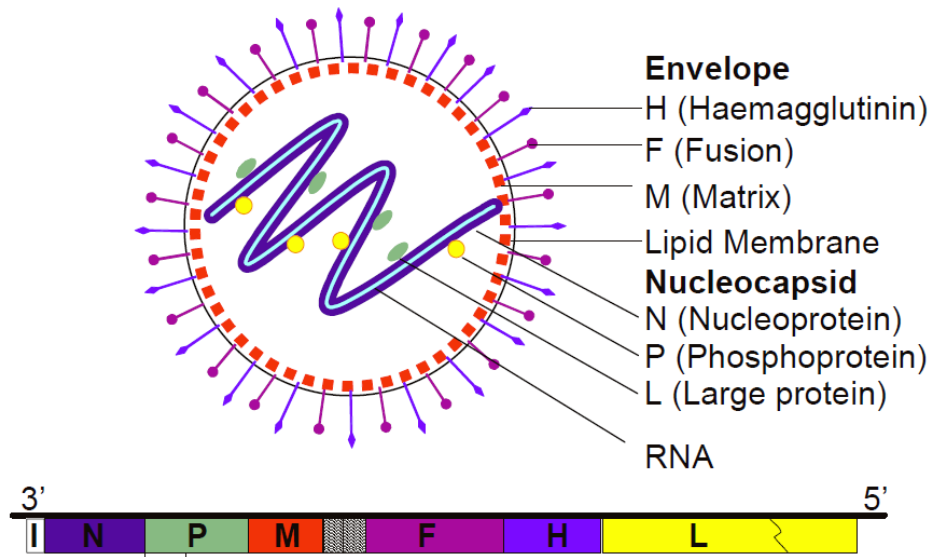


**Figure 1: Schematic diagram of the measles virus particle correlated with the genetic map (WHO, 2007).**

The NP mRNA is the first transcribed from the genome and the NP protein (525 aa) is the most abundant protein both in the virion and in the infected cell. Every NP protein binds to six nts, so the NP polymer entirely covers the complete MV genome and makes it resistant to nucleases. Thus the NP protein encapsidates the genomic RNA, associates with the P/L polymerase complex, so it is required for transcription and replication and most likely interacts with the M protein during virus assembly (Longhi, 2009). The highly conserved amino-terminal part ( $N_{CORE}$ , aa 1 to 400) is required for self-assembly, RNA binding and P protein binding, whereas the extremely variable carboxyl-terminal domain ( $N_{TAIL}$ , aa 401 to 525) can interact with several host proteins and also the P protein (Bankamp et al., 1996, Bourhis et al., 2005). The NP protein is a ubiquitous antigen in infected cells and is the first target of the immune response, though antibodies are not neutralising due to its unavailability at the virus surface (Graves et al., 1984).

The P protein (507 aa) is a highly phosphorylated, modular protein, which links L to NP to form the replicas complex (Curran et al., 1995). The amino-terminus (PNT) is poorly conserved, binds to  $N_{CORE}$  and is required for replication. In contrast, the carboxyl-terminus (PCT) is well conserved, binds to  $N_{TAIL}$  and

contains all domains required for transcription. Beside the P protein the P gene also encodes non-structural virulence factors in particular the C (186 aa) and V (299 aa) proteins (Bellini et al., 1985). The V protein shares the first amino-terminal 231 aa with the P protein, but its 68 carboxyl-terminal aa are translated from a different open reading frame (ORF), accessed by RNA editing of a non-encoded guanosine residue. The C protein is translated using the second ORF of the P gene, 19 nts downstream of the P/V start codon (Devaux & Cattaneo, 2004). Both V and C proteins interact with cellular proteins, play a role in the regulation of transcription and translation and contribute to immune evasion (Palosaari et al., 2003, Reutter et al., 2001, Shaffer et al., 2003, Takeuchi et al., 2003a). A third accessory protein encoded by the P gene is the so called R protein (299 aa). The first 294 aa of the amino-terminus are in common with the P protein, fused to a 5 aa carboxy-terminus derived from the V ORF, created by ribosomal frame-shifting (Liston & Briedis, 1995).

The M protein (335 aa) is a basic protein with several hydrophobic domains and links the RNP complex with H and F proteins during assembly. Thus it plays a key role in the maturation, stabilisation and budding of the virion (Hirano et al., 1993).

The F protein (550 aa) is a type I trans-membrane glycoprotein synthesized as an inactive precursor  $F_0$  and cleaved enzymatically by furin in the trans-golgi network to yield the functional, disulphide linked  $F_1$  and  $F_2$  subunits (Wild & Buckland, 1997). This protein, associated with the H protein, mediates membrane fusion and virus entry.

The H protein (617 aa) is a type II trans-membrane protein expressed as disulfide-linked homodimer on the surface of the virion and infected cells (Hu et al., 1994). Its amino-terminus acts as a membrane anchor and is essential for transport to the cell membrane, whereas the carboxyl-terminus has key function in receptor binding. The binding sites on the H protein for these receptors overlap

and MV strains differ in their efficiency to use a receptor (details about MV receptors, please see section 1.3). The H protein is closely associated with the F protein, allowing viral entry into the cell by attaching and fusing the viral envelope to the host cell membrane (Griffin, 2007, Moss & Griffin, 2006).

The L protein (2,183 aa) is a multi-domain protein, represented only in small quantities (< 50 copies) inside the virion. The amino-terminus contains domains important for binding the L to the P protein, in order to form the polymerase complex (Horikami et al., 1994). Both proteins together are important for transcription and replication.

### **1.3. Cellular receptors**

Until now two main receptors are identified for MV: signalling lymphocyte activation molecule (SLAM/CD150) and the complement regulatory molecule CD46 (Naniche et al., 1993, Tatsuo et al., 2000).

CD46, the receptor for vaccine and laboratory adapted MV strains, is expressed on all nucleated cells. It normally protects cells from autologous complement, being a cofactor for the serine protease factor I to inactivate C3b and C4b (Riley-Vargas et al., 2004). Four different isoforms, derived from alternative splicing of a single gene, are common on human cells and all serve as receptors for MV (Gerlier et al., 1994). CD46 is a type I membrane glycoprotein and the amino-terminus of each isoform consists of four tandem complement control protein repeats (CCPs), followed by one or two serine/threonine/proline-rich domains (STP) that are heavily O-glycosylated (Figure 2a). The STP region is followed by a trans-membrane domain and two alternative cytoplasmic tails. The MV-H protein binds to the two external CCP modules (CCP1/2), whereas CCP2/3/4 are essential for complement inactivation. Both cytoplasmic tails comprise signaling motifs and are associated with adaptor proteins or intracellular kinases and cross-linking of CD46 leads to cell activation events (Riley-Vargas et al., 2004).

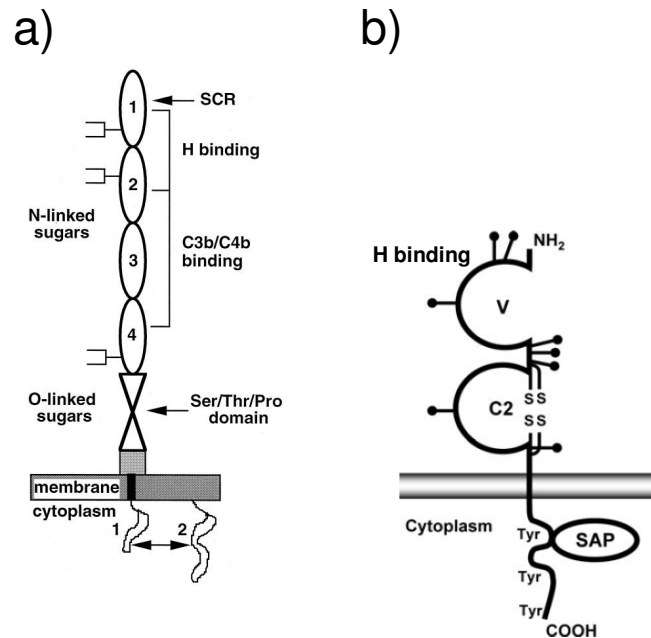


**Figure 2: Structure of human MV receptors.**

a) membrane cofactor protein/CD46 (Griffin, 2007) and b) signaling lymphocyte activation molecule/SLAM (Yanagi et al., 2002). On the CD46 receptor MV-H binds to complement control protein/CCP1 and CCP2. On the SLAM receptor MV-H binds to immunoglobulin like domain V.

SLAM/CD150, the MV wild-type (wt) receptor, is expressed on activated lymphocytes, mature dendritic cells, macrophages, thymocytes as well as on human and mice platelets (Griffin, 2007). It is a membrane glycoprotein with two highly glycosylated extracellular immunoglobulin like domains (V and C2) (Figure 2b). The cytoplasmic tail with three tyrosine-based motifs is surrounded by SH2 domain-binding sequences. It has the ability to bind tyrosines and SH2 domain-containing adaptor proteins like SLAM-associated protein (SAP), protein tyrosine phosphatase SHP-2 and inositolphosphatase SHIP, all important for cell signaling (Sayos et al., 1998, Shlapatska et al., 2001, Yanagi et al., 2002). Wang et al. (Wang et al., 2004) showed that SLAM also plays a role in activation of lipopolysaccharide induced production of interleukin 12 (IL-12), tumor necrosis factor (TNF-alpha) and nitric oxide by macrophages in mice. The amino-terminal V domain is necessary and sufficient to interact with the MV-H protein and allows MV entry (Ono et al., 2001).

Beside CD46 and SLAM, other receptors like a putative receptor on epithelial cells, dendritic cell specific intercellular adhesion molecule-3-grabbing non-integrin (DC-SIGN) and neurokinin-1 are discussed (de Witte et al., 2006, Makhortova et al., 2007, Takeuchi et al., 2003b).

## 1.4. Virus Replication

Aerosols and respiratory secretions from measles infected persons function as vehicles of transmission by delivering infectious virus to epithelial cells of the upper respiratory tract of susceptible hosts. The identification of SLAM as the MV wt receptor supports a new model of MV dissemination, postulating a primary infection of SLAM-expressing lymphatic cells in the tonsils, following a rapid spreading to all lymphatic organs (Navaratnarajah et al., 2009).

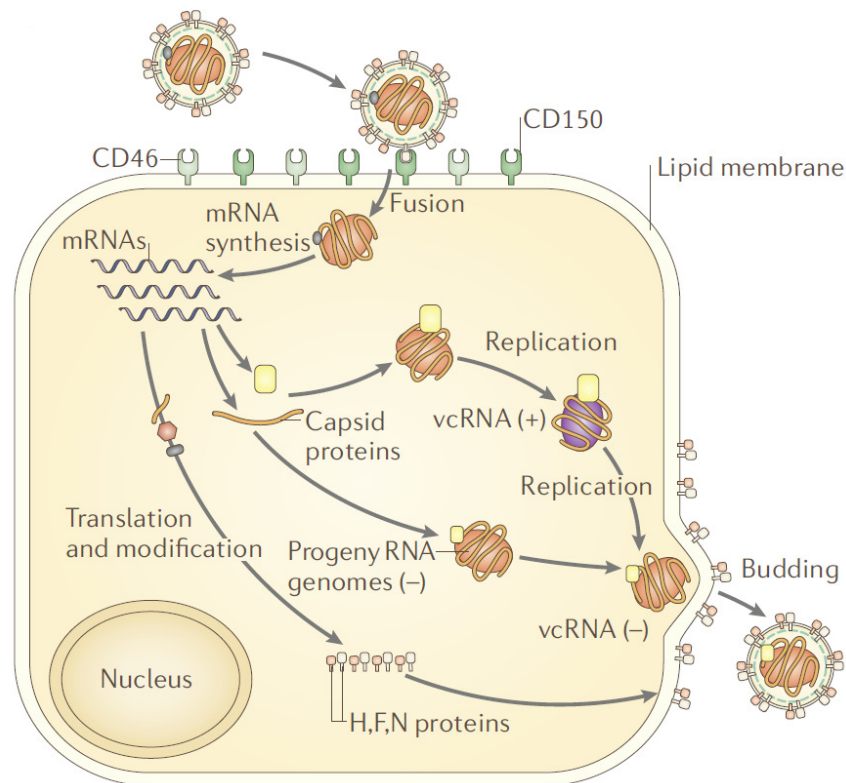


**Figure 3: MV replication cycle.**

(Moss & Griffin, 2006).

Attachment of the H protein to the receptor (CD46 or SLAM) on the surface of the host cell triggers a conformational change within the F protein and leads to the fusion of the viral membrane with the cellular plasma membrane (Figure 3). Next the RNP complex is released into the cytoplasm of the cell and serves as a template for both primary transcription from and replication of the genomic RNA. The main location of the large viral factories is perinuclear, especially in the early stage of the infection (Wileman, 2007). The RNA-dependent RNA polymerase, made of L and P proteins, initiates the transcription from a single promoter at the 3'-end of the genome. Reaching an intergenic junction the polymerase recognizes the gene end and terminates the synthesis. Following, either the gene start of the downstream gene is recognized and the transcription started again or the polymerase fails and detaches from the template, explaining the attenuated viral transcription gradient (Cattaneo et al., 1987). Except for the glycoproteins H and F that are translated at the endoplasmatic reticulum, all other proteins are synthesized from free ribosomes in the cytosol.

During transcription the polymerase sometimes ignores all polyadenylation/termination signals to form a full-length antigenome nucleocapsid. Following generation of this bicistronic mRNAs, the polymerase switches to the replication mode and synthesizes a full-length positive-sense RNA genome utilising the upstream replication genomic promoter (Plumet et al., 2005). During this replication process the genome is simultaneously encapsidated by the N protein. Together with the L and P proteins, the RNA-N protein complex is assembled into the RNP complex. As last step after the assembly the RNP complex is enwrapped into the envelope. The M protein seems to have a key role in this, concentrating F and H proteins as well as the RNP at the site of virus assembly (Vincent et al., 2000).

In cell culture monolayers as well as in infected tissues *in vivo*, MV replication leads to the cytopathic effects (CPE) of syncytia-formation (Figure 4), due to cell-cell fusion. This effect is facilitated by the interaction of surface expressed H and F proteins and actin-filament plasma membrane cross-linker moesin (Doi et al., 1998).



**Figure 4: Typical cytopathic effect of syncytia formation associated with MV replication in Vero/hSLAM cells.**

## **2. Molecular Epidemiology**

### **2.1. Usefulness of Molecular Epidemiology**

Since the introduction of measles vaccination, the global burden of measles disease has continuously decreased. Significant progress has been made during the last decade, with the elimination of measles from the Americas and a dramatic reduction in measles mortality worldwide (Rota et al., 2009). Although measles induced death were reduced during 2000 to 2008 from 733.000 to 164.000 cases (reduction of 78%), the disease still remains a serious public-health problem with more than 10 million cases annually (WHO, 2008). Measles

continues to be endemic in many developing countries and to certain extend also in industrialized countries (Papania & Orenstein, 2004).

Molecular epidemiology of MV has proven to be a very useful tool for monitoring the progress in measles control (Rota & Bellini, 2003). First in 1998, following the spring meeting of the World-Health-Organization (WHO), standardized analysis protocols for virus surveillance and a uniform nomenclature for MV strains were established, facilitating the comparison of data created in different laboratories. Based on the fact that the 450 nts encoding the carboxyl-terminal 150 aa of the N gene (MV-NP HVR) are the highest variable region of the MV genome (up to 12% sequence divergence among wt strains) the WHO recommends this as the minimal sequence data required for MV genotyping (Xu et al., 1998). Additionally, the complete H gene sequence (up to 6.1% sequence divergence among WHO reference strains) should be obtained, if a new genotype is suspected (Bankamp et al., 2008, Rota et al., 2009).

## **2.2. Measles genotyping and surveillance**

Although MV is serologically a monotypic virus, the genetic characterisation identified so far eight clades A-H, further sub-divided into 24 genotypes (A, B1-B3, C1 and C2, D1-D11, E, F, G1-G3, H1 and H2) (Table 1) (Rota et al., 2009, Zhang et al., 2010). Several of these genotypes B1, D1, E, F, G1 seem to be extinct or inactive, since they have not been detected during the last 15 years (Rota & Bellini, 2003). The combination of MV genotyping and standard case classification/ reporting are important tools of measles surveillance to document chains of transmission, discriminate between imported or indigenous viruses and monitor elimination programs. Laboratory-based surveillance, including the characterisation of wt strains, is performed throughout the world by the WHO Measles and Rubella Laboratory Network including 166 countries.

Based on the extensive measles surveillance, three different patterns of genotype distribution have been observed (Rota et al., 2009). In countries where

measles are still endemic, most cases are caused by relative few endemic genotypes. In these cases co-circulation of different variants is quite common. In countries that have eliminated measles, small outbreaks are caused by a number of different genotypes imported from other regions. The third pattern occurred in countries with very good measles control, but increasing numbers of susceptibles (perhaps due to “Vaccine fatigue”). This situation allows reintroduction of measles and leads to large outbreaks associated with a single genotype with nearly the same sequence. The geographic distribution of MV genotypes is shown in Figure 5.

**Table 1: WHO reference strains for measles genotyping 2010**

(Rota et al., 2009, Zhang et al., 2010).

Genotype	Status <sup>a</sup>	WHO Reference name <sup>b</sup>	MV-H gene accession <sup>c</sup>	MV-N gene accession <sup>c</sup>
A	Active	Edmonston-wt.USA/54	U03669	U01987
B1	Inactive	Yaounde.CAE/12.83 "Y-14"	AF079552	U01998
B2	Active	Libreville.GAB/84 "R-96"	AF079551	U01994
B3	Active	New York.USA/94	L46752	L46753
		Ibadan.NIE/97/1	AJ239133	AJ232203
C1	Active	Tokyo.JPN/84/K	AY047365	AY043459
C2	Active	Maryland.USA/77 "JM"	M81898	M89921
		Erlangen.DEU/90 "WTF"	Z80808	X84872
D1	Inactive	Bristol.UNK/74 (MVP)	Z80805	D01005
D2	Active	Johannesburg.SOA/88/1	AF085198	U64582
D3	Active	Illinois.USA/89/1 "Chicago-1"	M81895	U01977
D4	Active	Montreal.CAN/89	AF079554	U01976
D5	Active	Palau.BLA/93	L46757	L46758
		Bangkok.THA/93/1	AF009575	AF079555
D6	Active	New Jersey.USA/94/1	L46749	L46750
D7	Active	Victoria.AUS/16.85	AF247202	AF243450
		Illinois.USA/50.99	AY043461	AY037020
D8	Active	Manchester.UNK/30.94	U29285	AF280803
D9	Active	Victoria.AUS/12.99	AY127853	AF481485
D10	Active	Kampala.UGA/51.00/1	AY923213	AY923185
D11	Active	MVi/Menglian.Yunnan.CHN/47.09	GU440571	GU440576
E	Inactive	Goettingen.DEU/71 "Braxator"	Z80797	X84879
F	Inactive	MVs/Madrid.SPA/94 SSPE	Z80830	X84865
G1	Inactive	Berkeley.USA/83	AF079553	U01974
G2	Active	Amsterdam.NET/49.97	AF171231	AF171232
G3	Active	Gresik.INO/17.02	AY184218	AY184217
H1	Active	Hunan.CHN/93/7	AF045201	AF045212
H2	Active	Beijing.CHN/94/1	AF045203	AF045217

<sup>a</sup>Active genotypes that have been isolated within the past 15 years, <sup>b</sup>WHO name-quotation mark indicates other name that has been used in the literature, <sup>c</sup>NCBI accession number.

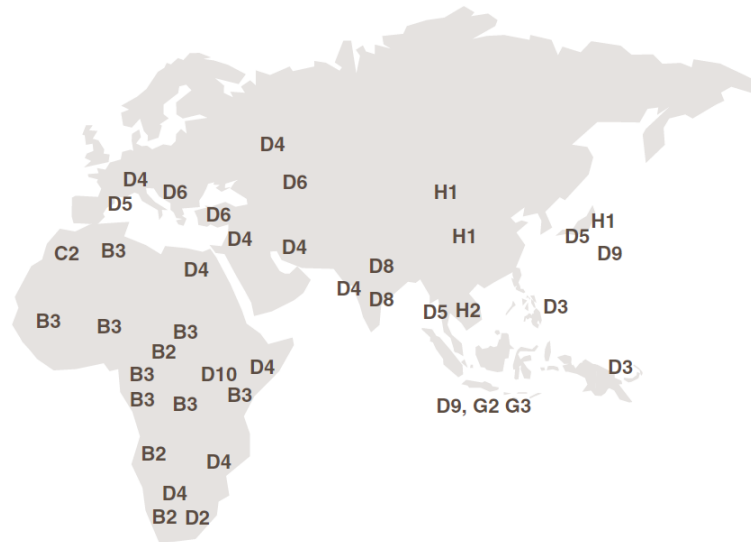


**Figure 5: Geographical distribution of MV genotypes.**

Based on surveillance data from 1995-2008. Americas and Australia are not shown since they have eliminated measles. In European Region only genotypes from major outbreaks 2005-2008 are shown (Rota et al., 2009).

### 3. Measles disease and host defense

#### 3.1. Clinical features and complications

The Measles virus is a highly contagious agent that spreads by the respiratory route and outbreaks can occur in populations in which less than 10% of individuals are susceptible (WHO, 2007). It is typically a childhood disease with an incubation period of 10 to 14 days. Upon contact, the virus replicates first in the upper respiratory tract and local lymph nodes leading to a primary viremia. Five to seven days after exposure, a second viremia occurs accompanied by characteristic lymphopenia and virus spread to multiple organs including lymph nodes, kidney, gastrointestinal tract, liver, skin and in monocytes, macrophages and lymphocytes (Moss & Griffin, 2006)(Figure 6).

First non specific symptoms of measles disease are fever, cough, coryza and conjunctivitis. First pathognomonic signs are the so called “Koplik`s spots”. This prodrome period of 2-3 days is followed by a characteristic maculopapular rash (3-5 days) that starts behind the ears and on the face and then spreads centrifugally to the trunk and extremities. The onset of rash indicates the activation of measles specific humoral and cellular immunity and initiation of virus clearance (Griffin, 2007). In uncomplicated cases an effective immune response leads to decreased symptoms and virus clearance 7-10 days after onset of rash. Recovery from natural measles infection is accompanied by a lifelong immunity (Black & Rosen, 1962, Graves et al., 1984, Panum, 1938).

However the long-lasting immunosuppression caused by measles can lead to sever complications including encephalitis, diarrhea and pneumonia. In rare cases (1 per 100.000) measles can also cause subacute sclerosing panencephalitis (SSPE), a fatal degenerative disease of the central nerve system (Griffin, 2007). Case-fatality rates in developing countries are ranging between 1-5% (Nandy et al., 2006) in contrast to <0.1% in many industrialized regions (WHO, 1999).

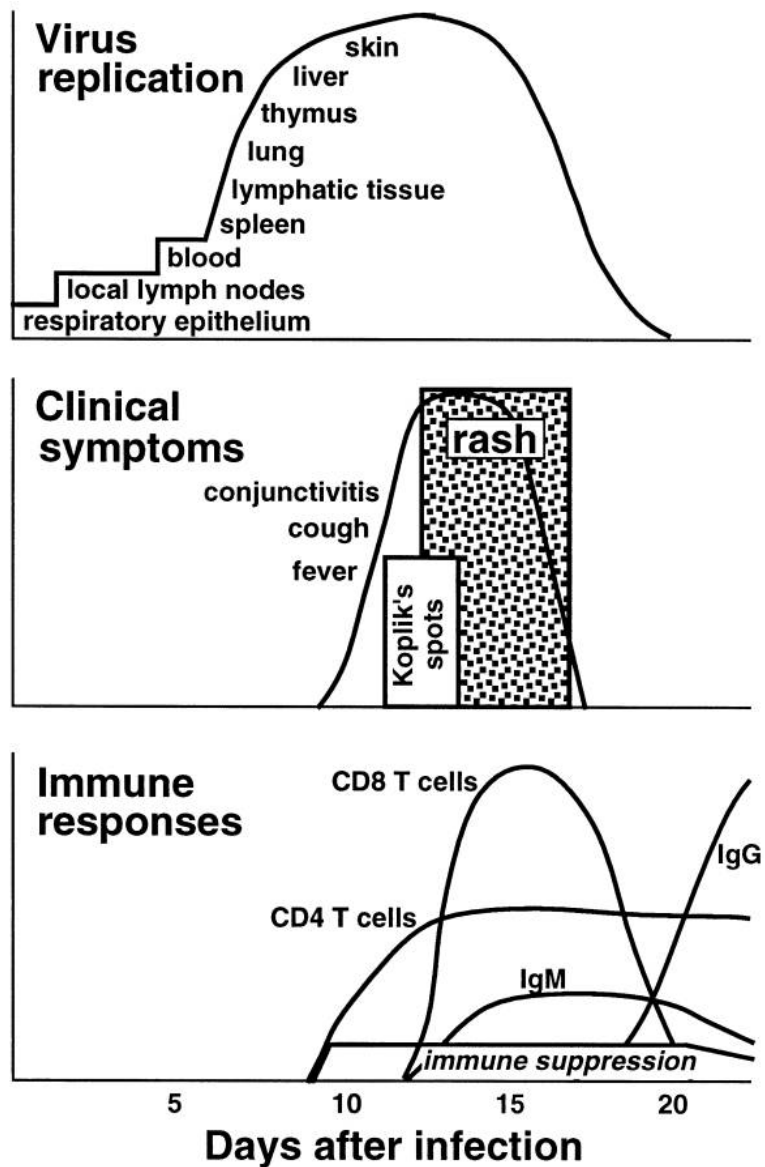


**Figure 6: Basic pathogenesis of MV infection.**

MV is spread from the respiratory epithelium to local lymph nodes and during second viremia virus spread to multiple organs including kidney, gastrointestinal tract, liver and skin. The rash appears simultaneously with the virus specific immune response and clearance of the virus is coincident with fading of the rash (Griffin, 2007).

### 3.2. Immune response against measles virus infection

The first immune response to be activated by viral infections is the innate immune response. Viral RNA sensing by different host cell receptors including Toll-like receptors (TLRs) TLR-3/7 and 9, cytoplasmic protein kinase R (PKR) or RNA-helicases like retinoic acid inducible gene I (RIG-I) and melanoma differentiation–associated gene-5 (MDA-5) leads to the activation of different transcription factors like interferon regulatory factor 3 (IRF-3) or NfκB, which mediate the expression of inflammatory cytokines and chemokines like IFN-alpha/beta, TNF-alpha, IL-1 beta, IL-5, IL-6, IL-8, IL-10, MCP-1 or RANTES (Ebihara et al., 2007, Indoh et al., 2007, Moriuchi et al., 1997, Ozato et al., 2007, Poeck et al., 2010, Shakhov et al., 1990, Wickremasinghe et al., 2004). IFN-alpha/beta binds to its common receptor on the cell surface, to activate the JAK/STAT signalling pathway. This ultimately leads to the expression of IFN-response genes including PKR, 2',5'-oligoadenylate synthetase (2-5AS) and myxovirus resistance A (MxA), most of which have antiviral activities (Haller et al., 2007, Haller et al., 2009, Sadler & Williams, 2008)

Both humoral and cellular immune responses are also involved in virus clearance. Anti-MV specific IgMs are the first detectable antibodies already 72h after onset of rash (Figure 6) and lasting for about 2 month (Naniche, 2009). IgA and IgG are detectable a few days after onset of rash (IgG peak 3-4 weeks later) and remain for life. The IgG antibodies are in majority targeting the most abundant N protein, but they are also directed against H, F and M proteins (Graves et al., 1984, Norrby et al., 1981, Stephenson & ter Meulen, 1979). Only Anti-H and Anti-F antibodies contribute to the neutralisation of the virus (de Swart et al., 2005) and the majority of neutralising antibodies are specific for the H protein (Black, 1989, Malvoisin & Wild, 1990). During acute phase of measles infection mostly IgG1 and IgG3 are predominant, whereas during the convalescent phase as well as long-term humoral memory IgG1 and IgG4 are dominant and IgG3 decreases.

Both CD4<sup>+</sup> and CD8<sup>+</sup> cells, specific for various measles proteins and specific epitopes, are activated during measles infection. T cells recognizing almost all MV proteins based on either MHC class I or class II presentation are described. CD8<sup>+</sup> cells are activated during the prodrome, eliminating infected cells via the MHC class I pathway. During the acute phase a CD4<sup>+</sup> Th1 response profile (including cytokines IFN-gamma and IL-2; activation of macrophages) is found, whereas in the convalescent phase a Th2 response profile (including cytokines IL-4, IL-5 and IL-10; B cell growth and differentiation, macrophage deactivation) is prevalent. The Th1 response is essential for virus clearance, while a Th2 response promotes the induction of protective MV-specific antibodies (Griffin, 1995).

However, *in vivo* as well as *in vitro* a long-lasting immune suppression has been described following measles disease. This measles induced immune suppression starts with the onset of clinical symptoms and persists over weeks (Hirsch et al., 1984, Marie et al., 2001, McChesney et al., 1989, Tamashiro et al., 1987). During this period patients are highly susceptible for secondary bacterial and viral infections causing diarrhoea, otitis media, bronchitis or pneumonia, explaining the high mortality rates especially in developing countries with poor health care systems. Pneumonia is the most common fatal complication and occurs in 56-86% of measles related death (Duke & Mgone, 2003).

## **4. Measles eradication strategies**

### **4.1. Measles vaccines**

Following the successful isolation of MV in cell culture in 1954 by Enders and Peebles (Enders & Peebles, 1954), intensive work was spent on this so called Edmonston isolate. Formalin- and Tween-ether inactivated vaccines as well as

live attenuated vaccines were produced. The inactivated vaccines provided only insufficient protection since antibody levels declined fast, recipients became again susceptible for measles and reinfection with wt virus induced a more severe disease called “atypical measles” (characterized by higher and more prolonged fever, unusual skin lesions and severe pneumonitis). These inactivated vaccines were soon replaced by the live attenuated vaccines that had been passaged intensively on various human and non-human cell lines (like successive passages on human kidney cells, human amnion cells, embryonated hens eggs and finally chicken embryo cells) (Katz, 2009). The first attenuated vaccine (Edmonston B) was licensed in 1963, but was associated with a high frequency of fever and rash in immunized children (Katz et al., 1960). This Edmonston B strain was further passaged on chicken embryo fibroblasts to generate a more attenuated vaccine (Schwarz vaccine) that was licensed in 1965. Schwarz and Edmonston-Zagreb vaccines are widely used throughout the world, whereas the Moraten strain is used primarily in the USA (Moss & Griffin, 2006). In the early 1960s different groups from Japan, USA and the Soviet Union worked simultaneously on the design of measles vaccines, so several attenuated vaccine strains were developed (Figure 7). Although these vaccine strains have a different passage history, they only show a maximal genetic divergence of 0.6% in their MV-NP HVR.

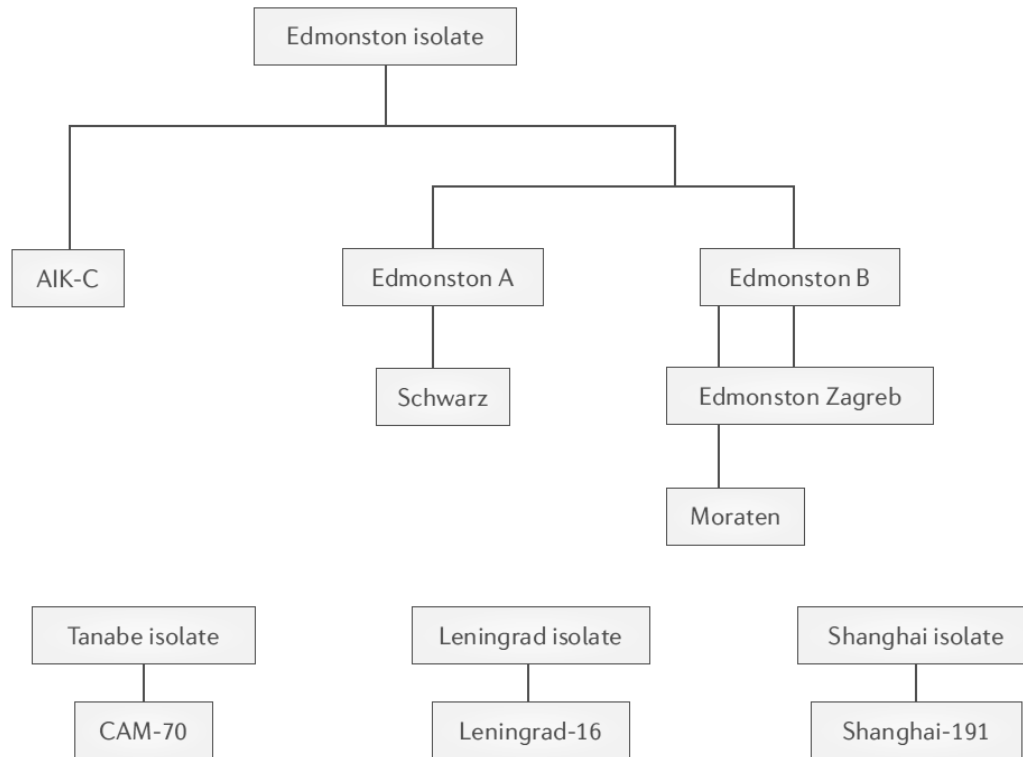


**Figure 7: MV vaccines.**

Most attenuated vaccines are derived from the original Edmonston-wt isolate. Nowadays the Schwarz and Edmonston-Zagreb vaccines are widely used throughout the world, whereas the Moraten strain is used primarily in the USA (Moss & Griffin, 2006).

Despite the large public health benefits, all the licensed vaccines have some drawbacks that are important for the global measles elimination. Currently used attenuated vaccines are light and temperature sensitive, requiring a continuous cold-chain and protection from sunlight (reconstituted vaccines lose half their potency already after storage for 1h at 20°C). The vaccination is done subcutaneously or intramuscularly so trained healthcare workers are obligatory. An important limitation is also that both maternally acquired antibodies as well as immunological immaturity of young infants reduce the efficacy of measles vaccination and hinder the effective immunization of young children.

The recommended age for a first vaccination boost is 12 month (infants in developing countries with 9 months) followed by a second boost at the age of five

to six years (Weiss, 1992). Nowadays the WHO recommends to use the trivalent MMR vaccine (Measles, Mumps, Rubella vaccine) that induce both humoral and cellular immune response (WHO, 2007). Previously it has been assumed that approximately 85% of children immunized at 9 month develop protective antibody titers, whereas in case of a later vaccination with 12 month 90-95% show protective antibodies (Cutts et al., 1995).

## **4.2. Eradication efforts**

Prior to the widespread use of measles vaccine more than 130 million cases and >2.5 million measles related death occurred annually and almost everybody was infected during childhood (Clements et al., 1992). Due to massive global vaccination campaigns over recent years remarkable progress has been made in reducing measles incidence and mortality during the last decades (Figure 8).

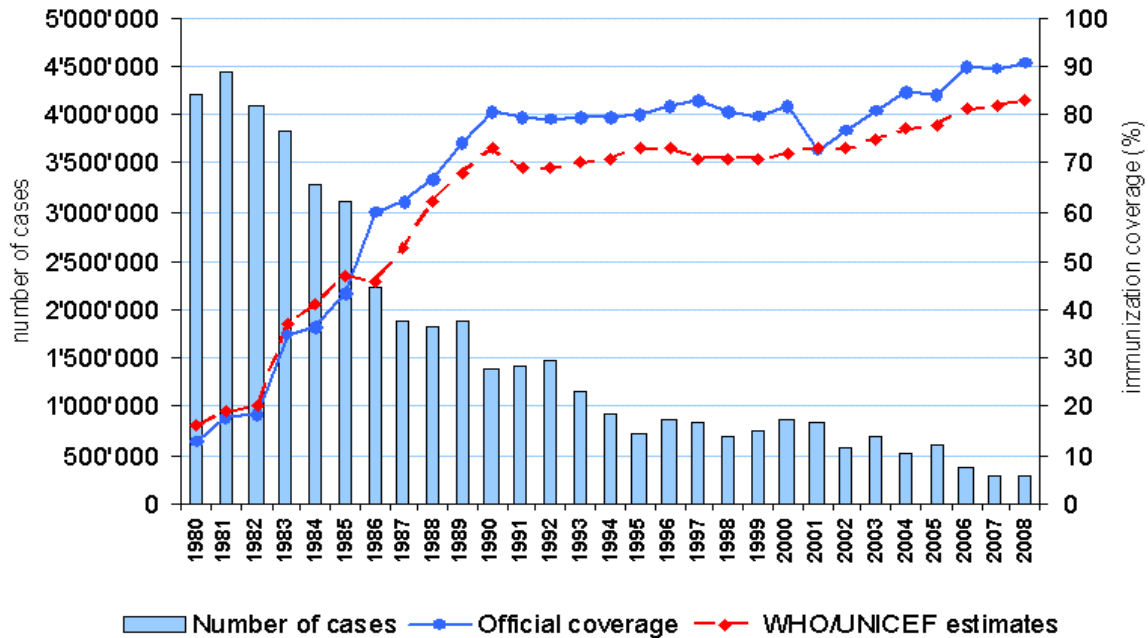


**Figure 8: Overview about global annual reported measles cases and measles vaccine coverage during 1980 to 2008.**

(WHO, 2009b).

In 2001 the WHO and United Nations International Children's Emergency Fund (UNICEF) implemented the measles mortality reduction strategy with focus on 1) achieving and maintaining >90% vaccine coverage with the first immunization by the age of 12 month, 2) ensuring that all children receive a possibility for a second vaccination, 3) surveillance of measles cases and 4) establishment of appropriate case management (WHO & UNICEF, 2001). During 2000-2008, global measles mortality declined by 78%, from an estimated 733,000 deaths in 2000 to 164,000 in 2008 (WHO, 2008). As one of the most successful and cost-effective medical interventions the measles vaccination campaigns have resulted in the interruption of indigenous measles circulation in a number of developed countries (Papania & Orenstein, 2004).

### **4.3. Measles today**

Despite achieving and sustaining global measles vaccination coverage > 80% over the past decade, worldwide measles remains the fifth leading cause of mortality among children below five years of age (Strebel et al., 2003). Especially unvaccinated pre-school-aged children are susceptible to measles and provide the fuel for new epidemics. This explains the importance of vaccinating each new cohort of infants soon after they lose the protection by maternal antibodies.

In the last years especially in resource-rich countries a loss of public confidence in vaccines as well as vaccine fatigue significantly impaired elimination efforts. Following a publication in 1998 that misleadingly purported an association between the MMR vaccine and autism (Wakefield et al., 1998) the MMR-immunization rates in England nosedive from 94 to 75% (Offit and Coffin 2003). As a consequence, measles outbreaks became more frequent and larger in size in the United Kingdom. Regardless of the huge efforts in measles control, the highest number of measles cases since more than a decade was observed in 2008 in several European countries and the US, and the virus was again declared endemic in the United Kingdom (Plempner & Snyder, 2009). Between January and June 2010 already more than 40,300 measles cases were reported by the WHO worldwide. Ongoing measles disease burden demonstrate the requirement to strengthen global efforts to control measles. Nevertheless other experiences demonstrate that interruption of measles transmission can be achieved and sustained over a long period of time (Orenstein et al., 2004).

## 5. Objectives of this study

Despite enhanced vaccination efforts, measles is still responsible for more than 50% of vaccine-preventable childhood deaths. Most deaths are attributed to secondary infections, facilitated by a long-lasting immunosuppression following measles disease. The molecular bases of MV induced immunosuppression and of the attenuation process of vaccine strains are still only partially understood.

The innate immunity is critical to control viral infections during the development of the adaptive immune response. Phenotypic differences between MV strains, relating to cytokine induction and signalling, may influence virus spread and severity of disease.

Distinct MV genotypes are endemic in most areas with high mortality rates. Usually the high mortality rates are attributed to specific host factors and to the quality of the public health system in the corresponding region. However, the pathogenicity of different genotypes has never been systematically compared. A better understanding of the characteristic differences between vaccine and wt strains as well as among various wt strains will be crucial to understand measles pathogenesis, immunosuppression and *in vivo* tropism of different strains. This knowledge may help to develop alternative vaccines or to test new antiviral agents in the future.

The genetic characterisation of wt strains provides a powerful tool of the laboratory-based measles surveillance. Molecular characterisation of viruses allows monitoring the transmission of MV during and after an outbreak, to detect interruptions of indigenous virus circulation and so differentiate ongoing transmission of endemic viruses from new imported sources of viruses, as well as to estimate the number of co-circulating variants. However, with the enhanced vaccination efforts the genetic variability of circulating strains continues to decline and identical sequences of the MV-NP highly variable region (routinely used for MV genotyping) have been found for several years in a same region. Very similar sequence variants were found throughout Europe and beyond. Thus it becomes

increasingly difficult to determine the origin of a virus analysing only this part of the viral genome. Therefore, sequencing of other variable regions of the MV genome, such as the entire MV-P and H genes may help to confirm epidemiological links between cases.

The aim of the present project was to identify phenotypic differences between attenuated and wt strains and/or between different wt strains and to analyse the genetic variability of MV strains (vaccine and wt). Specifically the following points were investigated:

- Part I: Genetic and Phenotypic characterisation of various MV strains
  - Differences in replication fitness
  - Interaction with the innate immune response *in vitro*
  - Effects of multiple passaging on the wt phenotype
  - Relationship of phenotypic differences and genetic characteristics
- Part II: Proteome profiling of MV host interaction in human lung cells comparing wild type and attenuated strains
  - Host cell proteome changes induced by different MV strains
- Part III: MV induced cytokine response in humans
  - Effects of two different MV genotypes on cytokine response
  - Interaction with the early immune response
- Part IV: Investigation of MV outbreaks
  - Genetic characterisation of new MV variants
  - Improvement of genotype classification

## **Chapter II**

---

## **Materials and Methods**

---

## Materials

All cell lines and virus strains used in part I of the Result Section are described under “Cells and Viruses” in this chapter. Following, all human sera analysed in part III of the Result Section are listed under “Patient sera”. Subsequently all samples investigated in part IV of the Result Section are described under “Clinical specimens”.

### 1. Cells and Viruses

#### 1.1. Cells

**Table 2: Cell lines used in part I of the Result Section**

cell name	Culture medium	cell type	species	source / reference
A549/hSLAM	DMEM, 10% FBS, 1% P/S, 1% Ultra-Glu	SLAM-transfected and expressing alveolar epithelial cells	Human ( <i>Homo sapiens sapiens</i> )	Yusuke Yanagi, Faculty of Medicine, Fukuoka, Japan, (Takeda et al., 2005)
Vero	DMEM, 7.5% FBS, 1% P/S, 1% Ultra-Glu	Kidney cells, fibroblasts	African green monkey ( <i>Chlorocebus aethiops</i> )	Yusuke Yanagi, Faculty of Medicine, Fukuoka, Japan, (Yasumura & Kawakita, 1963)
Vero/hSLAM	DMEM, 7.5% FBS, 1% P/S, 1% Ultra-Glu	SLAM-transfected and expressing Vero cells	African green monkey ( <i>Chlorocebus aethiops</i> )	Yusuke Yanagi, Faculty of Medicine, Fukuoka, Japan, (Tatsuo et al., 2000)

## 1.2. Viruses

Table 3: MV strains used in part I of the Result Section

ID	genotype	Strain name	Source	Isolated on	genbank acc# NP	genbank acc# P,V,C
<b>isolated on SLAM positive cells</b>						
MV030	B2	Mvi/Kinshasa.DRC/50.04	LNS, Luxembourg	Vero/hSLAM	FN668709	FN668713
MV112	B3	Mvi/Ibadan.NIE/8.98/9	LNS, Luxembourg	B95a	AJ232209	AM943859
MV215	C2	Mvi/Wincrange.LUX/22.96/3	LNS, Luxembourg	B95a	FN668710	FN668715
MV022	D10	Mvi/London.UNK/07.03	HPA, London	B95a	FN668708	FN668712
MV705	D2	NC1/95	NIV, Johannesburg	B95a	U64581	FN668724
MV032wt	D4	Mvi/Bucharest.ROU/04.06/3	LNS, Luxembourg	Vero/hSLAM	FN668702	FN668718
MV033wt	D4	Mvi/Bucharest.ROU/04.06/8	LNS, Luxembourg	Vero/hSLAM	FN668704	FN668720
MV034wt	D4	Mvi/Bucharest.ROU/04.06/9	LNS, Luxembourg	Vero/hSLAM	FN668706	FN668722
MV035	D4	Mvi/Athens.GRC/25.06	LNS, Luxembourg	Vero/hSLAM	AM850906	FN668714
MV005	D7	Mvi/Mainz.DEU/06.00	RKI, Berlin	B95a	AF277805	FN668711
MV801	D8	Mvi/Janakpur.NEP/2.99/1	LNS, Luxembourg	B95a	AJ250069	FN668725
MV409	G2	Mvi/Amsterdam.NET/49.97	Erasmus MC, Rotterdam	BLCL	AF171232	EU090818
MV336	G3	Mvi/Gresik.INO/17.02	CDC, Atlanta	Vero/hSLAM	DQ390233	EU090819
MV407	H1	Mvi/Amsterdam.NET/27.97	Erasmus MC, Rotterdam	BLCL	AF193512	FN668723
MV335	H2	Mvi/Beijing.CHN/94-1	CDC, Atlanta	B95a	AF045217	EU090821
<b>isolated or passaged on SLAM negative cells</b>						
MV501	A	Schwarz	RIMEVAX, GSK, Belgium	Vero	AF266291	AF266291
MV506	A	Hallé	INSERM, Lyon	Vero	X13480	EU332920
MVEdm	A	Edmonston-wt	ATCC	Human kidney cells	U01987	AF266288
MV326	D3	TX-92	CDC, Atlanta, USA	Vero	L46764	FN668716
MV032VCA	D4	Mvi/Bucharest.ROU/04.06/3_VCA	LNS, Luxembourg	Vero	FN668703	FN668717
MV033VCA	D4	Mvi/Bucharest.ROU/04.06/8_VCA	LNS, Luxembourg	Vero	FN668705	FN668719
MV034VCA	D4	Mvi/Bucharest.ROU/04.06/9_VCA	LNS, Luxembourg	Vero	FN668707	FN668721

wt: wild type strain; VCA: Vero cell adapted strain (10 times passaged on Vero cells before use)

## 2. Patients sera for cytokine analysis

In total, 41 human sera from laboratory confirmed measles patients, collected in Nigeria, Spain and Luxembourg were available for our pilot study described in part II of the result section (Table 4). The 13 Nigerian sera (genotype B3) were obtained from patients with clinical measles (7 to 60 years) collected during a measles outbreak in February and March 1998 in Ibadan. These samples were mainly collected from the pediatric out-patients department of three public hospitals (Adioyo State Hospital, n=7; Oni Memorial Children Hospital, n=4; University Collage Hospital, n=1) and one private hospital (St. Mary`s Hospital, n=1). The 14 sera from Spain (genotype B3) were collected from patients (1 to 32 years) during an MV outbreak in Almeria in 2003. The 14 Luxembourgish sera (genotype C2) were obtained during an outbreak in two primary schools in March and Mai 1996 from children with clinical measles (1 to 12 years). All sera were from uncomplicated measles cases collected between day 0 and day 8 after onset of rash. The control sera were from ten healthy Luxembourgish children vaccinated against MV (12 to 13 years) (Table 5). All samples have been stored appropriately at -20°C. The measles diagnosis was based on typical clinical symptoms confirmed by measles-specific IgM ELISA (Enzygnost, Dade Behring) as well as PCR for the MV-NP HVR (Kremer et al. 2007) to determine the genotype. Nigerian samples were all tested negative for HIV and HBV infection.

**Table 4: Patient sera used in part III of the Result Section**

ID number	gender	Age (years)	Days after onset of rash
<b>Patient sera from Luxembourg (genotype C2)</b>			
3005	m	6	2
3012	m	1	2
3013	f	8	1
3017	m	10	1
3018	m	10	3
3046	f	12	5
3055	m	10	3
3023	m	2	2
3040	f	6	3
3020	f	7	5
3021	m	6	3
3061	f	9	2
3070	m	11	4
3071	m	10	1
<b>Patient sera from Nigeria (genotype B3)</b>			
10037	uk	15	2
10041	uk	37	5
10043	uk	17	3
10044	uk	27	3
10055	uk	15	2
10581	uk	22	3
10924	uk	60	1
10931	uk	7	1
10951	uk	48	1
10952	uk	17	5
10965	uk	7	1
10967	uk	16	4
10970	uk	24	4
<b>Patient sera from Spain (genotype B3)</b>			
345	f	27	4
347	m	22	3
466	f	32	0
1244	m	8	1
396	m	1	0
372	m	18	3
342	m	23	4
362	m	26	8
339	f	28	0
245	m	12	0
312	m	28	3
309	m	21	1
316	f	19	2
306	m	19	1

f: female, m: male, uk: unknown

**Table 5: Control sera used in part III of the Result Section**

<b>ID number</b>	<b>Age (years)</b>
6007	12
6010	12
6011	12
6012	13
6013	12
6014	12
6016	11
6018	11
6020	13
6021	12

All control sera were positive for measles-specific IgG and negative for measles-specific IgM. Information about patient gender was not available.

### **3. Clinical specimens for virus characterization**

A total of 73 strains from four epidemiological settings in Europe and Africa were analyzed in part IV of the Result Section (Table 6). Clinical specimens from 13 patients were collected between April and June 2006 from 11 different locations in North-Rhine Westphalia (NRW, Germany). Samples from ten patients were collected between March and September 2006 from three different areas in Belarus: Minsk city (n=1), Minsk region (n=4) and Grodno region (n=5). 31 clinical samples were collected throughout the Russian Federation, Uzbekistan, Kazakhstan and Kyrgyzstan during March 2003 and May 2007. 18 samples were collected between December 2004 and February 2006 in three different regions of the Democratic Republic of Congo (DR-Congo): Bas-Congo (n=4), Kinshasa (n=12) and Kasai-Oriental (n=3). Most cases were serologically confirmed by measles specific IgM detection in serum, using a commercial ELISA kit (Enzygnost, Dade Behring, Germany).

Table 6: List of clinical specimens analysed in part IV of the Result Section

Strain name	Country	Region	NCBI acc# NP-HVR	NCBI acc# P	NCBI acc# H	MV genotype	sample material
MV/s/Bonn.GER/15.06/1	Germany	NRW	HM802073	HM801972	HM801915	D6b	TS
MV/s/Leching.GER/15.06/2	Germany	NRW	HM802074	HM801973	HM801916	D6b	OF
MV/s/Dortmund.GER/16.06	Germany	NRW	HM802075	HM801974	HM801917	D6b	OF
MV/s/Neunkirchen.GER/17.06/1	Germany	NRW	HM802076	HM801975	HM801918	D6b	OF
MV/s/Duisburg.GER/17.06/2	Germany	NRW	HM802077	HM801976	HM801919	D6b	OF
MV/s/Moenchengladbach.GER/17.06/3	Germany	NRW	HM802078	HM801977	HM801920	D6b	TS
MV/s/BadNeunahr.GER/21.06/1	Germany	NRW	HM802079	HM801978	HM801921	D6b	OF
MV/s/Borken.GER/21.06/2	Germany	NRW	HM802080	HM801979	HM801922	D6b	U
MV/s/Essen.GER/24.06/1	Germany	NRW	HM802082	HM801981	HM801924	D6b	TS
MV/s/Duisburg.GER/24.06/2	Germany	NRW	HM802083	HM801982	HM801925	D6b	OF
MV/s/Essen.GER/14.06	Germany	NRW	HM802084	HM801983	HM801926	D6b	TS
MV/s/Rheinberg.GER/15.06/3	Germany	NRW	HM802085	HM801984	HM801927	D6b	OF
MV/s/Dormagen.GER/15.06/4	Germany	NRW	HM802086	HM801985	HM801928	D6b	TS
MV/i/Minsk.BLR/12.06/3	Belarus	Minsk city	HM802062	HM801961	HM801904	D6b	ISO
MV/i/Smorgon.BLR/20.06/2	Belarus	Grodno region	HM802063	HM801962	HM801905	D6b	ISO
MV/i/Molodechno.BLR/28.06	Belarus	Minsk region	HM802064	HM801963	HM801906	D6b	ISO
MV/i/Vilejka.BLR/28.06	Belarus	Minsk region	HM802065	HM801964	HM801907	D6b	ISO
MV/i/Smorgon.BLR/28.06 **	Belarus	Grodno region	HM802066	HM801965	HM801908	D6b	ISO
MV/i/Smorgon.BLR/31.06 **	Belarus	Grodno region	HM802067	HM801966	HM801909	D6b	ISO
MV/i/Vilejka.BLR/33.06	Belarus	Minsk region	HM802068	HM801967	HM801910	D6b	ISO
MV/i/Volozhin.BLR/34.06 *	Belarus	Minsk region	HM802070	HM801969	HM801912	D6b	ISO
MV/i/Smorgon.BLR/36.06/1	Belarus	Grodno region	HM802071	HM801970	HM801913	D6b	ISO
MV/i/Smorgon.BLR/36.06/2	Belarus	Grodno region	HM802072	HM801971	HM801914	D6b	ISO
MV/i/Kinshasa.DRC/50.04	Congo	Kinshasa	HM802061	HM801886	HM802018	B2	ISO
MV/i/Mbujimayi.COD/06.06/2	Congo	Kasai-Oriental	HM802052	HM801887	HM802020	B2	TS
MV/s/Bas-Congo.COD/06.06/9	Congo	Bas-Congo	HM802053	HM801888	HM802021	B2	TS
MV/s/Bas-Congo.COD/06.06/3	Congo	Bas-Congo	HM802056	HM801884	HM802022	B2	TS
MV/s/Bas-Congo.COD/06.06/6	Congo	Bas-Congo	HM802054	HM801885	HM802023	B2	TS
MV/s/Kinshasa.COD/19.05/11	Congo	Kinshasa	HM802038	HM801890	HM802024	B2	SA
MV/i/Kinshasa.COD/19.05/15	Congo	Kinshasa	HM802039	HM801891	HM802025	B2	ISO
MV/i/Mbujimayi.COD/06.06/4	Congo	Kasai-Oriental	HM802051	HM801892	HM802026	B2	TS

Table 6: (continued) List of clinical specimens analysed in part IV of the Result Section

Strain name	Country	Region	NCBI acc# NP-HVR	NCBI acc# P	NCBI acc# H	MV genotype	sample material
MVs/Kinshasa.COD/41.05/9	DR-Congo	Kinshasa	HM802047	HM801894	HM802028	B2	SE
MVs/Kinshasa.COD/19.05/10	DR-Congo	Kinshasa	HM802040	HM801895	HM802029	B2	SA
MVs/Kinshasa.COD/18.05/2	DR-Congo	Kinshasa	HM802041	HM801896	HM802030	B2	SA
MVs/Kinshasa.COD/41.05/6	DR-Congo	Kinshasa	HM802044	HM801897	HM802031	B2	SE
MV/I/Mbujimayi.COD/06.06/3	DR-Congo	Kasai-Oriental	HM802049	HM801898	HM802032	B2	SA
MVs/Kinshasa.COD/19.05/4	DR-Congo	Kinshasa	HM802042	HM801899	HM802033	B2	SA
MVs/Kinshasa.COD/41.05/1	DR-Congo	Kinshasa	HM802045	HM801900	HM802034	B2	SA
MVs/Kinshasa.COD/42.05/3	DR-Congo	Kinshasa	HM802046	HM801901	HM802035	B2	SA
MV/I/Kinshasa.COD/42.05/4	DR-Congo	Kinshasa	HM802048	HM801902	HM802036	B2	SA
MV/I/Boma.COD/06.06/1	Congo	Kinshasa	HM802050	HM801903	HM802037	B2	ISO
MV/I/Moscow.RUS/13.03/2	Russia	Moscow	HM802087	HM801986	HM801929	D6a	ISO
MV/I/Moscow.RUS/5.04/1	Russia	Moscow	HM802088	HM801987	HM801930	D6a	ISO
MV/I/Moscow.RUS/7.04	Russia	Moscow	HM802089	HM801988	HM801931	D6a	ISO
MV/I/Moscow.RUS/14.04	Russia	Moscow	HM802090	HM801989	HM801932	D6a	ISO
MV/I/S-Petersburg.RUS/16.04/1	Russia	St. Petersburg	HM802091	HM801990	HM801933	D6a	ISO
MV/I/S-Sahalinsk.RUS/19.04/1	Russia	St. Sahalinsk	HM802092	HM801991	HM801933	D6a	ISO
MV/I/Rostov-na-Donu.RUS/15.05	Russia	Rostov-na-Donu	HM802093	HM801992	HM801935	D6a	ISO
MV/I/Rostov-na-Donu.RUS/17.05/2	Russia	Rostov-na-Donu	HM802094	HM801993	HM801936	D6a	ISO
MV/I/NizhnyNovgorod.RUS/35.05	Russia	Nizhny Novgorod	HM802095	HM801994	HM801937	D6a	ISO
MV/I/Moscow.RUS/19.06/1	Russia	Moscow	HM802097	HM801996	HM801939	D6a	ISO
MV/I/Moscow.RUS/25.03/1	Russia	Moscow	HM802098	HM801997	HM801940	D6a	ISO
MV/I/Moscow.RUS/11.06/10	Russia	Moscow	HM802099	HM801998	HM801941	D6a	ISO
MV/I/Orenburg.RUS/12.06	Russia	Orenburg	HM802100	HM801999	HM801942	D6a	ISO
MV/I/Tver.RUS/14.06	Russia	Tver	HM802101	HM802000	HM801943	D6a	ISO
MV/I/Orenburg.RUS/16.06	Russia	Orenburg	HM802102	HM802001	HM801944	D6a	ISO
MV/I/NizhnyNovgorod.RUS/10.07/1	Russia	Nizhny Novgorod	HM802103	HM802002	HM801945	D6a	ISO
MVs/NizhnyNovgorod.RUS/26.05	Russia	Nizhny Novgorod	HM802104	HM802003	HM801946	D6a	RNA
MV/I/Moscow.RUS/25.03/2	Russia	Moscow	HM802105	HM802004	HM801947	D6a	ISO
MV/I/Moscow.RUS/29.03/1	Russia	Moscow	HM802108	HM802007	HM801950	D6a	ISO
MVs/Moscow.RUS/16.07/2	Russia	Moscow	HM802110	HM802009	HM801952	D6a	RNA
MVs/Moscow.RUS/19.07	Russia	Moscow	HM802111	HM802010	HM801953	D6a	RNA
MV/I/Novokuzneck.RUS/44.03/1	Russia	Novokuzneck	HM802113	HM802012	HM801955	D6a	ISO
MV/I/N.Osetiya.RUS/51.03	Russia	N. Osetiya	HM802114	HM802013	HM801956	D6a	ISO
MV/I/Moscow.RUS/3.04/1	Russia	Moscow	HM802115	HM802014	HM801957	D6a	ISO

**Table 6: (continued) List of clinical specimens analysed in part IV of the Result Section**

Strain name	Country	Region	NCBI acc# NP-HVR	NCBI acc# P	NCBI acc# H	MV genotype	sample material
MV/Moscow.RUS/3.04/2	Russia	Moscow	HM802116	HM802015	HM801958	D6a	ISO
MV/Moscow.RUS/4.04	Russia	Moscow	HM802117	HM802016	HM801959	D6a	ISO
MV/Toshkent.UZB/07.06/2	Uzbekistan	Toshkent	HM802096	HM801995	HM801938	D6a	ISO
MVs/Toshkent.UZB/07.06/3	Uzbekistan	Toshkent	HM802106	HM802005	HM801948	D6a	RNA
MVs/Toshkent.UZB/07.06/4	Uzbekistan	Toshkent	HM802107	HM802006	HM801949	D6a	RNA
MVs/Almaty.KAZ/36.06	Kazakhstan	Almaty	HM802109	HM802008	HM801951	D6a	RNA
MVs/Chuy.KGZ/17.07	Kyrgyzstan	Chuy	HM802112	HM802011	HM801954	D6a	RNA

NRW: North-Rhine Westphalia; DR-Congo: Democratic Republic of Congo; TS: throat swab; OF: oral fluid; U: urine; ISO: cell culture isolate; SA: saliva; SE: serum; RNA: unknown sample source, RNA received from collaborators; \*\* Epidemiological link to the Ukraine; \* Imported from Grodno region to Minsk region

## 4. Chemicals, Buffers and Solutions

### 4.1. Chemicals

Commonly used chemicals were purchased from Sigma Aldrich (Belgium) or Merck (Germany). All cell culture media and reagents were purchased from Lonza (Switzerland).

<b>Compound</b>	<b>Supplier</b>
Agarose	Lonza
Ampicillin	Sigma
Dithiothreitol (DTT) 0.1 M	Invitrogen
dPBS 10x w/o Ca and Mg	Lonza
Dimethylsulfoxide (DMSO)	Sigma
Dulbecco`s modified Eagle`s medium (DEMEM ) w/o Glutamine	Lonza
Ethanol 100%	Merck
Ethylendiaminetetraacetic acid (EDTA)	Biorad
Fetal bovine serum (FBS)	Lonza
Ultra-Glutamine	Lonza
Glycerol	Sigma
IFN-alpha/beta	R&D Systems
MgCl <sub>2</sub> 50 mM	Invitrogen
Nucleotides (dNTPs)	Invitrogen
Oligonucleotides/primers	Eurogentec
Orange G	Invitrogen
PCR buffer without MgCl <sub>2</sub> 10x	Invitrogen
Penicillin G-Streptomycin 100x	Sigma/Lonza
Sodium acetate	Merck
SYBR <sup>®</sup> Green <sup>™</sup> nucleic acid stain 10 000x	Molecular Probes
SYBR <sup>®</sup> Safe <sup>™</sup> DNA Gel Stain 10 000x	Invitrogen
Tris(hydroxymethyl)aminomethane (Tris)	Sigma
Trypan blue	Sigma

## 4.2. Buffers and Solutions

The water used for the buffers and solutions was purified using the Barnstead TII Water System (Thermo Scientific).

Buffer name	Reagents	Volume
DNA loading dye (6x)	Orange G Sucrose (40%) ddH <sub>2</sub> O store at 4 °C	25 mg 4 g up to 10 ml
TAE-buffer (50x)	Tris Sodium acetate EDTA Adjust pH 7.8	2 M 25 mM 0.5 M
PBS-EDTA (10x)	EDTA PBS w/o Ca/Mg (10x)	1 g 500 ml

## 5. Commercial kits

Commercial name	Supplier
QIAamp <sup>®</sup> Viral RNA Mini kit	Qiagen
RNeasy Mini kit	Qiagen
QIAquick Gel Extraction <i>Kit</i>	Qiagen
MagMAX <sup>™</sup> AI/ND Viral RNA Isolation kit	Ambion
Jet Quick PCR Purification Spin <sup>®</sup> kit	Genomed
Big Dye Terminator v3.1 Cycle Sequencing <sup>®</sup> kit	Applied Biosystems
MycoAlert <sup>®</sup> Mycoplasma Detection Kit	Lonza
IFN-beta ELISA kit: EIA-2088	DRG
RANTES ELISA kit: BMS287/2INST	VWR
CBA Flex sets (for IL-5, IL-6, IL-8, IL-10 and MCP-1)	BD
Enzygnost Anti-MV IgM and IgG	Dade Behring
2D-Clean-Up-Kit	GE Healthcare
2D-Quant-Kit	GE Healthcare

## 6. 2D-DIGE Material

Compound	Supplier
SYPRO® Ruby protein gel stain	Invitrogen
DTT	Sigma-Aldrich
CyDye DIGE Fluor Cy3 minimal dye, 25 nmol	GE Healthcare
CyDye DIGE Fluor Cy5 minimal dye, 25 nmol	GE Healthcare
CyDye DIGE Fluor Cy3 minimal dye, 25 nmol	GE Healthcare
Immobiline DryStrip pH 3-7, 24 cm	GE Healthcare
IPG Buffer pH 3-7	GE Healthcare
Immobiline DryStrip Cover Fluid	GE Healthcare
Paper Wicks	GE Healthcare
Reference markers (for robot spot picking)	GE Healthcare
PlusOne Ammonium Persulfate	GE Healthcare
PlusOne N,N'-Methylene-bisacrylamide	GE Healthcare
PlusOne N,N'-Methylene-bisacrylamide 2% Solution	GE Healthcare
PlusOne AcrylamidePAGE	GE Healthcare
PlusOne UREA	GE Healthcare
Thiourea	GE Healthcare
PlusOne Glycerin	GE Healthcare
PlusOne Tris	GE Healthcare
PlusOne SDS	GE Healthcare
CHAPS	GE Healthcare
Iodoacetamide	GE Healthcare
Potease Inhibitor Mix	GE Healthcare
PlusOne Bromophenol Blue	GE Healthcare
PlusOne Triton X-100	GE Healthcare
PlusOne Glycerol	GE Healthcare
Nuclease mix	GE Healthcare
Lava Purple gel strain	Gel Company

## 7. 2D-DIGE Buffers and Solutions

Buffer name	Reagents	Volume/Concentration
CHAPS Lysis buffer	Tris Cl (1 M, pH not adjusted)	30 mM
	Thiourea	2 M
	Urea	7 M
	CHAPS	4 % (w/v)
	Complete Protease Inhibitor Mix	1x
	Nuclease Mix	1x
	Isopropanol	12 %
	dd H <sub>2</sub> O	up to 100 ml
	pH	8.5
Rehydration buffer	CHAPS	4 %
	Thiourea	2 M
	Urea	7 M
	DTT	13 mM
	IPG buffer	1 %
	Bromphenol blue	trace
	dd H <sub>2</sub> O	25 ml
SDS equilibration buffer	Tris Cl (1.5 M, pH 8.8)	50 mM
	Urea	6 M
	Glycerol (50 %)	30 % (v/v)
	SDS	2 % (w/v)
	Bromphenol blue	trace
	dd H <sub>2</sub> O	80 ml
Equilibration buffer for reduction	SDS equilibration buffer	40 ml
	DTT	0.5 % (w/v)
Equilibration buffer for alkylation	SDS equilibration buffer	40 ml
	IAA	4.5 % (w/v)

Tris 1.5 M, pH 8.8	Tris	1.5 M
	HCL (6 M)	~150 ml
	dd H <sub>2</sub> O	up to 3 l
12 % 2D-PAGE gel	Acrylamid/Bisacrylamid 30 % (w/v)	250
	Tris Cl (1.5 M, pH 8.8)	150
	10 % SDS	6
	TEMED	0.2
	APS	3
20x SDS Running Buffer	Tris	25 mM
	Glycine	192 mM
	SDS	0.2 % (w/v)
Agarose sealing solution	1x SDS Running Buffer	100 ml
	Agarose	0.5 %
	Bromphenol blue	trace

## 8. Enzymes

Enzyme	Supplier
Platinum <sup>®</sup> Taq DNA polymerase	Invitrogen
RNaseOUT <sup>™</sup> (Recombinant Ribonuclease Inhibitor)	Invitrogen
SuperScript <sup>™</sup> III Reverse Transcriptase	Invitrogen

## 9. Primers

Primer name	5' - 3' sequence	Annealing (°C)	Reference
MN5	GCCATGGGAGTAGGAGTGG AAC	55	(Santibanez et al., 2002)
MN6	CTGGCGGCTGTGTGGACCTG		
Nf1a	CGGGCAAGAGATGGTAAGGAGGTCAG	58	(Kremer et al., 2007)
Nr7a	AGGGTAGGCGGATGTTGTTCTGG		
MVTaqfw	CCCTGAGGGATTCAACATGATTCT	60	(Hubschen et al., 2008)
MVTaqprobe	FAM-TCTTGCTCGCAAAGGCGGTTACGG-BHQ1		
MVTaqrv	ATCCACCTTCTTAGCTCCGAATC		
MV-P1 (fw)	CTTAGGAACCAGGTCCACACA	65	(Bankamp et al., 2008)
MV-P1 (rv)	GAGGGTGA CTTTCGAGCACAT		
MV-P2 (fw)	GCACTTCCGAGACACCCATTC		
MV-P2 (rv)	GAGGCAATCACTTTGCTCCTAAGT		
MV-H1	TTAAAACTTAGGGTGCAAGATCATCCACA	58	(Kessler et al. 2010 in preparation)
MV-H2	ACTTGGTTAGTGTACTACAGTGGG		
MV-H3	CACCTCAGAGATTCACTGACCTAGT		
MV-H4	TATCCCTCATGCTGAAGTCTCTAG		
MV-H5	GTACCGAGTGTTTGAAGTAGGTGTTA		
MV-H6	AACTCGTTGGTCAGTCATTACCAG		
MV-H7	GATCTGAGTCTGACAGTTGAGCTTA		
MV-H8	TAACTAGTGTGTGCCGAGTCC		
MxA TaqMan <sup>®</sup>	TaqMan GE assay Mx1 (no sequence available)		(Applied Biosystems)
beta actin (fw)	GGCCACGGCTGCTTC	60	(Schote et al., 2007)
beta actin (rv)	GTTGGCGTACAGGTCTTTGC		
TNF-alpha (fw)	TGCTGCACTTTGGAGTGATCG	62	(Kessler et al. 2010 in preparation)
TNF-alpha (rv)	CCTCAGCTTGAGGGTTTGC		
IL-1 beta (fw)	AGATGATAAGCCCACTCTACAG		
IL-1 beta (rv)	TTCAGCACAGGACTCTCTGG		
2-5AS (fw)	TTAAATGATAATCCCAGCCC	60	(Fujii et al., 1999)
2-5AS (rv)	AAGATTACTGGCCTCGCTGA		
MV396	TATAAGCTTACCAGACAAAGCTGGGAATA GAACTTCG	54	(Shingai et al., 2007)
MV402	TTTATCCAGAATCTCAARTCCGG		
MV403	CGAAGATATTCTGGTGTAAAGTCTAGTA		

## 10. Bioinformatics

Detailed information about phylogenetic analysis can be found in Chapter II, Methods.

<b>Program name</b>	<b>Reference</b>
Opticon Monitor™ v3.1	BioRad
FastPCR v. 3.7.8	(R. Kalender, University of Helsinki, Finland)
BLAST	<a href="http://ncbi.nlm.nih.gov/BLAST">http://ncbi.nlm.nih.gov/BLAST</a>
SeqScape	Applied Biosystems
BioEdit	<a href="http://www.mbio.ncsu.edu/BioEdit">http://www.mbio.ncsu.edu/BioEdit</a>
CLUSTAL W	(Thompson et al., 1994)
MEGA 4.0	(Tamura et al., 2007)

## 11. Additional programs

<b>Program name</b>	<b>Reference</b>
TCID <sub>50</sub> calculation	NCBI ID-50 v5.0
SigmaStat v3.11 and SigmaPlot v9.01	Systat Software
Adobe Photoshop and Illustrator	Adobe Systems
Delta2D v.4.0	Decodon

## 12. Instruments

Instruments	Supplier
Centrifuges	Pico 17, Heraeus; Megafuge <sup>®</sup> 1.0R, Heraeus
Balance	UNIVAP 150H, UniEquip SARTORIUS Precision balance
Electrophoresis power supply	E835, Consort
Electrophoresis power supply EPS 3501 XL	GE Healthcare
Ettan IPGphor II	GE Healthcare
Ettan Dalt picking robot	GE Healthcare
FACS Canto II	BD
Fluorescence/Luminescence reader	GENios Plus, Tecan
Gel tank and casting form	Biozyme
InGenius Gel documentation system	InGenius, Syngene
Heating block	Thermomixer Comfort, Eppendorf
Incubator	HERAcell <sup>®</sup> 150, Heraeus
KingFisher Flex	Thermo Scientific, VWR
Microscope	Leica
PCR machine	Mastercycler <sup>®</sup> Gradient, Eppendorf
Real time PCR machines	Opticon <sup>®</sup> 2 DNA Engine, Chromo4 <sup>™</sup> , CFX, MiniOpticon, Biorad, ABI7500Fast, Applied Biosystems
Shaker	Multitron 2, INFORS-HT
Sequencer	ABI PRISM <sup>®</sup> 3130xl Genetic Analyzer, Applied Biosystems
Safe Imager <sup>™</sup>	Invitrogen
SPECTRAmax PLUS microplate reader system	Molecular Devices
Typhoon 9400	GE Healthcare
Ultraflex TOF/TOF	Bruker Daltonics
UNIVAP 150 H	UniEquip
Vortex	Vortex-Genie <sup>®</sup> 2, Scientific Industries <sup>1</sup>

### Comment

Company and product denominations mentioned in this document, such as: Invitrogen, Merck, Biorad, Sigma, Eurogentec, Qiagen, Genomed, Applied Biosystems, Heraeus, UniEquip, Eppendorf, Tecan, R&D Systems, Finnzymes, Biozyme, Syngene, Biotage, Roche Diagnostics, may be trademarks or registered trademarks of their respective trademark owners.

## Methods

The following methods were used to generate and collect the results described in Chapter III. Additional information about specimens and clinical samples are described in the respective parts of Chapter II, Materials.

### 13. Cell cultures

#### 13.1. Cell lines

##### Vero

The Vero cell line was derived from kidney epithelial cells of an adult African Green Monkey (*Chlorocebus aethiops*) in 1962 (Yasumura & Kawakita, 1963). Since Vero cells are susceptible for a broad range of viruses, including measles, rubella and rabies viruses, this adherent mammalian continuous cell line is commonly used in molecular research. Unlike normal mammalian cells, Vero cells are IFN-deficient, so they do not secrete type I IFN after virus stimulation, but respond normally to external type I IFN stimulation (Emeny & Morgan, 1979). Cells were seeded in 175 cm<sup>2</sup> flasks and cultivated in 30 ml cell culture medium under sterile standard cell culture conditions. Depending on cell growth, cells were passaged by splitting every 2-3 days. Reaching 100% confluent monolayer, cells were once washed with 10 ml 1x PBS and afterwards incubated (37°C) for 20-30 min in 10 ml 1x PBS-EDTA. Detached cells were swirled gently, transferred to a 50 ml tube and centrifuged 5 min at 1200 rpm. The remaining supernatant was discarded and the cell pellet resuspended in 10 ml fresh culture medium. To estimate the cell number 10 µl cell suspension were mixed with 10 µl trypan blue,

transferred to a Neubauer Haemocytometer and the following formula was used to determine the number of cells per ml suspension:

$C = N \times 10^4 \times 2$  (C = cells/ml; N = average of cells counted in two haemocytometer chambers;  $10^4$  = volume conversion factor; 2 = correction of trypan blue dilution). Approximately  $2.5 \times 10^6$  cells were transferred back into the 175 cm<sup>2</sup> culture flask with maximal 30 ml fresh culture medium.

### Vero/hSLAM and A549/hSLAM

Both cell lines have been transfected with a plasmid encoding the gene for the human signalling lymphocyte activation molecule (SLAM) and are constitutively expressing SLAM, the receptor for both MV-wt and laboratory-adapted strains (Ono et al., 2001, Takeda et al., 2005). Vero/hSLAM cell are originally derived from the Vero cells, described above. The A549/hSLAM cell line was generated in 2005 by Takeda et al. (Takeda et al., 2005) using A549 cells. The A549 cells are human carcinomic alveolar basal epithelial cells, which were first developed in 1972 by D.J Giard and further characterised by Lieber et al 1976. In the past, this cell line has been extensively referenced in the toxicology literature. Vero/hSLAM as well as A549/hSLAM cells were propagated as described for the above Vero cells.

## 13.2. Freezing and thawing cells

As described above, 100% confluent cells were detached from the culture flask using 1x PBS-EDTA, centrifuged and counted. Afterwards  $2-3 \times 10^6$  cells/ml were resuspended in cold freezing medium, containing 70% culture medium, 20% FBS and 10% DMSO. The freezing solution was distributed into 1 ml cryo-vials, tubes were transferred into a special freezing container (Mr Frosty) and stored for at least 24 h at -80°C to perform the freezing procedure with a cooling rate of

1 °C/min. Long-time storage was done in the N<sub>2</sub>-tank. In order to thaw cells, a 75 cm<sup>2</sup> culture flask was filled with 15 ml cell culture medium and pre-warmed in the incubator at 37 °C and 5% CO<sub>2</sub>. The cryo-vials were placed directly from the N<sub>2</sub>-tank into a 37 °C water bath. Subsequently, the thawed cell suspension was transferred into the prepared 75 cm<sup>2</sup> flask and placed back into the incubator at 37 °C. The next day, the culture medium was changed in order to wash dead cells away.

### 13.3. Mycoplasma test

Mycoplasma are obligate parasitic bacteria, depending on their hosts for many nutrients, due to their limited biosynthetic capabilities. On a monthly basis a mycoplasma test was performed, using the MycoAlert® Kit from Lonza. This is a selective biochemical test, which exploits the activity of certain mycoplasmal enzymes. For 10-25 tests the lyophilized MycoAlert® Reagent and lyophilized MycoAlert® Substrate were each reconstituted in 600 µl MycoAlert® Assay Buffer and incubated for 15 min at RT, to ensure complete rehydration. 2 ml of cell supernatant were centrifuged for 5 min at 1500 rpm to remove dead cells and cell debris. In a white wall luminescence compatible 96 well plate, 100 µl of the cleared supernatant were mixed with 100 µl of the before prepared MycoAlert® Reagent and incubated for 5 min at RT. Afterwards the luminescence of reaction one was measured using the luminescence reader from Tecan. Subsequently 100 µl MycoAlert® Substrate were added to each sample and incubated for 10 min at RT. The luminescence of reaction two was measured and the following formula was used to determine whether the cell culture was contaminated by mycoplasma: Ratio = Reaction 2/Reaction 1. Ratios below 1 designated uninfected cells, ratios between 1 and 1.3 were suspected to be positive, quarantined and retested after 24 h. Ratios above 1.3 clearly highlighted a contamination with mycoplasma.

## 14. Virus cultures

### 14.1. MV isolation and virus propagation

MV can be isolated using a broad range of clinical specimens including peripheral blood mononuclear cell (PBMCs), throat or nasopharyngeal swabs, nasal aspirates or urine collected as soon as possible after rash onset. The virus isolation is most successful for samples collected between day one and three after onset of rash (WHO, 2007). The preparation of samples for virus isolation and the process of virus inoculation on Vero/hSLAM cells have been done in BSL3 facilities. As described in the (WHO, 2007), Vero/hSLAM cells stable express SLAM also without Geneticin in the cell culture medium, for at least 15 cell passages. Another advantage of this cell line is that they are not persistently infected with virus, and therefore, are not considered as hazardous material like previously used B95a cells. Hence, for inoculation  $1 \times 10^6$  Vero/hSLAM cells were seeded into a 25 cm<sup>2</sup> culture flask in normal cell culture medium. Next day, cells were 85-90% confluent and up to 1 ml of the clinical sample was added onto the culture. Inoculated cells have been observed by light microscopy for CPE on a daily basis. Following 5 days inoculation, 1 ml of CPE negative culture supernatant was transferred to a fresh cell culture (blind passage of virus). When CPE reached approximately 75-85% cells and culture supernatant were harvested using a cell scraper, transferred into a 15 ml tube and stored at -80 °C. After 24 h at -80 °C, this first generation virus batch was thawed, centrifuged 15 min at 3000 rpm, 1-2 ml aliquots of the clear supernatant prepared and these were afterwards used for growing user batches.

User batches were grown in 175 cm<sup>2</sup> flasks and the complete culture was harvested when the CPE reached 85-95%, using the procedure described above (in general after 2-4 days). TCID<sub>50</sub> was determined for each virus batch separately.

## 14.2. Virus titration (TCID<sub>50</sub> determination)

The 50% tissue culture infective doses (TCID<sub>50</sub>) determination calculates the amount of virus required to produce CPE in 50% of inoculated cells. Vero/hSLAM cells from a continuous culture (passage < 15) were detached using 1x PBS-EDTA, counted and diluted to 7.5x 10<sup>4</sup>/ml in normal culture medium. Each well of two sterile 96-well flat-bottom cell culture plates was filled with 100 µl cold (4°C) culture medium, 100 µl virus solution was added to each well of column 1 of plate 1. Beginning in column 1 of plate 1 the solution was mixed by pipetting 100 µl three times up and down using an eight channel pipette. Following, a serial dilution was performed, transferring always 100 µl of one column to the following one, after mixing three times. So 100 µl of column 1 were transferred to column 2, mixed 3 times, filter-tips were changed and 100 µl of column 2 were transferred to column 3, this procedure was repeated until column 11 of plate 2. Column 12 of plate 2 was the negative control. Afterwards 100 µl of previously prepared 7.5x 10<sup>4</sup>/ml Vero/hSLAM cell solution was added to each well, starting at column 12 of plate 2. After five days incubation (37°C, 5% CO<sub>2</sub>) wells positive for CPE were counted and TCID<sub>50</sub> calculation was performed using the program ID-50 v5.0 (NCBI).

## 14.3. Virus Concentration (Amicon<sup>®</sup> Ultra filtration)

In order to increase the amount of infective particles after MV propagation, the virus user batch was ultrafiltrated using Amicon<sup>®</sup> Ultra-15 centrifugal filter devices (100k, Millipore, Belgium). This Amicon<sup>®</sup> Ultra filtration method enables the recovery of the concentrated sample (retained in the filter unit) and the ultrafiltrate. Up to 15 ml of virus solution was transferred to the Amicon filter unit. Capped filter devices were centrifuged up to 30 min at 3000 rpm at 4°C. The

concentrate (maximal 2 ml) was collected from the filter unit using a normal 1000 µl pipette and TCID<sub>50</sub> was determined as described above.

## **15. Enzyme-Linked-Immuno-Sorbent-Assay (ELISA)**

The Enzyme-Linked-Immuno-Sorbent-Assay (ELISA) is a fundamental tool of clinical immunology, and is mainly used to detect the presence of an antibody or an antigen in different specimens (like urine, serum or cell culture supernatant) usually performed in microwell plates. The basic principle of an ELISA is the recognition by enzyme linked antibodies of antigens, adsorbed onto a specially treated plastic support. The enzyme converts a colorless substrate to a colored product, indicating the presence of antigen/antibody binding. A Sandwich ELISA is based on the following steps: 1) The micro-well plate is coated with the capture antibody, 2) the specimen is added to the plate and any antigen present, binds to a capture antibody, 3) unbound antigens are washed away, 4) the detection antibody is added and binds to the antigen, 5) the secondary enzyme-linked antibody is added and binds to the detection antibody, 6) in the last step the enzyme substrate is added, is converted by the enzyme to a detectable form and the color change is measured by a spectrophotometer. An ELISA can be used to detect either the presence of antigens or antibodies in a specimen, depending on the design of the test.

Human IFN-beta and RANTES protein concentrations in cell culture supernatant as well as in human sera were determined using commercial ELISA Kits (IFN-beta: EIA-2088, DRG, Germany and RANTES: BMS287/2INST, VWR, Belgium) according to the manufactures instructions.

Briefly IFN-beta ELISA: The lyophilised enzyme-labelled-antibody was dissolved in 6 ml ice cold dilution buffer (both contained in the kit). To prepare the HuIFN-beta standard solution, the lyophilisate was dissolved in 1 ml ice cold distilled water. Following this solution was further diluted in ice cold distilled water to obtain a standard dilution series (200, 100, 50, 20, 10, 5, 2.5 IU/ml, dilution buffer

was used as negative control). The concentrated washing solution was mixed with 450 ml distilled water. The colour-developer-solution was freshly prepared each time, substrate A was mixed with substrate B in a ratio 20 to 1. To prime the ELISA plate, it was placed for 10 min at RT. Afterwards each well was washed with 400 µl washing solution, using an eight channel pipette. Subsequently 50 µl enzyme-labelled-antibody was added to each well and mixed with 100 µl sample or HuIFN-beta standard solution (0-200 IU/ml). The plate was placed for 2 h at RT on a plate shaker. Following the solution was carefully aspirated and each well was washed twice with 400 µl washing solution. 100 µl colour-developer-solution was added to each well and the plate was shaken 30 min at RT. Finally the reaction was stopped by adding 100 µl reaction-stopper-solution to each well and the measurement was performed at 450 nm in a plate reader.

Briefly RANTES-ELISA: The wash buffer concentrate (25 ml) was diluted in 475 ml distilled water and adjusted to pH 7.4. The 5 ml assay buffer concentrate was diluted in 95 ml distilled water. The ELISA plate was used immediately after removing from -20°C. 140 µl distilled water were transferred to each sample and standard well. Following 10 µl of the sample were added to the designated wells, mixed and the plate was incubated 3 h at RT. Subsequently each well was carefully washed six times with 400 µl wash buffer. The plate was tapped on absorbent paper to remove excess wash buffer. 100 µl of TMB substrate solution was added to each well and incubated for 10 min at RT in the dark. Finally the enzyme reaction was stopped by pipetting 100 µl stop solution into each well and the absorbance was measured at 450 nm.

## **16. Cytometric bead array (CBA)**

The flow cytometric bead-based technology offers a new approach to simultaneously measure multiple analytes in biological or environmental samples. This method uses the broad dynamic range of fluorescence detection by flow cytometry and antibody-coated beads to efficiently capture analytes.

Particles (beads) with discrete fluorescence intensities or various sizes are coated with a capture antibody for a soluble protein and can be mixed and used simultaneously in a single reaction. Each bead provides a capture surface for a specific protein and is traced by detector antibodies, which are conjugated to a fluorescent dye. In comparison to a traditional ELISA this method requires a reduced sample volume. IL-5, IL-6, IL-8, IL-10 and MCP-1 protein concentrations in cell culture supernatant or human sera were determined using commercial cytometric bead arrays (CBA Flex sets, BD) according to the manufactures instructions.

Briefly: To prepare the standards, all lyophilized standard spheres from each Flex set that was tested, were pooled into one 15 ml tube and label as Top Standard. These spheres were all reconstituted in 4 ml assay diluent by pipetting the solution up and down and equilibrated 15 min at RT. From this Top Standard a serial dilution (1/2, 1/4, 1/8, 1/16, 1/32, 1/64, 1/128, 1/256) was performed in 500  $\mu$ l assay diluent; the negative control contained only assay diluent. The Flex set capture beads were 50 times concentrated and needed to be diluted into capture bead diluent. The exact calculation of this dilution step can be found in the manual and was performed using the FlexSet Calculator provided by the company. To Prepare the PE detection reagent, the concentrate (50x) was diluted in detection reagent diluent as calculated by using the FlexSet Calculator. To start the assay procedure 50  $\mu$ l of the prepared bead mixture was transferred into the designated tubes, mixed with 50  $\mu$ l of sample or standard and incubated 1 h at RT. Subsequently 50  $\mu$ l PE detection reagent were added to each tube, mixed and incubated for 2 h at RT in the dark. 100  $\mu$ l wash buffer were transferred to each tube, tubes were centrifuged for 5 min at 200 g and the supernatant was carefully descended. Finally the pellet was resuspended in 75  $\mu$ l 1% paraformaldehyd solution to inactivate infectious samples. The measurement was performed using a FACS Canto II (BD).

## 17. RNA extraction

### 17.1. QIAamp<sup>®</sup> Viral RNA Mini kit

Viral RNA was extracted from clinical specimens (nasopharyngeal sample, throat swab, oral fluid, urine, saliva or serum) and virus cell culture supernatant using the QIAamp<sup>®</sup> Viral RNA Mini kit (Qiagen) according to the manufacturers instructions. Briefly: 140 µl of sample were added to 560 µl of Lysis Buffer (AVL buffer) containing carrier RNA (both included in kit), vortexed for 10 s and incubated for 10 min at RT. Afterwards, 560 µl of 100% ethanol were added to the latter solution, vortexed for 10 s, transferred to the QIAamp<sup>®</sup> Mini spin column in a 2 ml centrifugation tube and centrifuged 1 min at 10.000 rpm. The flow through was discarded and the column was washed with 500 µl AW1 buffer (1 min at 10.000 rpm) and afterwards with 500 µl AW2 buffer (both included in kit). RNA was eluted in a final volume of 35 µl of distilled water and stored at -80 °C.

### 17.2. MagMAX<sup>™</sup>-96 AI/ND Viral RNA Isolation kit

For huge amounts of clinical samples the MagMAX<sup>™</sup>-96 AI/ND Viral RNA Isolation kit (Ambion, Netherlands) was used to extract measles virus RNA. This kit is based on microspherical paramagnetic beads with a large available binding surface. The beads can be fully dispersed in solution, allowing thorough nucleic acid binding, washing and elution. The procedure was performed in the KingFisher Flex robot (Thermo scientific), which is able to process in only 20 min up to 96 samples in a single run. The following protocol was used for parallel RNA isolation of 100 samples. For the Lysis buffer, 5 ml of Lysis binding solution concentrate and 100 µl of carrier RNA were mixed and afterwards 5 ml of 100% isopropanol was added. For the bead mix, 600 µl of bead resuspension solution, 400 µl of nuclease free water, as well as 400 µl of magnetic beads were well mixed, afterwards 600 µl 100% isopropanol was added. To Wash Buffer 1

concentrate 35 ml 100% isopropanol, as well as to the Wash Buffer 2 concentrate 80 ml 100% ethanol, were added to reach the working concentration. In order to perform the RNA extraction using the Kingfisher Flex Robot, following five 96-well plates were prepared: plate 1 (100 µl Lysis buffer and 20 µl of bead mix were added in each well); plate 2 (100 µl per well Wash Solution 1); plate 3 (100 µl per well of Wash Solution 2); plate 4 (100 µl per well of Wash Solution 2); plate 5 (50 µl per well of Elution buffer). Fifty µl of the clinical sample was added to plate 1 containing the Lysis buffer and the bead mix (well A1 to H12). A negative control replaced a clinical sample every 12 wells (sterile 1x PBS). The plates were placed in the KingFisher Flex in the given order (plate 1 to 5) and plate 5 was removed after finalization of the program containing the eluted RNA. Afterwards the RNA was transferred to a clean 1,5 ml tube and stored at -80 °C.

### **17.3. RNeasy® Protect Mini kit**

Total RNA from virus cell culture was purified using the RNeasy® Protect Mini kit (Qiagen), according to the manufacturers instructions. Buffers were prepared as follows: Lysis buffer: 10 µl beta-Mercaptoethanol per 1 ml RLT buffer; Wash buffer: 4 volumes of 100% ethanol were added to the RPE concentrate. The following protocol was used for 200.000 cells per well in a 24 well-plate. Cell culture supernatant was removed and cells were washed once with 500 µl 1x PBS. Afterwards 350 µl Lysis buffer (RLT + beta-Mercaptoethanol) was added to the cells, incubated for 1 min at RT and lysate was transferred to the QIAshredder spin column in a 2 ml centrifugation tube. Following centrifugation 2 min 13.000 rpm, the homogenized lysate was transferred to a gDNA eliminator spin column (included in the kit), placed in a 2 ml collection tube, centrifuged 1 min 13.000 rpm. 350 µl of 100% ethanol were mixed with the flow through and applied to the RNeasy-spin column in a 2 ml centrifugation tube and centrifuged 1 min 13.000 rpm. The column was afterwards washed with 700 µl RW1 buffer followed by two wash steps with 500 µl RPE buffer and finally dried by

centrifugation 1 min 13.000 rpm. RNA was eluted in a final volume of 35  $\mu$ l of distilled water and stored at  $-80^{\circ}\text{C}$ .

## 18. Reverse Transcription

During the Reverse Transcription, a single-stranded RNA template is reverse transcribed into a single stranded complementary DNA (cDNA) using the enzyme reverse transcriptase. Purified viral RNA was reverse transcribed for 80 min at  $50^{\circ}\text{C}$  using random primers and SuperScript III reverse transcriptase, brief work flow as shown below (all compounds were ordered at Invitrogen, Belgium). The resulting cDNA was afterwards used for PCR.

### Mix 1

Reagent	Volume ( $\mu$ l)	Concentration
Random primer	5	150 ng
dNTP mix	1	10 mM each
RNA	5	10 pg - 5 $\mu$ g
distilled water	1	

### Mix 2

Reagent	Volume ( $\mu$ l)	Concentration
DTT	2	5 mM
RNaseOUT™	0.5	20 units
5x First-Strand Buffer	4	1 x
SuperScript® III	1	200 units
distilled water	0.5	

Mix 1 was incubated 5 min at  $65^{\circ}\text{C}$ , afterwards kept on ice, supplemented with Mix 2 and incubated 5 min at  $25^{\circ}\text{C}$ . The Reverse Transcription was performed at  $50^{\circ}\text{C}$  for 80 min, followed by 15 min at  $72^{\circ}\text{C}$  for inactivation of the enzyme.

## 19. Polymerase Chain Reaction (PCR)

As the name implies, PCR is a chain reaction, where one DNA molecule is used to produce two copies, then four, then eight and so forth. This procedure amplifies double stranded PCR products, to quantify the presence of a specific DNA fragment, or to obtain sufficient DNA product for downstream applications. The reaction solution contains beside DNA molecules (to be copied), a set of oligonucleotides (forward and reverse primer, which specifically bind to a given sequence), a DNA-dependent-DNA-polymerase (which copies the DNA by starting at the forward primer and finishing at the reverse primer during multiple PCR cycles),  $MgCl_2$  (essential for enzyme activity and primer binding) and reaction buffer (ensuring the correct ionic strength and pH for the PCR). Each PCR cycle consist of the following three steps and is repeated up to 40 times: 1) Denaturation at 95°C (separates the double stranded DNA into single stranded molecules), 2) Primer Annealing usually at temperatures between 50-65°C (primers will bind specifically to designated positions on the single stranded molecules), 3) Elongation at 72°C (the polymerase will add further nts to the developing DNA strand, so copying the single stranded sequence between primers to a double stranded molecule; at the same time, any loose bonds that have formed between the primers and DNA segments that are not fully complementary are broken). Each time these three steps are repeated, the number of copied DNA molecules doubles and after 20 cycles about a million molecules are cloned from a single segment of double-stranded DNA. Normally, the result of the PCR is visualised using agarose gel electrophoresis.

In order to increase the sensitivity of the amplification, a nested or semi-nested PCR can be performed. In a nested PCR the first-round PCR product is used as template in a second PCR, with two new primers binding inside of the first-round product. Alternatively, in a semi-nested PCR only one primer is shifted (downstream for the forward primer or upstream for the reverse primer), whereas the second primer is unchanged.

Alternatively, by adding SYBRGreen<sup>®</sup> (a non-specific fluorescent dye that intercalates unspecific with any double-stranded DNA) (Invitrogen, Belgium) to the PCR reaction, it is possible to visualise the DNA amplification during each cycle and consequently simultaneously quantify the DNA; this method is called real-time PCR (RT-PCR). Other common methods to quantify specific DNA, are TaqMan<sup>®</sup> assays, they contain a third primer (probe) that is labelled with a fluorescent reporter and binds between the forward and reverse primers. During the elongation process, the DNA polymerase separates the initially non-fluorescent reporter from the probe, which then becomes fluorescent. Based on their high sequence specificity, TaqMan<sup>®</sup> assays are commonly used for diagnostic purposes.

### 19.1. MV genotyping PCR

The following PCR protocol was used for the MV genotyping first-round and nested PCR. For the first-round PCR: primer MN5 and MN6, Annealing at 55°C, five times diluted cDNA as template. For the nested PCR: primer Nf1a and Nr7a, Annealing at 58°C, 50 times diluted first-round product as template (Kremer et al., 2007, Santibanez et al., 2002). PCR reactions were performed on Opticon 2 (Biorad) thermocyclers.

#### PCR Mix

Reagent	Volume (µl)	Concentration
PCR Buffer (10x)	2.5	1x
MgCl <sub>2</sub>	0.91	1.8 mM
dNTP's	0.5	0.2 mM
primer fw	1	0.8 µM
primer rv	1	0.8 µM
SYBRGreen <sup>®</sup> (100x stock)	0.25	1x
Platinum Taq <sup>®</sup> polymerase	0.1	0.5 units
DNA template (diluted in distilled water)	5	
distilled water	13.74	

**PCR protocol**

Step	Temperature	Time	Cycle
Starting denaturation	94 °C	1 min 30 s	1x
Denaturation	94 °C	30 s	repeat 34 times
Annealing	55 °C or 58 °C	1 min	
Elongation	72 °C	1 min	
Final Elongation	72 °C	5 min	1x

According to the above described PCR setup all other RT-PCRs were performed, using different primers and annealing temperatures (details about primers please see chapter II, section 7). For further details please check the designated references.

**19.2. MV TaqMan<sup>®</sup> PCR**

The following TaqMan<sup>®</sup> assay was used for fast and highly sensitive MV detection of diverse specimens. As template five times diluted cDNA was used. PCR reaction was performed on a 7500 Fast Real-time PCR thermocycler (Applied Biosystems).

**TaqMan<sup>®</sup> Mix**

Reagent	Volume (µl)	Concentration
TaqMan <sup>®</sup> Fast Universal Master Mix (2x)	10	1x
MVTaqfw	1.8	0.9 µM
MVTaqrv	1.8	0.9 µM
MVTaqprobe	0.5	0.9 µM
DNA template (diluted in distilled water)	5	
distilled water	5.9	

**TaqMan<sup>®</sup> Fast PCR Protocol**

Step	Temperature	Time	Cycle
Starting denaturation	95 °C	20 s	1x
Denaturation	95 °C	3 s	repeat 44 times
Annealing and	60 °C	30 s	
Elongation			

## 20. Agarose gel electrophoresis

Agarose gel electrophoresis is used to separate DNA molecules by size. DNA molecules are negatively charged due to their high content of phosphates and migrate to the positively charged cathode, when they are exposed to an electric field (electrophoresis). Since agarose forms a tightly meshed structure, shorter molecules move faster and migrate farther than longer ones due to the sieving effect of the gel. To visualise the migration, the DNA was mixed with an ionic marker (Loading Dye 6x) which migrates as similar to a DNA molecule of 200 bp. In order to afterwards visualize the PCR products under UV light, SYBRSafe<sup>®</sup> (Invitrogen) (a dye which fluoresces only when bound to double stranded DNA) was added to the agarose gel.

Agarose gels (1.5%) were prepared by dissolving 1.5 g of powdered agarose in 100 ml of 1x TAE buffer using a microwave oven. Once completely dissolved, the mixture was allowed to cool to approximately 55°C, and 10 µl of SYBRGreen<sup>®</sup> were added and the liquid mixture was transferred into the casting form (14x12 cm) and the comb(s) were inserted (thickness of slots 1 mm). After 15 min the combs were removed from the polymerized agarose gel and the gel was transferred into the gel chamber. The gel was covered with 1x TAE running buffer. Before loading the DNA samples on the gel, 2 µl of 6x Loading Dye were mixed with 5 µl of PCR product. The gel was exposed for approximately 35-45 min to an electrical current of 130 V and images were taken after UV illumination at 300 nm wavelength with the InGenius Gel documentation system (Syngene).

## 21. Sanger sequencing

The dideoxynucleotide sequencing method that was used for de novo sequencing is based on the dye terminator method (Sanger sequencing). This technique utilizes 2',3'-dideoxynucleotide triphosphates (ddNTPs) molecules that differ from deoxynucleotides by having a hydrogen atom attached to the 3'

carbon rather than an OH-group. These molecules terminate the DNA chain elongation, since they cannot form a phosphodiester-bond with the next deoxynucleotide. Primer and DNA polymerase were mixed with dNTPs and a low concentration of fluorescently labelled, chain terminating dideoxynucleotides. Thus, these ddNTPs terminate DNA strand extension and result in DNA fragments of varying length. Each fragment terminates either with ddATP, ddCTP, ddGTP or ddTTP labelled with different fluorescent dyes (different wavelengths of fluorescence and emission). Using a poly-acrylamide gel the fragments are size-separated by capillary electrophoresis and at the end of the capillary the fluorescence is read with a laser. Sequences are assembled by comparing the size dependent order of appearance of fragments and the nucleotide specific fluorescence peaks (sequence electropherogram).

Prior the sequencing procedure, all samples were purified from residual primers and non-incorporated nucleotides using the Jetquick PCR product Purification Spin kit (Genomed). Briefly description of the method: 20 µl PCR product were mixed with H1 buffer (included in the kit), transferred to the Jet Quick Spin<sup>®</sup> column placed in a 2 ml collection tube and centrifuged 1 min at 10.000 rpm. The flow through was discarded and the column was washed with 500 µl H2 buffer (1 min at 10.000 rpm). The DNA was eluted in a final volume of 35 µl of TE buffer and stored at -20°C. Approximately 5-20 ng of DNA were required to sequence templates of 500 to 800 bp.

The sequencing PCR was performed using the BigDye Terminator<sup>®</sup> v3.1 Cycle Sequencing kit (Applied Biosystems) the and following protocol:

**Sequencing PCR reaction**

Reagent	Volume ( $\mu$ l)	Concentration
BigDye Terminator <sup>®</sup> Mix	1	1x
TE buffer	1.5	0.75
Primer fw	1	0.5 $\mu$ M
Primer rv	1	0.5 $\mu$ M
DNA template (diluted in distilled water)	max. 5	10 ng
distilled water	>0.5	
Total volume	10	

**Sequencing PCR protocol**

Step	Temperature	Time	Cycle
Denaturation	96 °C	1 min	repeat 25 times
Denaturation	96 °C	10 s	
Annealing	50 °C	5 s	
Elongation	60 °C	2 min	

Before sequencing the final PCR products, non-incorporated dyes were removed. All steps were performed in 96-well plates. So 5  $\mu$ l of 125 mM EDTA and 10 mM of distilled water were mixed with each sample and 60  $\mu$ l of 100% ethanol were added, samples were vortexed and incubated 15 min at RT in the dark. Afterwards the 96-well plate was centrifuged for 30 min at 3000 rpm and 4 °C. Subsequently, the ethanol was removed by flapping the plate on paper and additionally centrifuge for 60 s at 1000 rpm. The previous steps were repeated with 70% ethanol. Finally the plate was dried 15 min in a UNIVAP 150 H (UniEquip) and stored at 4 °C until use. For sequencing, samples were finally heated 5 min at 95 °C, complemented with 10  $\mu$ l HI-DI (Applied Biosystems) and again incubated 5 min at 95 °C and loaded on the capillary sequencer ABI PRISM<sup>®</sup> 3130 xl Genetic Analyzer (Applied Biosystems) (capillaries were 80 cm long).

## 22. Phylogenetic analysis

The SeqScape<sup>®</sup> program (Applied Biosystems) was used to convert the generated electropherograms into sequences, and individual sequences were combined to complete genes using a reference sequence (NCBI accession number: AF266291: MV Schwarz vaccine, complete genome). Sequences were imported into BioEdit (Hall, 1999) and further aligned using the internal algorithm ClustalW (Thompson et al., 1994). The MEGA 3 (Kumar et al., 2004) software was used to construct phylogenetic trees by the Neighbor-Joining method (Kimura 2-parameter or number of nucleotide differences) and the nucleotide distance was calculated.

A phylogenetic tree is a branching diagram showing the inferred evolutionary relationship for example among various viruses, based on nt differences among them. Sequences are linked by nodes (hypothetical ancestors or points of deviation) and connected by horizontal branches (length of lines is proportional to the genetic distance). Strains clustering on the same node belong to the same phylogenetic group.

The neighbour-joining method (Saitou & Nei, 1987) is a simplified version of the minimum evolution method, which uses distance measures to correct for multiple hits at the same sites and chooses a topology showing the smallest value of the sum of all branches as an estimate of the correct tree. The Bootstrap test was used to estimate the reliability of the calculated phylogenetic trees. For this bootstrapping, a tree is calculated on a sub-sample of the sites in an alignment. This computation is repeated multiple times ( $\geq 1000$ ) and the results allow estimating about the reliability of the particular cluster/group. The Bootstrap values are expressed as percentage, so high bootstrap values indicate significant nodes.

The Kimura 2-parameter model (1980) corrects the calculation by taking into account transitional and transversional substitution rates, while assuming that the four nt frequencies are the same and that rates of substitution do not vary among sites. This is one of the most widely used models and time-independent. The

number of substitutions between sequences usually reflects the evolutionary distance among sequences. Evolutionary distances are essential to study the molecular evolution of a virus.

### **23. 2D-DIGE Proteomics**

Two-dimensional Difference Gel Electrophoresis (2D-DIGE) is a special form of gel electrophoresis, commonly used to analyse proteins. The procedure consists of the following steps: sample preparation (cell lyses and protein purification), sample labelling (using up to three specific fluorescent dyes), sample fractionation (starts with separation in the first dimension based on the isoelectric points of the proteins, using isoelectric focusing; following the second dimension based on the molecular weight of the proteins, which is performed in an acrylamide gel), gel imaging and image analysis (using Typhoon scanner and Delta2D analysis software to identify differential expressed proteins) and finally spot picking and identification of differentially expressed proteins (using mass spectrometry).

Labelling proteins with fluorescent dyes prior to isoelectric focusing and SDS-PAGE allows detection and quantification of differences in protein abundance between different biological samples within one single gel (Unlu et al., 1997). Special charge- and size -matched cyanine CyDye™ DIGE fluor minimal dyes (Cy2, Cy3, Cy5) that react over an NHS-ester group with  $\epsilon$ -amino residues of lysine are commonly used for protein labeling. The three different CyDyes add approximately 450 Da to the protein mass. With this procedure approximately 3% of the available proteins are labeled (only on a single lysine per protein). In order to reduce to experimental gel-to-gel variation a pooled internal standard comprises of equal amounts of each sample is used.

The practical work concerning the following proteomics parts, as well as the results shown in Chapter III part II were performed together with Dr. Anja Billing

and Dominique Reverts from the Proteomics platform at the Institute of Immunology.

### **Protein extraction and CyDye labeling**

Treated cells were two times washed with ice cold 1x PBS, scrapped with a cell scraper in a final volume of 1 ml 1x PBS, transferred into a 1.5 ml tube. After centrifugation the pellet was stored at -80°C until parallel protein extraction. Protein extraction was performed for 30 min at RT in 150 µl lysis buffer (pH 8.5) containing 7 M urea, 2 M thiourea, 30 mM Tris, 4% CHAPS, protease inhibitors and nuclease mix. Subsequently proteins were acetone precipitated with 8 volumes ice-cold acetone over night at -20°C and washed with ice-cold 90% acetone/DDW. Protein was resuspended in 50 µl lysis buffer and quantified using the 2D Quant kit (GE Healthcare).

Protein samples and internal standard were labeled with CyDye™ Fluor minimal cyanin dyes (GE Healthcare) prior 2D gel electrophoresis according to standard protocol and as described previously (Billing et al., 2010). Briefly, 50 µg of protein per sample was labeled with 400 pmol CyDyes™ (GE Healthcare). Labeling was performed on ice for 30 min with pH adjusted (pH 8.5) protein samples. Lysine (10 mM) was used to quench the labeling reaction. We generated two internal standards, one for each time point. Therefore, 25 µg of all protein samples per time point was combined and labeled with Cy2. Biological triplicates were labeled with Cy3 or Cy5. Labeled samples were pooled (Cy2, Cy3, Cy5) and separated by 2D-DIGE. One gel for each time point was spiked with 200 µg unlabeled protein mix of MV infected cells to enable protein identification.

### **2D gel electrophoresis**

Immobiline DryStrips (GE Healthcare, 24 cm pH 3-7 NL) were rehydrated overnight with combined samples (Cy2, Cy3, Cy5) in 7 M urea, 2 M thiourea, 4% CHAPS, 13 mM DTT, 1% IPG buffer, traces of bromophenol blue in a total volume of 450 µl. Isoelectric focusing was carried out on an Ettan II (GE Healthcare) using the following protocol constant 300 V over 4 h, gradient to

1000 V over 4 h, gradient to 8000 V over 4 h and final focusing at 8000 V for 8 h. The cysteine sulfhydryl groups were reduced and carbamidomethylated with 10 mM DTT and 55 mM iodoacetamide for 15 min at RT. IPG strips were placed on top of 12% self-cast polyacrylamide gels and overlaid with 0.5 % agarose. SDS-PAGE was carried out on an Ettan DALTtwelve (GE Healthcare) at 30°C with 2 W per gel for 30 min and 4 W per gel until the bromophenol blue front left the gel. 2D DIGE gels were scanned on a Typhoon 9400 (GE Healthcare) directly between glass plates in a 16-bit TIFF file format with a resolution of 100  $\mu$ m using excitation/emission wavelength of 488/520 nm for Cy2, 532/580 nm for Cy3 and 633/670 nm for Cy5. Preparative gels backed on bind silane-treated glass plate were post-stained with LavaPurple (GelCompany). Gels were scanned with a resolution of 100 micron using 633/670 nm as excitation/emission wavelength.

### **Image analysis**

Images were analyzed with Delta2D v.4.0 (Decodon). We generated two projects; one for the 12 h and one for 32 h time point. All images belonging to the same project were aligned with the DIGE compatible in-gel standard warping method. This defines the best Cy2 image as a master to which all other Cy2 images are merged. A few vectors were set manually prior automatic match vector finding. Warping was evaluated and approved. Images with the best resolution were selected for generation of a fusion image, which contains all spots in the project. This fusion was used for automated spot detection. After evaluation and editing the spot pattern was transferred to all images. Quantitative analysis of protein expression based on normalized spot volumes (after background subtraction and normalization to the internal standard) was performed with student's t-test. Spots with a p-value  $\leq 0.05$  were considered to be significant different. Data are represented as fold changes for each treatment in comparison to the mock-infected control.

**Protein identification**

LavaPurple-post stained preparative gel images were included into the Delta2D projects and aligned to its corresponding Cy2 gel internal standard. Significant spots were selected and automatically excised, in-gel digested with trypsin and extracted peptides were spotted by Ettan Spot handling Workstation (GE Healthcare) and analyzed by ABI 4800 Proteomics Analyzer (Applied Biosystems). Proteins were identified using MASCOT by searching against the UniProt database (release 57.15, 02-Mar-2010). Protein scores greater than 65 were significant. All searches were carried out with a tolerance of 150 ppm for the precursor ion and 0.75 Da for fragment ions. Carbamidomethyl was set as fixed modification and oxidation of methionine as variable modification. A maximum of 2 missed cleavages were allowed.

Spot picking and protein identification was mainly performed by the Proteomics Service Centre at the CRP-Gabriel-Lippmann, therefore experimental details are not described.

**Bioinformatic pathway analysis**

Proteomic data sets were analyzed by Ingenuity Pathway Analysis. (Ingenuity® Systems, [www.ingenuity.com](http://www.ingenuity.com)). Functional module analyses were performed using data sets containing gene identifiers and corresponding expression values and functional groups were defined based on information contained in the Ingenuity Pathways Knowledge Base.

## **Chapter III**

---

## **Results and Discussion**

---

**Part I**

---

**Genetic and Phenotypic characterisation of various MV strains**

---

Manuscript of part I is submitted as:

*Interplay of measles virus with early induced cytokines reveals different wild type phenotypes.*

J. R. Kessler, J. R. Kremer, C. P. Muller

Differential effects of MV on the innate immune response may influence virus spread and severity of disease. Type I interferons (IFN) and IFN-response genes including 2',5'-oligoadenylate-synthetase (2-5AS) and myxovirus-resistance A (MxA), are essential mediators of the innate immune response against viral infections (Haller et al., 2007, Sadler & Williams, 2008) Viral RNA sensing by different host cell receptors, including RNA-helicases like retinoic acid inducible gene I (RIG-I), mediates the expression of inflammatory cytokines and

chemokines like IFN-alpha/beta, TNF-alpha, IL-1 beta, IL-6, IL-8, MCP-I or RANTES (Liao et al., 2008, Poeck et al., 2010, Wang et al., 2008, Wu et al., 2010). MV has been shown to induce IFN via different mechanisms: MV-N protein recognition by IRF-3; detection of MV 5`-triphosphate RNA or specific defective interfering RNA molecules (diRNA) by RIG-I (Plumet et al., 2007, Shingai et al., 2007, tenOever et al., 2002). These 5`copy-back diRNA molecules that have been intensively studied in Sendai virus and Vesicular stomatitis virus, are subviral replicons generated spontaneously during virus replication, due to an error of the polymerase complex. DiRNAs often represent only minor parts of the virus genome and are therefore only replicated in cells infected with the parent virus (Barrett & Dimmock, 1986, Enami et al., 1989, Marcus & Sekellick, 1977). MV has also the ability to suppress the innate immunity. Especially the P/C/V locus has been associated with host immune evasion, by prevention of IFN-biosynthesis (Childs et al., 2007, Pfaller & Conzelmann, 2008) or by interfering with IFN-signalling (Takeuchi et al., 2003a, Yokota et al., 2003).

Different MV genotypes are endemic in most areas with high mortality rates. Mortality is mainly caused by secondary infections, facilitated by an immunosuppression. Differences in mortality rates are usually attributed to specific host factors and poor supportive care. However, the pathogenicity of different strains or genotypes has never been systematically compared.

Here we compare for the first time 22 MV strains, representative of most circulating genotypes (n=14), for their ability to interfere with the early immune response of different host cells. We found that MV wt strains significantly differ in their sensitivity to type I IFN and their ability to induce this and other cytokines largely depends on the apparently haphazard induction of diRNA.

## 1. Results

### 1.1. MV wt strains are highly variable in their sensitivity to IFN-alpha

MV was grown in the presence of IFN-alpha on IFN-deficient Vero/hSLAM cells and virus titers were compared to cultures without IFN-alpha treatment. Virus proliferation of all 22 MV strains was reduced in the presence of IFN-alpha (Figure 9), but viruses differed considerably in their sensitivity to this cytokine. Three wt strains (MV112, MV022, MV705) produced only 1.5 to 2.1 times less infectious virus in the presence of IFN-alpha ( $p > 0.05$ ). Seven wt strains (MV801, MV035, MV407, MV409, MV034wt, MV326, MV336, and MV030) showed an intermediate sensitivity with 3.5 to 11.6-times lower TCID<sub>50</sub>/ml ( $p < 0.05$ ) in IFN-alpha treated cultures. The remaining wt viruses (MV005, MV215, MV033wt, MV335 and MV032wt) exhibited a high sensitivity to IFN-alpha treatment, with a 25 to 47-fold reduction in virus production ( $p < 0.05$ ). Virus titers obtained with Vero cell adapted (VCA) strains were in all cases lower (~2-fold), than those produced by their parental wt strains, but for each virus differences were not statistically significant (Figure 9). Clade A strains showed low (Schwarz) or intermediate (Edmonston-wt and Hallé) sensitivity to IFN-alpha. Some wt strains were more while others were less sensitive than the Schwarz vaccine and other clade A strains. Thus it was not possible to distinguish between vaccine and wt strains on the basis of their sensitivity to IFN-alpha treatment and Vero cell adaptation essentially did not change the sensitivity to IFN-alpha.

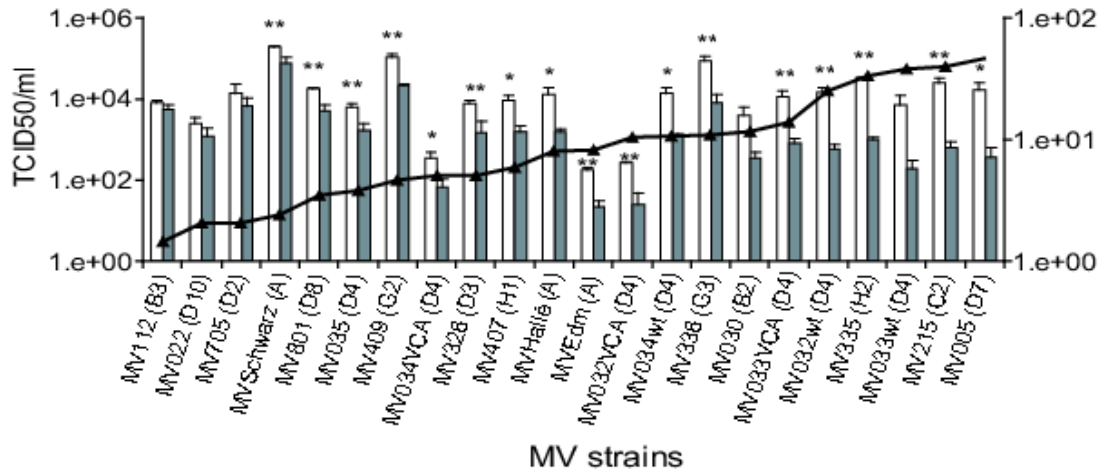


**Figure 9: MV production in IFN-alpha treated or un-treated Vero/hSLAM cells.**

MV production (TCID<sub>50</sub>/ml) in IFN-alpha treated (grey bars) or un-treated (open bars) Vero/hSLAM cells (MOI:0.0025) 48h p.i. (left y axis). MV sensitivity (black line and ▲) to type I IFN was defined as fold-decrease in viral titer, compared to untreated cultures (right y axis). Viruses are sorted by increasing sensitivity to IFN-alpha. Values represent means and standard errors of three biological replicates. Statistically significant differences are indicated by asterisks (Students t test: \*, p<0.05; \*\*, p<0.01). Genotypes are indicated in brackets behind the strain designation.

## 1.2. No sequence motif in the P/C/V-locus can be associated with the sensitivity to IFN-alpha

MV-P, V and C proteins have previously been associated with inhibition of IFN-signalling. Simultaneous amino acid (aa) mutations in the PNT region (Y110H) and the VCR region (C272R) of the V protein reverse their capacity to inhibit IFN signalling (Caignard et al., 2009, Ohno et al., 2004). Therefore complete P-genes, encoding the three proteins P, C and V were sequenced to assess, whether specific sequence motifs were associated with a high or low sensitivity to IFN-alpha treatment. The maximum aa diversity in P, C and V proteins of the 22 MV strains, was 10.1%, 7.5% and 11.4% respectively. None of the strains had

any of the above mutations, and no other sequence motif in the P/C/V-locus was preferentially associated with strains showing high or low sensitivity to IFN- $\alpha$ . Nevertheless, three characteristic aa substitutions were identified in the P and V protein (K/N51R, S83P and E225G) and one in the C protein sequence (R/M44G) of clade A strains compared to wt strains. The VCA strains MV032VCA and MV033VCA differed by one (V112A) and two (S63P and S66P) aa from their parental wt strains in the P and V proteins, as well as by F105L (MV032VCA) and V50A and V73A (MV033VCA) in the C protein. No aa difference in any of the three proteins was found between MV034VCA and its parental wt strain (MV034wt). Characteristic mutations in clade A or VCA strains may well be associated with their attenuated phenotype, but did not correlate with their sensitivity to IFN- $\alpha$ .

### **1.3. MV wt strains are low IFN-beta inducers unless they express diRNA**

We further investigated whether viruses that are sensitive to type I IFN avoid inducing this cytokine. Between <2.5 IU/ml (detection limit) and 750 IU/ml of IFN- $\beta$  was detected in the supernatant of MV infected A549/hSLAM cells 48h p.i. (Figure 10a). All clade A strains induced >600 IU/ml of IFN- $\beta$ . Two VCA strains (MV32VCA and MV34VCA) and the three wt strains MV112, MV035 and MV407 induced >250 IU/ml. All other wt strains induced <210 IU/ml of IFN- $\beta$ . Since it was previously shown that MV diRNAs are strong IFN- $\beta$  inducers (Shingai *et al.*, 2007) all strains were screened for these subviral replicons. DiRNA was detected only in A549/hSLAM cultures of two VCA strains (MV32VCA and MV34VCA) and three wt strains (MV112, MV035 and MV407) (Figure 10b i). MV034VCA and MV032VCA induced about four times ( $p < 0.001$ ) more IFN- $\beta$  than their parental, diRNA-negative wt strains, whereas MV33VCA, which remained negative for diRNA, induced 3.4 ( $p < 0.001$ ) times less

IFN-beta than the parental wt strain. The intensity of the corresponding bands in agarose gels, correlated with the concentration of IFN-beta in the culture supernatant (Figure 10a and b i).

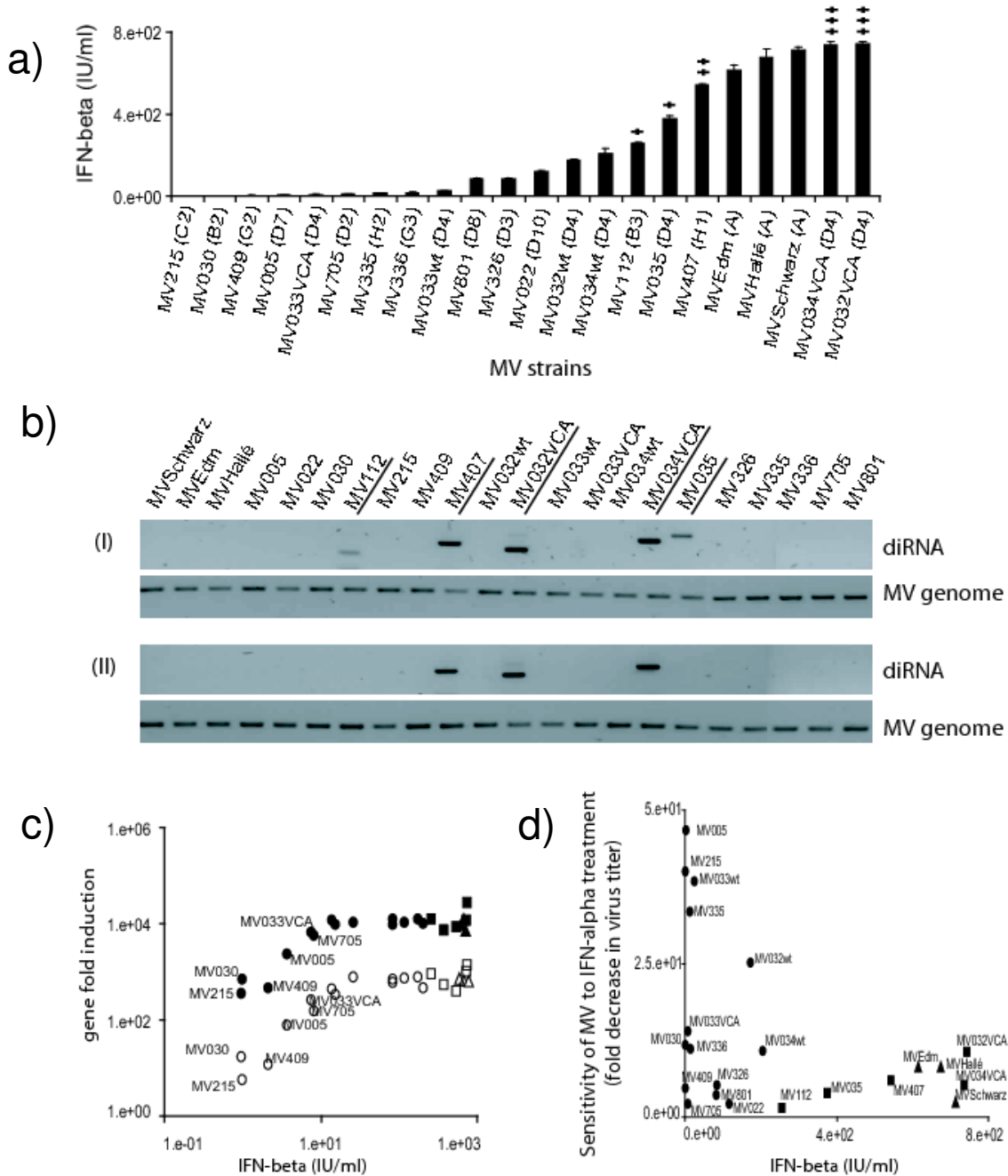


Figure 10: Effects of MV on host cells. Detailed figure legend please see next page.

**Figure 10: (see previous page). Effects of MV on host cells.**

a) Induction of IFN-beta in MV infected A549/hSLAM cells 48h p.i. (MOI:0.05). DiRNA carriers are marked with + (representing the amount of diRNA in agarose gel in Figure 10b I). Data are sorted by increasing IFN-beta induction. Values are expressed as mean and standard error of three biological replicates. Strain designation as in Figure 9. b) 5`copy-back diRNA in MV strains propagated on (I) A549/hSLAM or (II) Vero/hSLAM cells. DiRNA carriers are underlined. c) Fold induction of IFN response genes (MxA, closed symbols; 2-5AS, open symbols) in MV-infected A549/hSLAM cells normalizing against the housekeeping gene beta actin. ▲, clade A strains; ●, wt strains; ■, diRNA positive strains. IFN-beta levels measured in the supernatant of the same experiments are shown on the x-axis. d) Comparison of the sensitivity of MV to IFN-alpha treatment (measured in Vero/hSLAM) and the induction of IFN-beta in MV infected A549/hSLAM cells. ▲, clade A strains; ●, wt strains; ■, diRNA positive strains. Values are expressed as mean of three biological replicates.

DiRNAs were also detected in the stocks of MV strains (grown on Vero/hSLAM cells), which induced high levels of IFN-beta (MV032VCA, MV034VCA and MV407), whereas all other stocks were negative for diRNAs (Figure 10b II). Some of the other wt strains, inducing intermediate levels of IFN-beta, may express diRNAs below the limit of detection, but even after multiple passaging these strains did not necessarily induce detectable levels of diRNA (compare MV033wt and MV034wt in Figure 10a, Table 7).

In the same experiments the expression of type I IFN-inducible genes were also determined (Figure 10c). Up to 10 IU/ml IFN-beta the expression of MxA and 2-5AS increased with IFN-beta concentration, before reaching a plateau above 10 IU/ml. Several wt strains as well as the diRNA negative VCA strain (MV215, MV030, MV409, MV005, MV033VCA and MV705) triggered levels of IFN that induced low or sub-maximal levels of both response genes.

When the sensitivity to type I IFN of strains was compared with the level of IFN they induced, strains with a high sensitivity induce only low amounts of IFN (Figure 10d). On the other hand both strong and weak inducers were found among viruses with low or intermediated sensitivities.

Thus, the high levels of IFN-beta induced by clade A strains seemed to be independent of diRNAs, whereas wt strains induce high levels of IFN only in the presence of diRNA.

#### **1.4. MV wt strains induce significantly lower levels of cytokines than clade A strains, provided they are negative for diRNA**

In the above experiment on A549/hSLAM cells, diRNA positive strains (including the two VCA strains) also induced significantly more RANTES (26.8 fold), IL-6 (24.8 fold), IL-8 (3.2 fold), MCP-I (4.5 fold), TNF-alpha mRNA (21 fold) and IL-1 beta mRNA (14.3 fold) than diRNA negative wt strains ( $p < 0.005$ ) (Figure 11). On average diRNA positive strains did not induce significantly higher levels of the above cytokines than clade A strains. Wt in comparison to clade A strains induced significantly lower levels of IL-6 (13.5 fold), RANTES (37.3 fold), MCP-I (4.14 fold) and TNF-alpha mRNA (6.7 fold) ( $p < 0.005$ ). IL-8 and IL-1 beta mRNA inductions were also lower with wt strains, but the differences were not statistically significant.

Thus, in general wt strains induced low or undetectable levels of all cytokines, whereas clade A and diRNA positive strains (wt and VCA) induced intermediate or high levels.

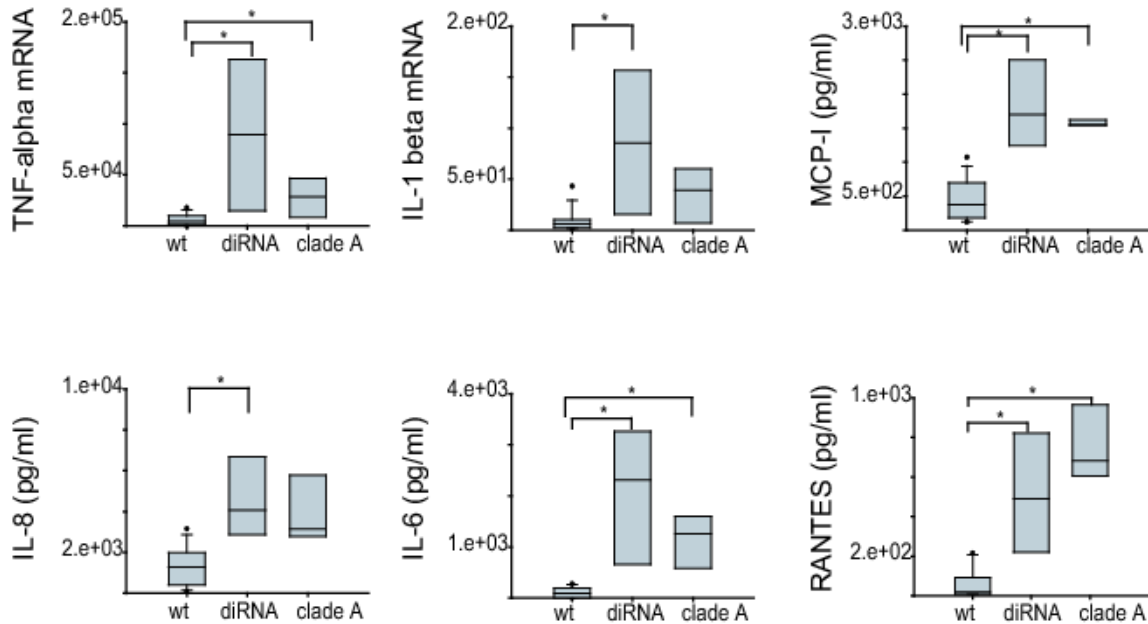


**Figure 11: Detection of RANTES, MCP-I, IL-8, L-6, TNF-alpha and IL-1 beta in MV infected A549/hSLAM cells.**

Detection of RANTES (pg/ml), MCP-I (pg/ml), IL-8 (pg/ml) and IL-6 (pg/ml) in the supernatant of MV infected A549/hSLAM cells (MOI:0.05). TNF-alpha and IL-1 beta are shown as fold induction of mRNA. MV strains are shown on the x axis: wt: all wt strains (negative for diRNA); diRNA: all strains positive for diRNA (wt and VCA); clade A: all strains from genotype A. Mann-Whitney rank sum test: \*, p<0.05)

### 1.5. DiRNA induce TNF-alpha expression during early MV infection in Vero cells

In our previous experiment (Figure 9, open bars) we showed that diRNA positive VCA strains produced much less virus than their diRNA negative parental wt strains. This suggests that in IFN-deficient Vero/hSLAM cells diRNA activates an antiviral mechanism that is independent of IFN, such as TNF-alpha (Herbein & O'Brien, 2000, Shingai et al., 2007, Wang et al., 2008). We compared the induction of TNF-alpha in Vero/hSLAM cells infected with diRNA positive or

negative MV stocks as an alternative antiviral mechanism at an early time point of infection (Figure 12). The diRNA positive strains induced up to 540-fold more TNF-alpha ( $p < 0.05$ ), than their diRNA negative counter parts. Thus, in Vero/hSLAM cells only diRNA positive strains induced significant levels of TNF-alpha already early during infection.

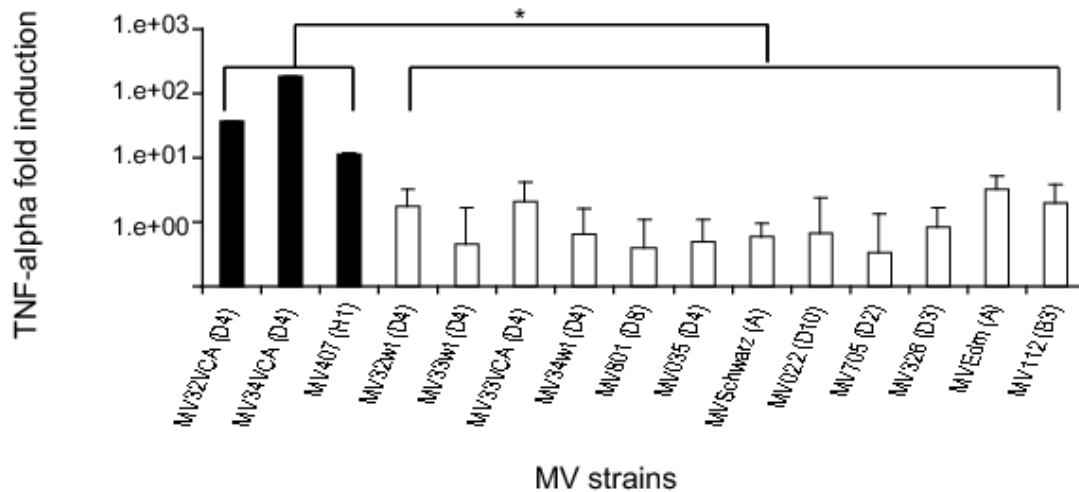


**Figure 12: mRNA expression level of TNF-alpha in MV infected Vero/hSLAM cells**

(MOI:0.05). DiRNA positive strains are indicated as closed bars; diRNA negative strains as open bars. Values are expressed as mean plus standard error of three biological replicates. Mann-Whitney rank sum test \*,  $p < 0.05$ ). Strain designation as in Figure 9.

## 1.6. Multiple passaging induces diRNA in MV culture

To investigate whether diRNA formation is influenced by IFN-competency/IFN-deficiency or whether SLAM expression affects this, three MV strains (MV032wt, MV033wt and MV034wt) were passaged ten times on type I IFN-deficient, SLAM-negative (Vero) or SLAM-positive (Vero/hSLAM), as well as IFN-competent SLAM-positive A549/hSLAM cells (Table 7). DiRNAs emerged during passaging, irrespective of the cell line, but not in all virus strains. MV032wt remained negative for diRNA both on Vero/hSLAM and A549/hSLAM cells, although diRNA

developed on Vero cells. DiRNA positive virus MV034VCA continued to express similar levels of diRNA throughout five additional passages in all three cell lines, showing that diRNA positive MV continues to be produced even in IFN-competent A549/hSLAM cells. The MV Schwarz strain developed a single diRNA in passages  $\geq 9$  on Vero/hSLAM cells, but remained negative on A549/hSLAM cells. The sizes of these diRNAs were calculated as described before (Shingai et al., 2007) (Table 8). Partial diRNA sequences showed that the switch of the MV polymerase from the positive to the negative strand RNA occurred in different positions, despite identical sequences of MV032VCA and MV034VCA in this region (Figure 13).

**Table 7: DiRNA production in MV strains passaged on Vero, Vero/hSLAM and A549/hSLAM cells**

Strain	Cell line	No of passages	diRNA in passage	Intensity of diRNA in agarose gel
MV032wt	Vero	10	$\geq 8$	+++
	Vero/hSLAM	10	not detected	-
	A549/hSLAM	10	not detected	-
MV033wt	Vero	10	not detected	-
	Vero/hSLAM	10	$\geq 7$	+++
	A549/hSLAM	10	$\geq 7$	+++
MV034wt	Vero	10	2 and 4 to 7 (multiple size) $\geq 8$ single size	++ +++
	Vero/hSLAM	10	$\geq 8$ multiple size	++
	A549/hSLAM	10	not detected	-
MVSchwarz	Vero/hSLAM	10	$\geq 9$	+
	A549/hSLAM	10	not detected	-
MV034VCA (diRNA positive)	Vero	5	$\geq 1$	+++
	Vero/hSLAM	5	$\geq 1$	+++
	A549/hSLAM	5	$\geq 1$	+++

+: intensity of diRNA in agarose gel, -: no diRNA detected

**Table 8: Characteristics of MV 5' copy-back diRNAs**

<b>MV name (genotype)</b>	<b>diRNA size (nt)</b>	<b>Stem size (nt)</b>	<b>Loop size (nt)</b>	<b>Jump point position (nt)</b>
MV032VCA (D4) p8 to 10	461	131	199	15763
MV034VCA (D4) p8 to 10	533	136	261	15758
MV034VCA (D4) p4 to 7	1204	190	824	15704
MV034VCA (D4) p2,4 to7	755	210	335	15684
MV035 (D4)	581	214	153	15680
MV112 (B3)	408	136	136	15758
MV407 (H1)	504	103	298	15790

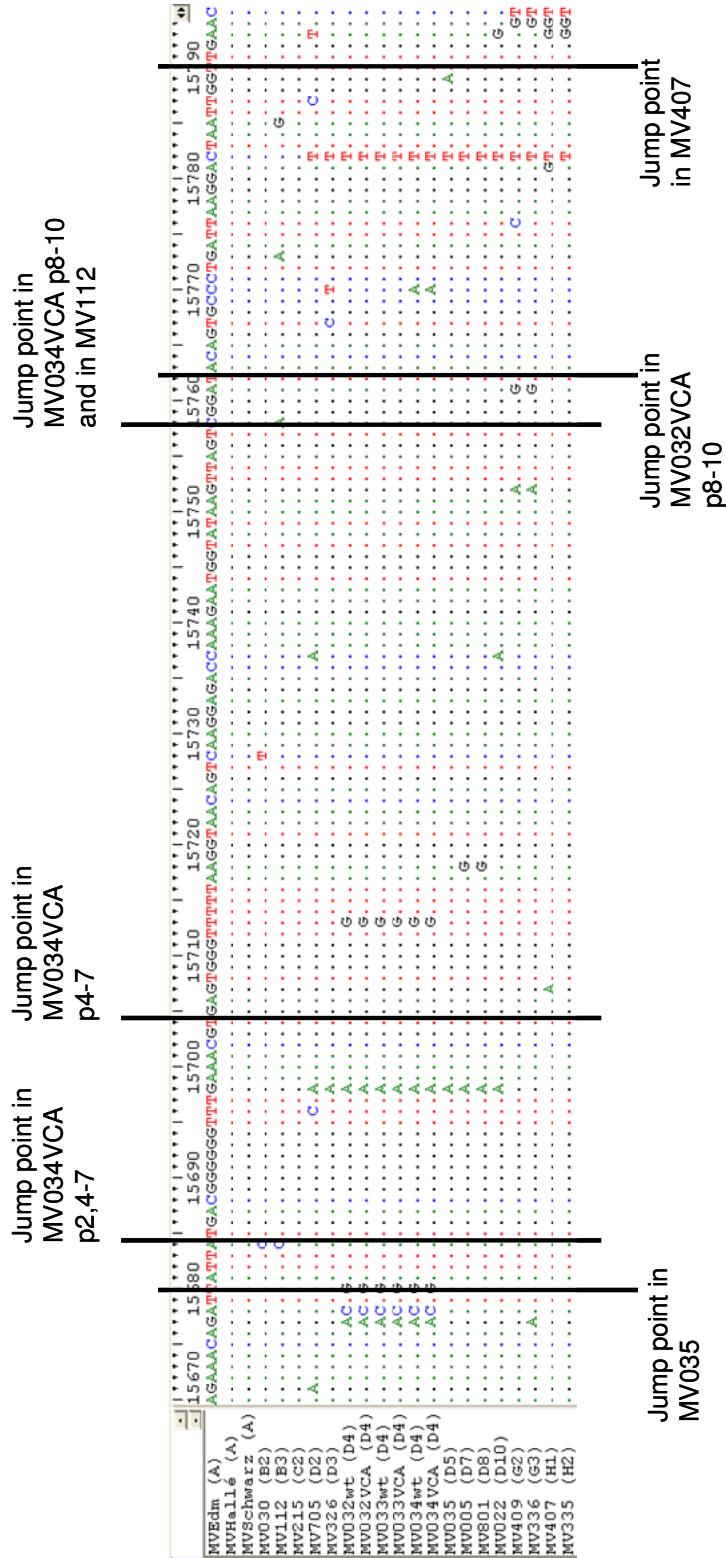


**Figure 13: MV genome nt positions 15670 to 15795 of MV strains used in this study.** Polymerase jump points are marked with black lines. Sequences have been submitted to NCBI, accession numbers are FN687774 - FN687795.

## 1.7. Clinical samples do not contain diRNA

To investigate whether such subviral replicons are also produced during natural MV infection, 64 clinical samples (PBMCs, oral fluid, throat swab or urine) from patients infected with either one of the 4 different genotypes B3, C2, D4 or D6 were analyzed. No diRNA was detected in any of the clinical specimens, suggesting that diRNA positive MVs are generated only during multiple passaging in cell culture (data not shown).

## 2. Discussion

The interplay between MV and type I IFN has been investigated in a number of studies (Caignard et al., 2009, Fontana et al., 2008, Naniche et al., 2000, Ohno et al., 2004). However, most of these studies compared differences between MV vaccine and a few wt strains. This is the first study of a broad set of MV wt strains, including at least one representative of each clade, and 14 of the 19 currently circulating genotypes.

We showed for the first time that MV wt viruses differ significantly in their sensitivity to type I IFN. Some wt strains were more, whereas others were less sensitive to IFN-alpha than vaccine strains. Thus, using a large panel of wt strains our observations reconcile earlier reports that wt strains are more sensitive to IFN-alpha than vaccine strains (Naniche et al., 2000), with those that reported the opposite (Ohno *et al.*, 2004). Considering that also vaccine strains differ in their sensitivity to type I IFN, previous results probably reflect differences between individual strains, rather than differences between attenuated and wt virus in general. The D7, C2 and one D4 strain were the most sensitive wt strains to IFN, whereas the B3 strain was least sensitive to IFN-alpha. Interestingly, this seems to agree with *in vivo* pathogenicity studies in rhesus macaques, where a B3 strain was more pathogenic than a C2 strain (El Mubarak et al., 2007).

Although sensitivity to IFN- $\alpha$  does not seem to be associated with attenuation of vaccine strains, this may nevertheless account for differences in pathogenicity between wt strains. However, this can only be confirmed by animal experiments.

It has been suggested that the sensitivity of MV strains to IFN correlates to some extent with the capacity of their P, C and V proteins to interplay with IFN biosynthesis and signalling (Caignard et al., 2009, Fontana et al., 2008, Naniche et al., 2000, Ohno et al., 2004). Nevertheless, in this study no sequence motif in the MV-P gene was preferentially associated with a high or low sensitivity to IFN- $\alpha$ , in particular none of the mutations associated with impaired inhibition of the JAK/STAT signalling (Caignard et al., 2009, Ohno et al., 2004).

We also showed that MV strains considerably differ in their ability to induce type I IFN, IL-6, IL-8, RANTES, MCP-I, TNF- $\alpha$  and IL-1 beta. While clade A, as well as diRNA positive wt and VCA strains induced high levels of these cytokines, diRNA negative wt strains induced only low levels. This reconciles earlier *in vitro* and *in vivo* findings that MV induces the latter cytokines (Helin et al., 2001, Sato et al., 2005, Schneider-Schaulies et al., 1993, Xiao et al., 1998), with those reporting the opposite (Haspolat et al., 2001, Ichiyama et al., 2006, Manchester et al., 1999, Naniche et al., 2000, Saruhan-Direskeneli et al., 2005) and which did not test for diRNA. In contrast to (Shingai et al., 2007) we did not detect diRNA in our Edmonston-wt and Schwarz isolates, probably because of differences in passage history and sample sources. It was suggested before that MV wt strains actively suppress IFN- $\beta$  induction, rather than failing to activate this cytokine (Childs et al., 2007, Nakatsu et al., 2008). Our findings suggest that this is only true for diRNA independent type I IFN induction, which is in line with the results from Naniche and colleagues (Naniche *et al.*, 2000).

In our hands diRNA was not required for clade A strains to induce high levels of IFN- $\beta$ . In contrast, wt strains did not induce IFN- $\beta$  in absence of diRNA. Thus mechanisms of IFN induction such as binding of uncapped MV triphosphate leader RNA to RIG-I or the direct interaction of nucleoprotein with IRF-3 are only pivotal in vaccine strains (Plumet et al., 2007, tenOever et al., 2002).

It has been suggested that adaptation of wt MV to Vero cells is sufficient, to change their phenotype from a non-inducing into a type I IFN-inducing strain (Naniche et al., 2000). In our hands only viruses that produced diRNA were able to induce IFN-beta and other cytokines. At least one strain (MV033VCA) was adapted to Vero cells, but did not induce diRNA or any of the measured cytokines. Thus cytokine induction seems to be a marker of diRNA rather than of Vero cell adaptation. It would thus be interesting to understand whether the attenuated phenotype of VCA strains depends on diRNA induced cytokines alone or whether other mechanisms are involved and whether diRNA negative VCA strains are closer to the wt or the vaccine phenotype of MV *in vivo*.

Among 64 samples from measles patients infected with either one of four different MV genotypes, no diRNA was detected. Nevertheless, it has been shown that brain cells of SSPE patients can contain MV-specific diRNA (Sidhu et al., 1994). Hence the generation of diRNAs seems to be a rare event in the course of natural measles infections in humans. Since diRNA carriers would induce a stronger innate immune response and consequently a more rapid viral clearance, these would have a selective disadvantage over diRNA negative strains (Barrett & Dimmock, 1986, Roux et al., 1991). Indeed, diRNA positive VCA strains produced significantly less infectious virus than their parental wt strains even in IFN-deficient Vero/hSLAM cells. In absence of type I IFN another mechanism must be responsible for reduced virus production. As reported here, the early expression of TNF-alpha in Vero/hSLAM cells and the strong induction of TNF-alpha in A549/hSLAM cells infected with diRNA positive MV, supports this hypothesis.

In conclusion, using a large panel of representative MV strains we found that both wt and vaccine strains differed considerably in their sensitivity to type I IFN and in their ability to induce IFN, TNF-alpha and other cytokines and that this variations may relate to differences in pathogenicity of wt viruses that were previously observed in monkeys. Some wt strains that were highly sensitive to IFN induced only suboptimal levels of cytokines. *In vitro*, in particular wt strains that produced diRNA, induced high levels of cytokines that otherwise were only

reached by vaccine strains. During acute measles diRNA was not detectable, but these subviral replicons were an important confounding parameter in passaged wt viruses which must therefore be carefully assessed in all *in vitro* studies.

**Part II**

---

**Proteome profiling of Measles Virus host interaction in  
human lung cells  
comparing wild type and attenuated strains**

---

Manuscript in preparation

Monitoring molecular changes within an infected host cell are key components in understanding biological events following a viral infection. The MV life cycle can be divided into different processes: virus entry and replication, virus interplay with cellular stress response and antiviral activity and finally assembling and budding of the virion from the host cell membrane. In the last years great efforts have been made to reveal mechanisms of MV host cell interactions. Nevertheless, the molecular bases of the interplay of MV with the innate immune response are only partially understood. In particular differences among various wild-type (wt) strains as well as wt compared to vaccine strains are discussed.

In contrast to basic virology research, only a few studies investigated viral-host interactions using a proteomic approach. Investigations regarding abundant changes in cellular proteins could help to characterize the physiological status of

an infected cell, highlighting new pathways involved in the viral life cycle or the antiviral response of the host cell.

In this study we describe the effects of MV infection on the proteome of human alveolar lung cells at different time points after infection, to especially explore changes in the protein profile induced by different MV strains. Main changes were found in proteins grouped as cytoskeleton, chaperones/stress response, metabolism, transcription/translation, immune response and mitochondria. Mostly structural proteins and proteins involved in stress response as well as in protein folding were affected.

## **1. Results**

### **1.1. Experimental design**

Since MV enters the human body via the respiratory route, human A549/hSLAM cells, a human lung carcinoma cell line that retains features of alveolar cells, was chosen to assess the effects of different MV strains on the host cell proteome. In the literature many discrepancies are found describing the characteristics of vaccine and wt MV strains (Naniche et al., 2000, Ohno et al., 2004) In this study, we used a common attenuated vaccine strain (MVSchwarz), two freshly isolated wt strains (MV34wt, MV37wt) and one Vero-cell adapted (VCA) strain (MV34VCA) that was passaged 10 times on SLAM-negative Vero cells. Three of the four MV strains have been intensively characterized in previous experiments (Table 9) (please see Chapter III Part I). In contrast to wt strains that mostly induced a weak cytokine response during 48 h p.i., both the vaccine and the VCA strain caused a high cytokine expression in infected cells. The presence of diRNA in the inoculum of the MV34VCA strain was correlated with the high cytokine response, whereas these subviral replicons were not detected in any

other strain used in the present study. Thus, our experimental design allowed to make the following comparisons: i) vaccine versus wt, ii) wt versus wt, iii) wt versus diRNA positive VCA strain and iv) vaccine versus diRNA positive VCA strain during early (12 h) and late (32 h) phase of the infection. Treatments with IFN-beta (IFNB) served as a positive control. Previously it has been shown that during the selected time points live or UV-inactivated MV strains do not differ in their effects on the cellular proteome (van Diepen et al., 2010). Thus we used live replicative MV strains for our experiments. Although viral cytopathic effects were visible at 32 h p.i. cells retained their viability.

**Table 9: Characterization of MV strains used in this study**  
(Kessler et al. 2010 in preparation\*)

strain name	diRNA	cytokine induction	CPE formation 32 h p.i.	passage history
MVSchwarz	no	++	++	attenuated vaccine strain
MV34wt	no	+	++	2x on Vero/hSLAM
MV37wt	no	nt	+++	2x on Vero/hSLAM
MV34VCA	+++	+++	+	10x on Vero

\* strain MV37wt was not included in this study, nt: not tested, +: indicates the intensity

The practical work concerning the following proteomics part as well as the protein identification was performed together with Dr. Anja Billing and Dominique Reverts from the Proteomics platform at the Institute of Immunology. -

## 1.2. 2D DIGE analysis

A549/hSLAM cells were treated for 12 h or 32 h with MVSchwarz, MV34wt, MV34VCA, MV37wt or IFNB. Total protein was extracted, CyDye labeled and separated by 2D-PAGE in 12% acrylamide gels within pH 3-7. For technical reasons proteins from 12 h and 32 h treatment were separately analyzed in two independent projects. In total, 738 and 882 spots were included in the statistical analysis for 12 h and 32 h, respectively. Significant differentially expressed spots

(Students t test  $p < 0.05$ ) were selected for automated spot picking, in-gel digestion and were identified by PMF combined with peptide sequencing using MALDI-TOF MS. Representative gel images with spot identifications of both 12 h and 32 h time points are shown in Figure 14a. For 12 h we identified 58 proteins from 79 spots and for 32 h 59 proteins from 91 spots. There was an overlap of 18 proteins within 12 h and 32 h treatment. In total, we identified 170 spots corresponding to 99 unique proteins (Tables 10 and 11). At 12 h we found 13, 15, 42 and 19 proteins differentially expressed for MVSchwarz, MV34wt, MV34VCA and IFNB, respectively. At 32 h we found 25, 24, 36 and 10 proteins differentially expressed for MVSchwarz, MV34wt, MV37wt and IFNB, respectively (Figure 14b).

**Figure 14: (see next page) Representative 2D gel maps of MV infected A549/hSLAM cells 12h and 32h p.i. and corresponding Venn diagrams.**

a) Representative 2D gel maps (24 cm IPG strip pH 3-7NL) for 12 h and 32 h of A549/hSLAM cells infected with MV strains (12 h: MVSchwarz, MV34wt, MV34VCA; 32 h: MVSchwarz, MV34wt, MV37wt) or treated with IFNB. Identified protein spots are annotated by UniProt ID. Multiple protein isoforms were numbered. b) Venn diagrams created with <http://bioinfo.gp.cnb.csic.es/tools/venny/index.html> for proteins identified at 12 h, 32 h and combined 12 h and 32 h time points.

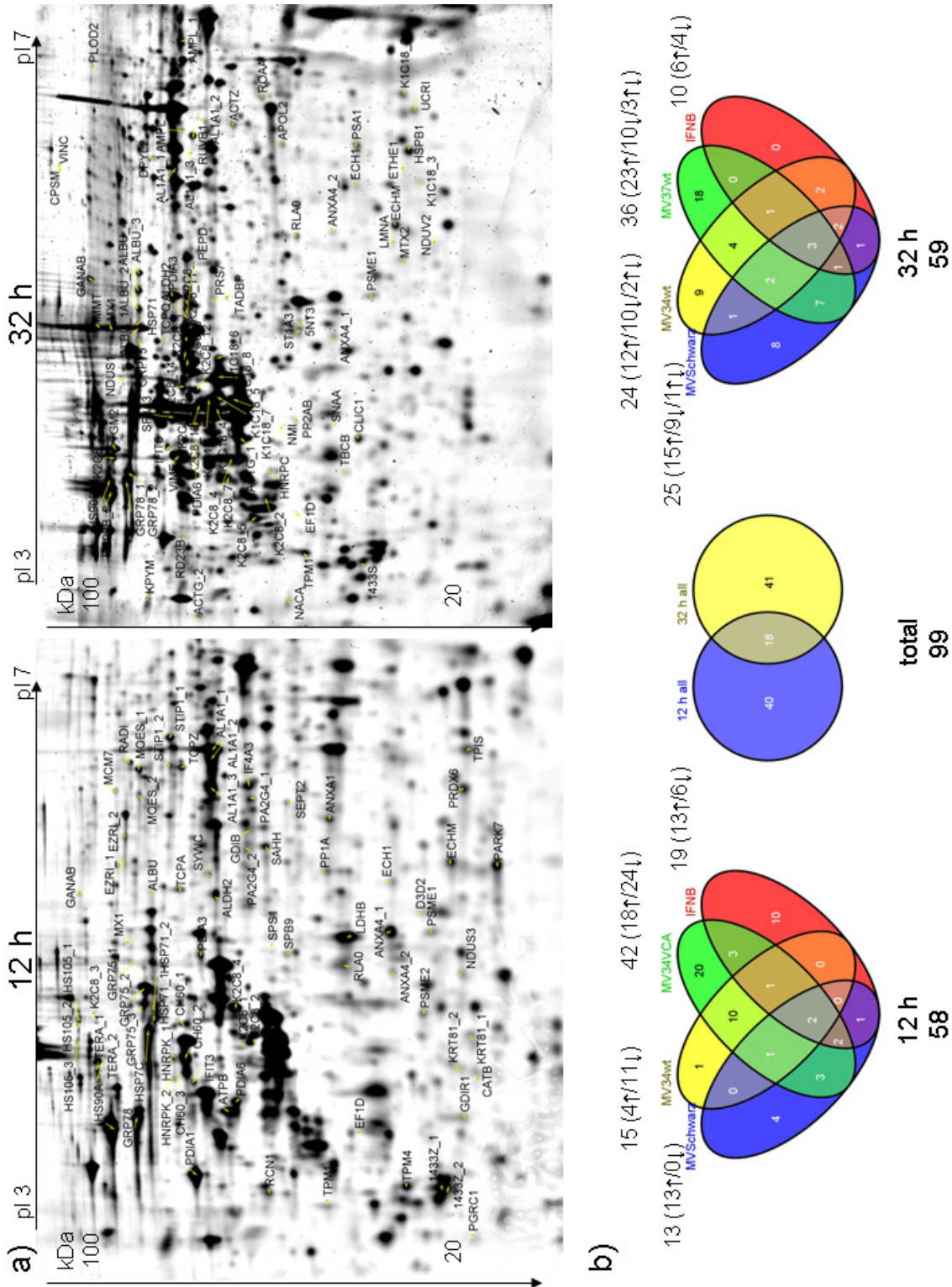


Figure 14: Representative 2D gel maps of MV infected A549/hSLAM cells 12h and 32h p.i. and corresponding Venn diagrams. Detailed figure legend please see previous page.

Table 10: Differentially expressed protein spots in A549/hSLAM cells 12 h p.i.

Accession	Protein Name (60)	MW	PI	Spot ID	PSC	TIS	TIC	PEP	MV Schwarz	MV 34wt	MV 34VCA	IFNB
	<b>CYTOSKELETON (8)</b>								<b>1</b>	<b>3</b>	<b>6</b>	<b>3</b>
EZRL_1	Ezrin	69484	5.94	202474	483	355	100.0	27			-1.63	
EZRL_2	Ezrin	69484	5.94	202475	109	60	100.0	12		-1.41	-1.44	
K2C8_1	Keratin, type II cytoskeletal 8	53671	5.52	202747	591	343	100.0	32			1.34	
K2C8_2	Keratin, type II cytoskeletal 8	53671	5.52	202764	572	338	100.0	31	1.07		1.17	
K2C8_3	Keratin, type II cytoskeletal 8	53671	5.52	202400	454	305	100.0	16	1.80			
K2C8_4	Keratin, type II cytoskeletal 8	53671	5.52	202729	747	504	100.0	31			1.52	
KRT81_1	Keratin, type II cuticular Hb1	56875	5.48	203101	384	286	100.0	16		-1.51	-1.61	
KRT81_2	Keratin, type II cuticular Hb1	56875	5.48	203091	507	342	100.0	25		-1.56	-1.57	
MOES_1	Moesin	67892	6.08	202510	504	353	100.0	31			-1.18	
MOES_2	Moesin	67892	6.08	202512	350	202	100.0	30			-1.57	1.25
RADI	Radixin	68635	6.03	202483	538	449	100.0	23				
SEPT2	Septin-2	41689	6.15	202842	662	518	100.0	17				1.43
TPM1	Tropomyosin alpha-1 chain	32746	4.69	202930	62	31	91.9	5		-1.29	-1.59	
TPM4	Tropomyosin alpha-4 chain	28619	4.67	203016	350	307	100.0	10				1.20
	<b>CHAPERONES/STRESS RESPONSE (11)</b>								<b>0</b>	<b>4</b>	<b>11</b>	<b>0</b>
GRP78	78 kDa glucose-regulated protein	72403	5.07	202491	1210	900	100.0	38			1.35	
HS105_1	Heat shock protein 105 kDa	97716	5.28	202353	499	297	100.0	26		-1.20	-1.42	
HS105_2	Heat shock protein 105 kDa	97716	5.28	202350	463	303	100.0	29			-1.31	
HS105_3	Heat shock protein 105 kDa	97716	5.28	202348	612	369	100.0	37			-1.33	
HS90A	Heat shock protein HSP 90-alpha	85006	4.94	202423	655	514	100.0	31			-1.26	
HSP71_1	Heat shock 70 kDa protein 1A/1B	70294	5.48	202556	969	707	100.0	34			-1.13	-1.21
HSP71_2	Heat shock 70 kDa protein 1A/1B	70294	5.48	202555	676	466	100.0	29			-1.12	-1.11
HSP7C	Heat shock cognate 71 kDa protein	71082	5.37	202524	960	750	100.0	31			-1.14	
PDIA1	Protein disulfide-isomerase	57480	4.76	202642	958	697	100.0	31			1.24	
PDIA3	Protein disulfide-isomerase A3	57146	5.98	202662	750	551	100.0	29			1.41	
PDIA6	Protein disulfide-isomerase A6	48490	4.95	202721	985	852	100.0	20			1.21	
STIP1_1	Stress-induced-phosphoprotein 1	63227	6.4	202579	363	165	100.0	33			-1.28	-1.33

Table 10: (continued) Differentially expressed protein spots in A549/hSLAM cells 12 h p.i.

Accession	Protein Name (60)	MW	PI	Spot ID	PSC	TIS	TIC	PEP	MV Schwarz	MV 34wt	MV 34VCA	IFNB
STIP1_2	Stress-induced-phosphoprotein 1	63227	6.4	202592	218	70	100.0	29		-1.28	-1.28	
TCPA	T-complex protein 1 subunit alpha	60819	5.8	202610	580	280	100.0	36		-1.28	-1.25	
TCPZ	T-complex protein 1 subunit zeta	58444	6.23	202614	694	453	100.0	32		-1.27	-1.18	
	<b>METABOLISM (10)</b>								3	1	6	2
AL1A1_1	Retinal dehydrogenase 1	55454	6.3	202630	564	437	100.0	20			-1.31	
AL1A1_2	Retinal dehydrogenase 1	55454	6.3	249214	537	378	100.0	23			-1.19	
AL1A1_3	Retinal dehydrogenase 1	55454	6.3	202668	597	425	100.0	24			-1.18	
CATB	Cathepsin B	38766	5.88	203274	305	243	100.0	8				-2.52
GANAB	Neutral alpha-glucosidase AB	107263	5.74	202354	249	208	100.0	15				-1.34
LDHB	L-lactate dehydrogenase B chain	36900	5.71	202939	569	343	100.0	25			-1.18	
PP1A	Serine/threonine-protein phosphatase -alpha	38229	5.94	202916	175	85	100.0	9		-1.22	-1.27	
PRDX6	Peroxiredoxin-6	25133	6	203316	402	249	100.0	18	1.16		-1.16	
SAHH	Adenosylhomocysteinase	48255	5.92	202782	269	178	100.0	13			-1.29	
SPS1	Selenide, water dikinase 1	43396	5.64	202822	228	176	100.0	11			2.27	
TERA_1	Transitional endoplasmic reticulum ATPase	89950	5.14	202404	847	631	100.0	35	1.21			
TERA_2	Transitional endoplasmic reticulum ATPase	89950	5.14	202407	106	51	99.9	15	1.29			
TPIS	Triosephosphate isomerase	26938	6.45	203097	390	256	100.0	16	1.38			
	<b>TRANSCRIPTION / TRANSLATION (8)</b>								1	2	5	4
EF1D	Elongation factor 1-delta	31217	4.9	202969	375	221	100.0	19		-1.37		
HNRPK_1	Heterogeneous nuclear ribonucleoprotein K	51230	5.39	249757	181	84	100.0	18			1.19	
HNRPK_2	Heterogeneous nuclear ribonucleoprotein K	51230	5.39	202599	218	82	100.0	21	3.03		2.17	1.95
IF4A3	Eukaryotic initiation factor 4A-III	47126	6.3	202739	552	395	100.0	25			-1.30	
MCM7	DNA replication licensing factor MCM7	81884	6.08	202452	548	344	100.0	30				1.50
PA2G4_1	Proliferation-associated protein 2G4	44101	6.13	202752	424	248	100.0	26		-1.24	-1.40	
PA2G4_2	Proliferation-associated protein 2G4	44101	6.13	202762	154	36	94.6	15			-1.24	1.13
PARK7	Protein DJ-1	20050	6.33	203418	124	62	100.0	8			1.23	
RLA0	60S acidic ribosomal protein P0	34423	5.71	202950	760	517	100.0	26			-1.17	1.23
	<b>IMMUNE RESPONSE (5)</b>								5	2	3	3
IFIT3	IFN-induced protein with tetrapeptide repeats	56691	5.12	202643	324	182	100.0	22	1.77	1.66	2.02	
MX1	Interferon-induced GTP-binding protein Mx1	75872	5.6	202487	279	162	100.0	21	5.29		3.83	3.30
PSME1	Proteasome activator complex subunit 1	28876	5.78	203049	246	155	100.0	13	1.28			1.13

Table 10: (continued) Differentially expressed protein spots in A549/hSLAM cells 12 h p.i.

Accession	Protein Name (60)	MW	PI	Spot ID	PSC	TIS	TIC	PEP	MV Schwarz	MV 34wt	MV 34VCA	IFNB
PSME2	Proteasome activator complex subunit 2	27515	5.44	203042	337	195	100.0	13	1.53		1.43	1.34
SYWC	Tryptophanyl-tRNA synthetase, cytoplasmic	53474	5.83	202675	228	116	100.0	18	1.24			
	<b>MITOCHONDRIMUM (8)</b>								<b>1</b>	<b>2</b>	<b>6</b>	<b>4</b>
ALDH2	Aldehyde dehydrogenase, mitochondrial	56859	6.63	202685	487	378	100.0	19			1.21	
ATPB	ATP synthase subunit beta, mitochondrial	56525	5.26	202702	848	596	100.0	28			1.31	
CH60_1	60 kDa heat shock protein, mitochondrial	61187	5.7	202583	931	731	100.0	30	1.12	1.50	1.39	
CH60_2	60 kDa heat shock protein, mitochondrial	61187	5.7	202590	1120	865	100.0	34			1.44	
CH60_3	60 kDa heat shock protein, mitochondrial	61187	5.7	202604	434	316	100.0	14				1.68
D3D2	3,2-trans-enoyl-CoA isomerase, mitochondrial	33080	8.8	203257	160	123	100.0	6			-1.98	
ECH1	Delta(3,5)-Delta(2,4)-dienoyl-CoA isomerase,	36136	8.16	203002	324	214	100.0	12				-1.33
ECHM	Enoyl-CoA hydratase, mitochondrial	31823	8.34	203348	360	261	100.0	13			1.24	-1.12
GRP75_1	Stress-70 protein, mitochondrial	73920	5.87	202492	57	18	0.0	8		1.57	1.45	
GRP75_2	Stress-70 protein, mitochondrial	73920	5.87	202497	859	615	100.0	33			1.31	
GRP75_3	Stress-70 protein, mitochondrial	73920	5.87	202507	841	601	100.0	34			1.40	
NDUS3	NADH dehydrogenase [ubiquinone]	30337	6.99	203092	477	229	100.0	25				-1.34
	iron-sulfur protein											
	<b>OTHERS (10)</b>								<b>2</b>	<b>0</b>	<b>5</b>	<b>3</b>
1433Z_1	14-3-3 protein zeta/delta	27899	4.73	203055	597	418	100.0	22				1.24
1433Z_2	14-3-3 protein zeta/delta	27899	4.73	203374	741	539	100.0	24				1.16
ALBU	Serum albumin	71317	5.92	202554	59	47	99.7	5			2.10	
ANXA1	Annexin A1	38918	6.57	202921	310	192	100.0	20				1.19
ANXA4_1	Annexin A4	36088	5.84	202990	757	550	100.0	27			-1.32	
ANXA4_2	Annexin A4	36088	5.84	203004	397	251	100.0	19	1.76			
GDIB	Rab GDP dissociation inhibitor beta	51087	6.11	202750	624	346	100.0	34			-1.28	
GDIR1	Rho GDP-dissociation inhibitor 1	23250	5.02	203099	379	256	100.0	14			-1.76	
PGRC1	Membrane-associated progesterone receptor	21772	4.56	203107	194	93	100.0	8				-5.74
RCN1	Reticulocalbin-1	38866	4.86	202802	120	78	100.0	7			1.20	
SPB9	Serpin B9	43004	5.61	202841	209	103	100.0	12	1.35			

MW molecular weight, PI isoelectric point, PSC total protein score, TIS total ion score, TIC total ion c.i.%, PEP peptide count

Table 11: Differentially expressed protein spots in A549/hSLAM cells 32 h p.i.

Accession	Protein Name (60)	MW	PI	Spot ID	PSC	TIS	TIC	PEP	MV Schwarz 4	MV 34wt 7	MV 37wt 6	IFNB
	<b>CYTOSKELETON (10)</b>											2
ACTG_1	Actin, cytoplasmic 2	42108	5.31	267195	523	411	100	17		1.20		
ACTG_2	Actin, cytoplasmic 2	42108	5.31	267085	255	174	100	10	-1.95			-1.69
ACTZ	Alpha-centractin	42701	6.19	267151	401	221	100	18		1.39		
K1C18_1	Keratin, type I cytoskeletal 18	48029	5.34	267099	560	357	100	27			-1.73	
K1C18_2	Keratin, type I cytoskeletal 18	48029	5.34	267628	514	384	100	19		3.24	12.75	
K1C18_3	Keratin, type I cytoskeletal 18	48029	5.34	267702	329	231	100	18		3.67	15.75	
K1C18_4	Keratin, type I cytoskeletal 18	48029	5.34	267102	736	513	100	27		-1.50	-1.64	
K1C18_5	Keratin, type I cytoskeletal 18	48029	5.34	267107	641	456	100	24		-1.44	-1.83	
K1C18_6	Keratin, type I cytoskeletal 18	48029	5.34	267092	582	400	100	25		-1.68	-1.98	
K1C18_7	Keratin, type I cytoskeletal 18	48029	5.34	267163	705	556	100	20			-1.68	
K1C18_8	Keratin, type I cytoskeletal 18	48029	5.34	267091	738	518	100	27		-1.60	-2.44	
K2C8_1	Keratin, type II cytoskeletal 8	53671	5.52	267015	714	416	100	35		-1.37	-1.48	
K2C8_2	Keratin, type II cytoskeletal 8	53671	5.52	267265	445	285	100	26				
K2C8_3	Keratin, type II cytoskeletal 8	53671	5.52	266761	134	53	99.93	18			1.62	
K2C8_4	Keratin, type II cytoskeletal 8	53671	5.52	267157	660	423	100	32	-1.90			
K2C8_5	Keratin, type II cytoskeletal 8	53671	5.52	267242	472	271	100	30			1.87	
K2C8_6	Keratin, type II cytoskeletal 8	53671	5.52	267006	659	413	100	33		-1.55	-1.72	
K2C8_7	Keratin, type II cytoskeletal 8	53671	5.52	267156	596	366	100	32		1.34		
K2C8_8	Keratin, type II cytoskeletal 8	53671	5.52	266998	502	264	100	32		-1.45	-1.48	
K2C8_9	Keratin, type II cytoskeletal 8	53671	5.52	267004	509	319	100	27		-1.37	-1.54	
K2C8_10	Keratin, type II cytoskeletal 8	53671	5.52	267004	639	395	100	33		-1.37	-1.54	
K2C8_11	Keratin, type II cytoskeletal 8	53671	5.52	266999	581	357	100	30		-1.62	-2.05	
K2C8_12	Keratin, type II cytoskeletal 8	53671	5.52	267059	686	430	100	34			2.15	
K2C8_13	Keratin, type II cytoskeletal 8	53671	5.52	267037	614	363	100	33			2.95	
K2C8_14	Keratin, type II cytoskeletal 8	53671	5.52	267011	535	330	100	30		-1.57	-1.89	
K2C8_15	Keratin, type II cytoskeletal 8	53671	5.52	269323	593	329	100	35	2.91	1.70	4.13	1.88
K2C8_16	Keratin, type II cytoskeletal 8	53671	5.52	269323	644	350	100	37	2.91	1.70	4.13	1.88

Table 11: (continued) Differentially expressed protein spots in A549/hSLAM cells 32 h p.i.

Accession	Protein Name (60)	MW	PI	Spot ID	PSC	TIS	TIC	PE P	MV Schwarz	MV 34wt	MV 37wt	IFNB
LMNA	Lamin-A/C	74380	6.57	267636	59	6	0	19			2.88	
TCPA	T-complex protein 1 subunit alpha	60819	5.8	202610	667	355	100	33				
TCPQ	T-complex protein 1 subunit theta	60153	5.42	266947	249	109	100	15		-2.73		
TPM1	Tropomyosin alpha-1 chain	32746	4.69	267381	302	269	100	10	3.22	3.12	2.98	
VIME	Vimentin	53676	5.06	266982	877	624	100	32			-1.40	
VINC	Vinculin	124292	5.5	266497	234	109	100	24	5	-3.62	-2.16	0
	<b>CHAPERONES/STRESS</b>											
	<b>RESPONSE (8)</b>											
GRP78_1	78 kDa glucose-regulated protein	72403	5.07	266790	1160	895	100	35	1.29			
GRP78_2	78 kDa glucose-regulated protein	72403	5.07	266800	1000	747	100	34	1.36			
HS90B_1	Heat shock protein HSP 90-beta	83554	4.97	269387	586	475	100	26		1.51		
HS90B_2	Heat shock protein HSP 90-beta	83554	4.97	266709	494	382	100	26		-1.27		
HSP71	Heat shock 70 kDa protein 1A/1B	70294	5.48	269216	531	321	100	30	1.76		1.82	
HSPB1	Heat shock protein beta-1	22826	5.98	267663	142	102	100	5			1.66	
PDIA3	Protein disulfide-isomerase A3	57146	5.98	266963	974	709	100	33	1.54			
PDIA6	Protein disulfide-isomerase A6	48490	4.95	267057	622	501	100	19	4.51		8.97	
TBCB	Tubulin-folding cofactor B	27594	5.06	267505	378	253	100	11	-3.02			
	<b>METABOLISM (13)</b>											
5NT3	Cytosolic 5'-nucleotidase 3	38266	6.67	267353	142	96	100	7	2.08	5	9	2
AL1A1_1	Retinal dehydrogenase 1	55454	6.3	266981	254	191	100	14			2.06	1.93
AL1A1_2	Aldehyde dehydrogenase, dimeric NADP-preferring	50746	6.11	270216	425	230	100	20	-2.31		1.40	
AL1A1_3	Aldehyde dehydrogenase, dimeric NADP-preferring	50746	6.11	267023	578	307	100	31			1.41	
AMPL_1	Cytosol aminopeptidase	56530	8.03	266984	519	310	100	28	1.17			
AMPL_2	Cytosol aminopeptidase	56530	8.03	270122	418	257	100	19			2.35	
DPYL2	Dihydropyrimidinase-related protein 2	62711	5.95	266908	311	170	100	16		-3.72		
GANAB	Neutral alpha-glucosidase AB	107263	5.74	266655	359	253	100	23			-1.98	
KPYM	Pyruvate kinase isozymes M1/M2	58470	7.96	266910	188	80	100	13		9.77	10.02	
PEPD	Xaa-Pro dipeptidase	55311	5.64	269180	278	154	100	20			-1.60	
PLOD2	Procollagen-lysine,2-oxoglutarate 5-dioxygenase 2	85373	6.24	266651	198	156	100	9			-1.99	

Table 11: (continued) Differentially expressed protein spots in A549/hSLAM cells 32 h p.i.

Accession	Protein Name (60)	MW	PI	Spot ID	PSC	TIS	TIC	PE P	MV Schwarz	MV 34wt	MV 37wt	IFNB
PP2AB	Serine/threonine-protein phosphatase 2A catalytic	36123	5.21	267349	128	46	99.55	9		3.25		
RD23B	UV excision repair protein RAD23 homolog B	43202	4.79	267034	172	91	100	14	-1.42			
SNAA	Alpha-soluble NSF attachment protein	33667	5.23	267470	208	84	100	14		2.07		
ST1A3	Sulfotransferase 1A3/1A4	34288	5.68	267357	172	86	100	14			2.10	
TGM2	Protein-glutamine gamma-glutamyltransferase 2	78420	5.11	266736	75	34	94.11	8	2.44	2.16	2.45	1.63
	<b>TRANSCRIPTION / TRANSLATION (7)</b>								<b>3</b>	<b>2</b>	<b>4</b>	<b>1</b>
EF1D	Elongation factor 1-delta	31217	4.9	267358	276	182	100	14	-9.05			
HNRPC	Heterogeneous nuclear ribonucleoproteins C1/C2	33707	4.95	267279	171	97	100	11	-1.86	-2.14		
RLA0	60S acidic ribosomal protein P0	34423	5.71	267330	692	516	100	21			3.43	
ROAA	Heterogeneous nuclear ribonucleoprotein A/B	36316	8.22	267247	244	184	100	9			-1.84	
RUVB1	RuvB-like 1	50538	6.02	267028	729	485	100	31			1.39	
SF3A3	Splicing factor 3A subunit 3	59154	5.27	266992	247	155	100	14		-1.18		-1.25
TADBP	TAR DNA-binding protein 43	45053	5.85	267131	165	118	100	6	-4.06		-2.78	<b>3</b>
	<b>IMMUNE RESPONSE (7)</b>								<b>3</b>	<b>3</b>	<b>3</b>	<b>3</b>
IFIT3	Interferon-induced protein with tetrapeptide repeats	56691	5.12	266975	373	241	100	21	3.06	3.07	2.24	3.35
MX1	Interferon-induced GTP-binding protein MX1	75872	5.6	266748	540	346	100	27	-1.58			
NACA	Nascent polypeptide-associated complex subunit alpha	23370	4.52	267344	99	51	99.95	7			-3.40	
NMI	N-myc-interactor	35206	5.24	267319	242	142	100	16			4.92	
PRS7	26S protease regulatory subunit 7	49002	5.71	267100	136	48	99.76	8		-2.21		-2.43
PSA1	Proteasome subunit alpha type-1	29822	6.15	267520	393	245	100	18		-1.68		
PSME1	Proteasome activator complex subunit 1	28876	5.78	267579	405	279	100	15	1.64			1.87
	<b>MITOCHONDRION (10)</b>								<b>3</b>	<b>3</b>	<b>6</b>	<b>0</b>
ALDH2	Aldehyde dehydrogenase, mitochondrial	56859	6.63	269156	301	220	100	16			-1.72	

Table 11: (continued) Differentially expressed protein spots in A549/hSLAM cells 32 h p.i.

Accession	Protein Name (60)	MW	PI	Spot ID	PSC	TIS	TIC	PE P	MV Schwarz	MV 34wt	MV 37wt	IFNB
CP5M	Carbamoyl-phosphate synthase [ammonia],	165975	6.3	266478	295	107	100	28		-8.58		
ECH1	Delta(3,5)-Delta(2,4)-dienoyl-CoA isomerase	36136	8.16	267519	567	370	100	24	-1.47			
ETHE1	Protein ETHE1, mitochondrial	28368	6.35	267662	260	147	100	15			3.88	
IMMT	Mitochondrial inner membrane protein	84026	6.08	266680	294	180	100	19			-2.01	
MTX2	Metaxin-2	30086	5.9	267668	190	117	100	11		2.70		
NDUS1	NADH-ubiquinone oxidoreductase 75 kDa subunit,	80443	5.89	266791	439	273	100	27		-1.35		
NDUV2	NADH dehydrogenase [ubiquinone] flavoprotein 2,	27659	8.22	267748	274	182	100	13			12.76	

MW molecular weight, PI isoelectric point, PSC total protein score, TIS total ion score, TIC total ion c.i.%, PEP peptide count

Proteins were grouped into cytoskeleton, chaperones/stress response, metabolism, transcription/translation, immune response, mitochondria and others. Mostly affected were structural proteins as well as proteins involved in stress response and protein folding. Multiple spots were identified as cytokeratins with up to 16 spots for K2C8 and 9 spots for K1C18. K2C8 was affected at the two time points, whereas KRT81 was only affected at 12 h, K1C18 only at 32 h. Cytokeratins were almost exclusively regulated after MV infection. At 12 h we observed average fold changes (FC) of -1.3 and 1.56 with maximal values for MX1 (FC 5.29) and PGRC1 (FC -5.75). At 32 h average fold changes were 3 and -2.18 with maximal values for K1C18 (FC 15.75) and EF1D (FC -9). The higher mean of expression changes at 32 h may reflect a stronger anti-viral response over time. Functional analysis of our data set revealed a strong enrichment for proteins linked to cell death and apoptosis, reflected by significant enrichment of mitochondrial proteins ( $1.9E-05$ ). Individual analysis for the 12 h time point showed significant enrichment for protein folding ( $1.56E-10$ ), endoplasmic reticulum stress ( $2.79E-09$ ), cell death ( $6.9E-09$ ), inhibition of apoptosis ( $3.24E-08$ ) and linkage of actin cytoskeleton ( $3.69E-08$ ). Top functions found for 32 h were cell death ( $2.84E-09$ ), apoptosis ( $1.52E-07$ ) and pneumonitis ( $5.5E-06$ ) (Table 12).

**Table 12: Molecular and cellular functions of differentially expressed proteins in A549/hSLAM cell 12 h and 32 h p.i.**

Molecular and cellular functions	12h*				32h*			
	MV Schwarz	MV 34wt	MV 34VCA	IFNB	MV Schwarz	MV 34wt	MV 37wt	IFNB
cell death	6	9	23	8	14	14	19	
inhibition of apoptosis	3	2	6		2		3	
apoptosis	5	5	17	6	10	12	16	
morphology of cell lines			4			3	5	
linkage of actin cytoskeleton		1	3					
shape change							5	
reorganization of cytoskeleton			4					
endoplasmic reticulum stress response	2	3	5		2		2	
growth of cells	5	8	15		9	7	8	
generation of reactive oxygen species					2		4	
allergy	2		5		5	3	4	2
pneumonitis	2		5		4	2	3	
folding of protein		3	7					
modification of protein		4	14					

\* Only number of proteins with significant changes are shown

### 1.3. Comparison of MV strains

#### **MV induced changes in cellular proteome 12 h p.i.**

The early response to the vaccine strain (MVSchwarz) was an overall induction of proteins (13 up) including all grouped as immune response (IFIT3, MX1, PSME1, PSME2, SYWC). Proteins classified for cytoskeleton, chaperones and metabolism were underrepresented. Four proteins were uniquely affected MVSchwarz (SPB9, SYWC, TERA, and TPIS). Cytokeratins were not affected by except for one cyto keratin 8 isoform (K2C8\_4). In contrast, the wt infection (MV34wt) dominantly led to protein down regulation (4 up, 11 down). Up regulated proteins were IFIT3, MX1, CH60 and GRP75. The majority of down regulated proteins included cytoskeletal proteins (EZRI, K2C8, KRT81, and TPM1) and chaperones (HS105, HSP71, STIP1, TCPA and TCPZ). In comparison to the latter wt and vaccine strain, most changes at 12 h were observed for the diRNA positive MV34VCA strain (18 up, 24 down). Among those proteins, 20 proteins were uniquely affected by MV34VCA. However, the relation to its parental wt strain (MV34wt) was still visible in the induced proteome changes. Of the 14 MV34wt modulated proteins 13 overlap with its VCA strain MV34VCA. Proteins grouped as chaperones/stress response were mostly down regulated by MV34VCA except for GRP78 and the phosphodiesterases PDIA1, PDIA3 and PDIA6. The mitochondrial chaperone CH60 was commonly induced by all viruses.

Indicator of an activated antiviral response was the induction of IFN-inducible proteins MX1 and IFIT3. At 12 h IFIT3 was similarly induced by all three MV strains (FC 1.77, 1.66, 2.02), but not by IFNB. Notably, CH60 and IFIT3 were the only common proteins at 12 h among virus infections. At the later time point IFIT3 was also induced by IFNB, again with a similar expression pattern (FC 3.06, 3.07, 2.24, 3.35). MX1 was significantly only induced at 12 h by MVSchwarz and MV34VCA (FC 5.29, 3.83) as well as IFNB (FC 3.3). Ten out of 19 proteins were uniquely expressed by IFNB treatment including PGRC1, CATB, NDUS3, GANAB, ECH1, 1433Z, ANXA1, TPM4, SEPT2, and MCM7.

**MV induced changes in cellular proteome 32 h p.i.**

During the late phase (32 h p.i.) virus infections induced more changes than IFNB alone. In contrast to the early phase more proteins were up regulated upon virus infection.

Comparing the MVSchwarz vaccine to both wt strains, six proteins showed similar expression when compared to MV37wt (HSP71, PDIA6, TADPB, 5NT3, UCR1, ECHM) and two proteins (HNRPC, APOL2) when compared to MV34wt. The two wt strains showed no broad overlap except for similar effects on the cytoskeleton (K1C18, K2C8, VINC) and one metabolic protein (KPYM). KPYM, equally induced by both wt strains (FC 9.77, 10.02), was the highest up regulated protein for MV34wt infection.

The dominantly suppressive phenotype of MV34wt (4 up, 11 down) at 12 h changed at 32 h showing equal up and down regulations (12 up, 10 down). Commonly induced by all virus strains and IFNB were two cytokeratin 8 isoforms (K2C8\_15, K2C8\_16), TGM2 and IFIT3. TGM2 and IFIT3 showed equal induction among viruses and IFNB, whereas the cytokeratin 8 isoforms were strongest induced by MV37wt. The two wt strains influenced multiple isoforms of cytokeratin 8 and 18, mostly by down regulation. Two cytokeratin 18 isoforms (K1C18\_2 and K1C18\_3) were induced by both wt viruses, but showing expression differences (MV34wt: 3.24, 3.67, MV37wt: 12.75, 15.75). Overall, MV37wt induced stronger expression changes than MV34wt. Among the unique proteins of MV37wt, 7 were more than 2-fold up-regulated: NMI, ETHE1, NDUV2, LMNA, AMPL\_2, ST1A3 and RLA0. Highest induction was observed for NDUV2 (12.76).

Similarly induced by all three viruses (vaccine and both wt), but not found for IFNB were TPM1 and ALBU. All three viruses showed some overlap, but also induced unique proteins. At 32 h p.i. there were 8, 9 and 18 unique affected proteins for MVSchwarz, MV34wt and MV37wt respectively. None was found for IFNB (at 32 h).

In general, we observed distinct proteome changes for the different MV strains. Proteins which were present in more than one treatment showed mainly expression changes in the same direction.

Comparing all proteins found to be affected at both early and late phase of the infection (combining time points 12 h and 32 h p.i.) by the different virus strains, we observed a profound part to be uniquely expressed for each treatment. We found 34, 36, 42, 36 and 28 total proteins for MVSchwarz, MV34wt, MV34VCA, MV37wt and IFNB, respectively. Among those were 7, 9, 14, 14 and 8 uniquely expressed after infection with MVSchwarz, MV34wt, MV34VCA, MV37wt or treatment with IFNB, respectively (Table 13).

**Table 13: Unique proteins affected by MV strains and IFNB**

	<b>MVSchwarz</b>	<b>MV34wt</b>	<b>MV34VCA</b>	<b>MV37wt</b>	<b>IFNB</b>
<b>total*</b>	<b>34</b>	<b>36</b>	<b>42</b>	<b>36</b>	<b>28</b>
<b>unique*</b>	<b>7</b>	<b>9</b>	<b>14</b>	<b>14</b>	<b>8</b>
	TERA	CPSM	D3D2	NACA	PGRC1
	SYWC	DPYL2	GDIR1	IMMT	CATB
	SPB9	TCPQ	RADI	PLOD2	NDUS3
	TPIS	PSA1	IF4A3	ROAA	1433Z
	TBCB	NDUS1	SAHH	PEPD	ANXA1
	RD23B	ACTZ	GDIB	VIME	TPM4
	CLIC1	SNAA	HS90A	RUVB1	SEPT2
		MTX2	LDHB	HSPB1	MCM7
		PP2AB	HSP7C	1433S	
			RCN1	ST1A3	
			PARK7	LMNA	
			PDIA1	ETHE1	
			ATPB	NMI	
			SPS1	NDUV2	

\*; whole data set (12 h and 32 h) was considered

## 2. Discussion

MV infection result in multiple effects in the host cell. The aim of this study was to compare proteome changes induced by different virus strains. Our quantitative proteomic approach and subsequently bioinformatics analyses displayed that different MV strains induced different alterations in the cellular host proteome.

The MV life cycle can be divided into different processes: virus entry and replication, virus interplay with cellular stress response and antiviral activity and finally assembling and budding of the virion from the cell membrane. During 12 h p.i. structural proteins and proteins involved in stress response or protein folding were mostly affected, reflecting mostly virus induced changes of the cellular machinery to replicate the virus. Most changes were found in the cytoskeleton, whether this is induced by the fusion of the virus with the cellular membrane or binding to the receptor on the cell surface, need to be further investigated. Previously it has been speculated that compounds of the cytoskeleton like cellular tubulin are necessary for MV RNA synthesis (Moyer et al., 1990) . At the later phase of the infection (32 h) mostly proteins of the cytoskeleton as well as cell death and apoptosis are influenced. For MV and other viruses it has been shown before that components of the cytoskeleton like actin, ezrin, moesin and tubulin play key functions during assembly and budding of the virion from the cell membrane (Berghall et al., 2004, Bohn et al., 1986, Cudmore et al., 1997). Moesin in interaction with the MV-H protein is involved in the cell-to-cell fusion process visible by CPE effect (Doi et al., 1998). Strain MV37wt that showed the strongest effect 32 h p.i. on proteins of the cytoskeleton also showed the highest amount of CPE. On the other hand, changes in cytoskeletal proteins indicated probably the loss of membrane integrity during the syncytia formation induced by MV. Functional analysis of our data set revealed a strong enrichment for proteins linked to cell death and apoptosis, reflected by a significant enrichment of mitochondrial proteins (1.9E-05). Changes in mitochondrial proteins are quite common during viral infections (Munday et al., Wang et al., 2009). Proteins

related to pneumonitis, a feature of MV infection (Moss & Griffin, 2006), were also found to be significantly affected.

Strain MV34VCA induced the most changes on the cellular proteome (42 proteins). Interestingly, this strain was the only diRNA positive strain in this study. It has been shown before that diRNAs can be detected from various sensors of the host cell, leading to a fast and strong antiviral response like activation of IFN as well as other cytokines (Shingai et al., 2007). Previous experiments displayed that compared to their parental wt strains Vero-cell adapted strains induce an attenuated phenotype in primates (Auwaerter et al., 1999). Whether this is linked to the appearance of diRNA or other molecular changes need to be further investigated. Our proteomics data revealed broad effects on proteins of all groups with chaperones and proteins involved in metabolism dominantly down regulated by MV34VCA, and immune response and mitochondrial proteins dominantly up regulated. In comparison to its parental wt strain MV34wt a slightly higher IFIT3 induction was observed in MV34VCA, as well as an induction of MX1 and PSME2 at 12 h p.i..

Notably, the evolutionary relation of MV34VCA and MV34wt was reflected by the largest overlap in commonly expressed proteins between those two strains. Three proteins were common only between MVSchwarz and MV34VCA, whereas no protein was common only between the vaccine and the original wt. This may reflect that the VCA strain evolves an intermediate phenotype like a hybrid of vaccine and the original wt strain. At 32 h p.i. the differences between MVSchwarz and MV34wt were still present, with one protein common only in the two strains. Closer to the vaccine strain was the MV37wt, with 7 proteins specifically overlapped between the two strains. The two wt strains showed not more similarities than compared to the vaccine. It has been speculated that wt strains in contrast to attenuated vaccine strains actively interact with the early innate immune response (Naniche et al., 2000). This we could not observe. We found a massive effect on cytokeratin isoforms mediated by the two wt strains and the attenuated MV34VCA. Huge differences found between the two wt strains 32 h p.i. underline the complex picture how wt strains interplay with the

cellular proteome and that they very likely differ in their phenotypic characteristics.

Despite inter strain differences we also observed some similarities which underline the potential power of the proteomics technique. IFIT3 (interferon-induced protein with tetratricopeptide repeats 3 or RIG-G) was induced similarly by all virus strains at both time points, whereas for IFNB treatment it was only detected at 32 h. IFIT3 can be induced by type I IFN but also by IRF3 (Andersen et al., 2008). This suggests that both attenuated and wt MV leads to the activation of IRF3 at comparable levels. Serum albumin was induced by all viruses at 32 h p.i., but not by IFNB. It has been shown that albumin-uptake in lung cells by receptor-mediated endocytosis and pinocytosis is a mechanism for alveolar clearance (Hastings et al., 2004). It has been suggested that intracellular albumin influence increased glutathione levels, which leads to a decrease in TNF-alpha-mediated NF-kappaB activation (Cantin et al., 2000) and prevents apoptosis of endothelial cells (Zoellner et al., 1996). Notably, the attenuated MV34VCA already showed albumin uptake at 12 h p.i.. TGM2 (protein-glutamine gamma-glutamyltransferase 2) catalyzes transamidation and produces polyaminated or deamidated proteins. Recently a growing number of viral proteins, as well as cellular proteins with which they interact, have been found to be modified by TG2, suggesting a novel function for TG2 in viral pathogenesis (Maggio et al., 2006). Protein disulfide isomerases PDIA1, 3 and 6 were moderate induced by MV34VCA during early phase of infection, whereas PDIA6 became strongly induced by the vaccine strain and MV37wt at the late phase of the infection. PDIA6, redox chaperones, mainly present in the endoplasmic reticulum but also at cell surface, have been linked to virus-uptake (Santos et al., 2009) and MHC I degradation (Lee et al., 2010). NMI (N-Myc interactor), a transcription co-factor to enhances the association of CPB/p300 to STAT1 and STAT5 (Zhu et al., 1999), was solely induced by MV37wt at 32 h p.i.

This is the first study that offers a global overview of the host cell response to different MV strains. This opens up new potential targets for antiviral treatments and a deeper understanding of differences in MV phenotypes.

---

## Part III

---

---

### MV induced cytokine response in humans

---

The human immune system continuously tries to limit pathogen invasion and tissue damage and to efficiently protect the organism against invaders. The immunity against pathogens is orchestrated by an intimate interaction between the natural (innate) and acquired (adaptive) immunity. After recognition of pathogens various cytokines are released by activated tissue and inflammatory cells to trigger the diverse networks of defense mechanisms.

Despite intensive analyses of genetic differences of MV genotypes, little is known about biological differences among members of the different clades. Recently speculations occurred about differences in the level of pathogenicity among various wt strains, since Mubarak et al. (Chernoff et al., 1995, Opal et al., 1998, Sieling et al., 1993) found variations in clinical parameters and immune response in macaques following the infection with either MV genotype C2 or B3. Also in our IFN sensitivity study (part I of the Result Section) these MV strains behaved differently. Our C2 strain was one of the most sensitive wt strains to IFN, whereas the B3 strain was least sensitive to IFN-alpha treatment.

In the following pilot study we investigated the concentration of cytokines in human sera after natural measles infection with either one of the two mentioned genotypes (genotype C2 or B3). In agreement with previous studies we could detect interleukin 5 (IL-5), IL-6, IL-8 and IL-10 during the first eight days after onset of rash of the measles disease (Moss et al., 2002).

IL-6 and IL-8 are among the most prominent pro-inflammatory cytokines. IL-6 plays an important role in the acute-phase innate response and is involved in stimulating T-cell proliferation, T and B-cell differentiation and antibody production (Schneider-Schaulies & ter Meulen, 2002). IL-6 is one of the most important mediators of fever. IL-8 supports the induction of the local immune response, mucosal inflammation and mucus secretion required for rapid virus clearance (El Mubarak et al., 2007). IL-5 is a pleiotropic cytokine, enhances the mediator release from human basophils and plays a pivotal role in the chemoattraction, proliferation, differentiation, survival and activation of eosinophils (Moss et al., 2002, Sato et al., 2008). IL-10 plays a major role in the late-phase of the infection, enhancing B-cell proliferation (Kenis et al., 2002, Thavasu et al., 1992). However, IL-10 down-regulates cytokine synthesis, suppresses macrophage activation and T-cell proliferation and promotes the release of cytokine inhibitors (Kenis et al., 2002). Thus it was speculated that these inhibitory effects of IL-10 contribute to the prolonged immune suppression following measles disease (Papania & Orenstein, 2004).

## 1. Results

The comparison of cytokine levels in the sera from laboratory confirmed measles showed that in the Luxembourgish patients infected with genotype C2, the median cytokine levels of IL-5, IL-6, IL-8 and IL-10 were lower than in the genotype B3 infected patients from Spain and Nigeria (Figure 15). In B3 infected patients (Spain and Nigeria) was the cytokine level for IL-6 >2.5 fold higher ( $p < 0.05$ ) than in C2 infected patients. A similar pattern was found for IL-8 and IL-10 respectively. Spanish and Nigerian B3 sera showed a >2.6 fold and >3 fold higher level of IL-8 and IL-10 ( $p < 0.05$ ) than Luxembourgish C2 sera. IL-5 was detectable only in a few samples, since most of them were under limit of

detection. Nevertheless the Spanish B3 sera showed a higher induction of IL-5 than the Luxembourgish C2 ( $p > 0.05$ ) and control samples ( $p < 0.05$ ).

To monitor the kinetics of cytokines during acute measles related to different genotypes we analyzed the cytokine changes during different days after onset of rash. We separated the patients into two groups, one group (<3days) with all patients for which sera between day zero and day three after onset of rash were collected and the second group (>3days) included all sera collected later than day three (Figure 16). Overall in B3 infected patients the cytokine average levels in group one (<3days) were significantly higher for IL-6 and IL-8 than in C2 infected patients ( $p < 0.05$ ). The same pattern was found for sera of group two (>3days), but only IL-6 was significantly different in B3 sera. Interestingly, in C2 sera a slight decrease in IL-6 and IL-8 levels was found between group one (<3days) and group two (>3days), whereas in case of B3 sera a slight increase in these cytokine levels was observed.

So in this study we could show that in great contrast to B3 infected patients (Spain and Nigeria) the cytokine response in C2 infected patients (Luxembourg) seems to be alleviated.

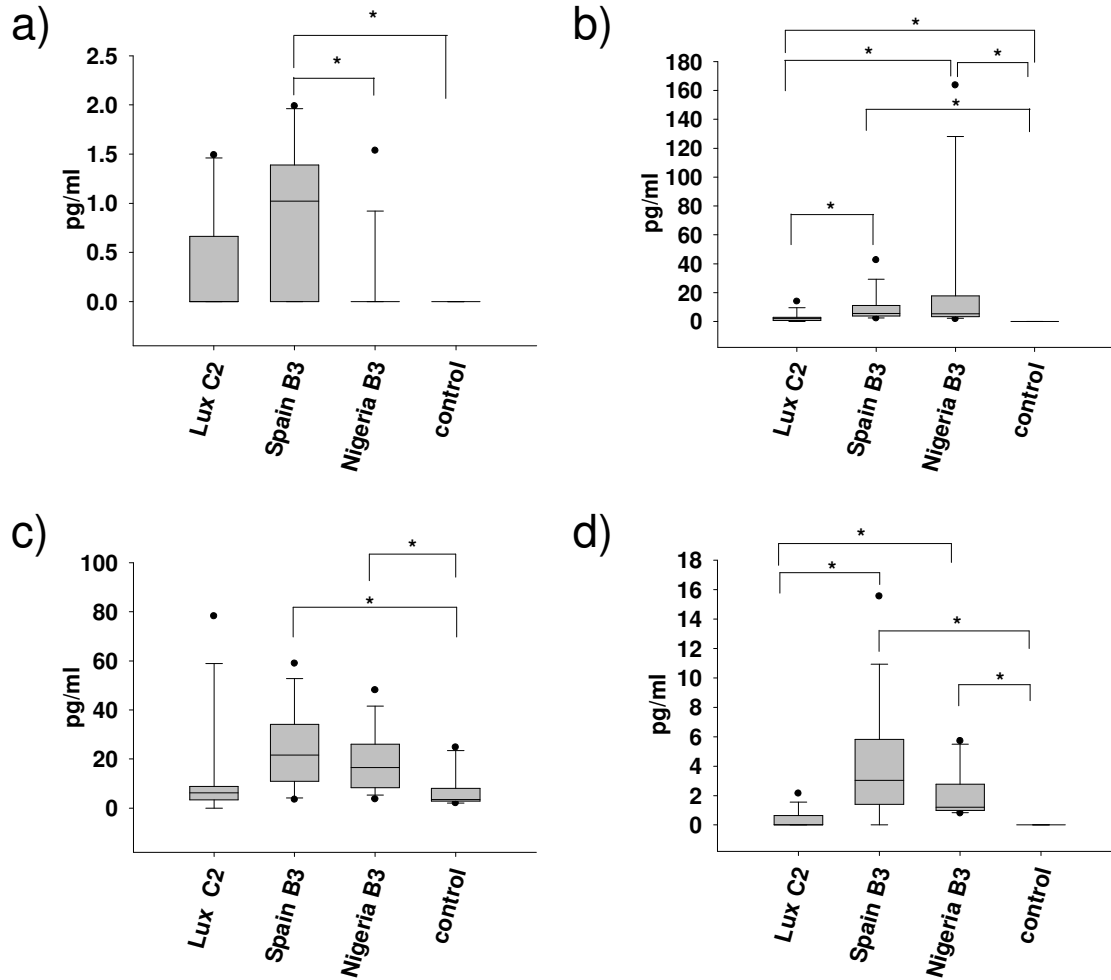


**Figure 15: Cytokine induction of IL-5, IL-6, IL-8 and IL-10 in sera of patients infected with either MV genotype C2 or B3.**

Overall cytokine induction of a) IL-5, b) IL-6, c) IL-8 and d) IL-10 in sera of patients infected with MV genotypes C2 from Luxembourg (Lux) or B3 from Nigeria and Spain and healthy control group. All sera were collected during day 0 and 8 after onset of rash. All sera were measured in triplicates, except those from Nigeria, which were measured in duplicates only (due to low sample volume). Analysis of statistical significance was performed using Mann-Whitney rank sum test (\*,  $p < 0.05$ ).

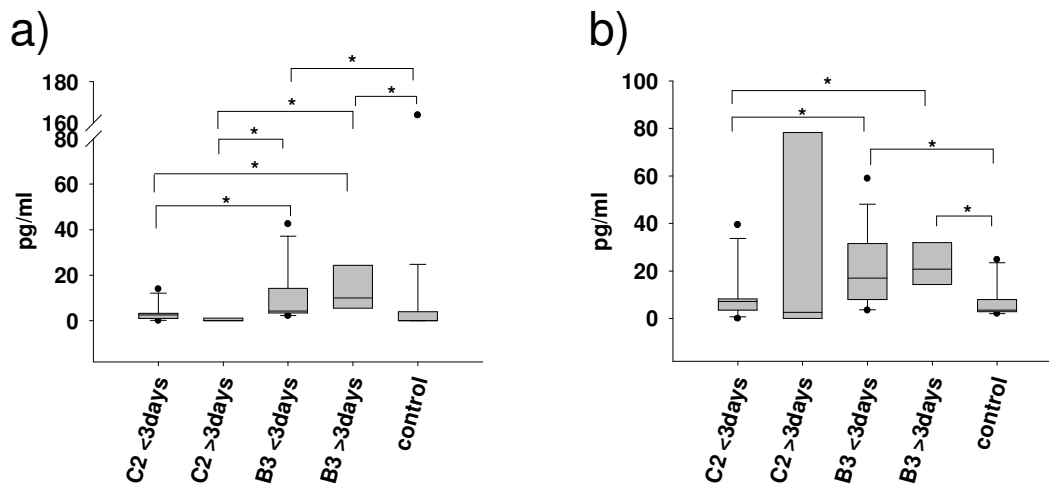


**Figure 16: Cytokine induction of IL-6 and IL-8 stratified according to onset of rash.**

Cytokine induction of a) IL-6 and b) IL-8 in sera of patients infected with MV genotypes C2 (from Luxembourg) or B3 (fused data from Nigeria and Spain) and healthy control group. Sera were stratified according to onset of rash: <3days or >3days. Analysis of statistical significance was performed using Mann-Whitney rank sum test (\*,  $p < 0.05$ ).

## 2. Discussion

The immune reaction against viral infections starts with the recognition of the pathogen by the innate immune system, followed by a specific B- and T-cell response, which normally terminates the infection and the inflammatory response. In this study we investigated the cytokine response during acute measles infection in humans infected with either genotype C2 or B3. Interestingly B3 and C2 infected patients showed important differences in their immune response. The B3 infections consistently induced high cytokine levels. In contrast, C2 infections induced a slower progression of the immune response characterized by lower cytokine levels. C2 sera differed from B3 sera especially by the higher levels of IL-6, IL-8 and IL-10.

On the one hand, a fast and strong induction of cytokines may lead to inhibition of virus replication and fast clearance of the virus, whereas a low cytokine level

would support virus spread and severity of disease. However these effects would only play a role if all MV wt strains have the same sensitivity to cytokines. In our previous study (see part I of the Result Section) we demonstrated significant variations in the sensitivity to IFN-alpha among wt strains. We showed that the B3 strain had the lowest sensitivity to IFN-alpha treatment, whereas the C2 strain was among the most sensitive strains. Taking this into account, we hypothesise that the C2 strain could be cleared faster than the B3 strain, although this induced higher amounts of cytokines, but is less sensitive to them.

Until now it was commonly assumed that MV wt strains do not differ in terms of pathogenicity or neurovirulence at least in humans and explanations were always given by host determinants, such as age, nutrition status and particular immunocompetence (Riddell et al., 2005). Nevertheless, Mubarak et al. (WHO, 2007) showed differences in pathogenicity between B3 and C2 strains in infected macaques. Animals infected with the B3 strain had an earlier and longer viremia as well as a more rapid onset of MV-specific IgM. It would thus be interesting to know the sera cytokine concentrations in these animals and whether they are in agreement with our findings in humans. IL-10 is known to negatively influence the immune response by suppressing macrophages activation, inhibition of cytokines synthesis and T-cell proliferation (Rota et al., 2009). Thus, higher levels of IL-10 leading to longer immunosuppression, would result in increased susceptibility to severe secondary infections like pneumonia or diarrhea, especially in B3 infected patients. However, whether the stronger induction of cytokines in the case of human B3 infection corresponds to differences in pathogenicity requires further investigation.

Two types of biases can influence our results. First, the biological variability of cytokine levels, which is influenced by seasonal and diurnal fluctuations, age, gender, the menstrual cycle and other conditions that effects the cytokine concentration *in vivo* (Rota et al., 2009). On the other hand may experimental variability due to blood sampling, sera preparation and storage play a role. Since we analyzed sera collected in 1996, 1998 and 2003, there is a difference in storage time, but sampling and storage conditions were comparable.

Nevertheless, both B3 cohorts collected 1998 in Nigeria or 2003 in Spain showed a higher cytokine concentration than the C2 sera collected 1996 in Luxembourg. It has been shown before that especially IL-6 and IL-10 are quite stable and can be stored for several years at -20 °C, including up to 4 times repeated freeze-thaw cycles, without significant decline in concentration (Kremer et al., 2008). Thus, the difference in storage time should not impact our findings.

Although we have used small cohorts in this study, we could demonstrate that B3 strains collected during two outbreaks (1998 and 2003) and in patients from Africa and Europe induce higher levels of cytokines than the C2 strains. So the results obtained here support the hypotheses that MV genotypes differ in their pathogenicity in human. At least we could demonstrate large differences in the induction of cytokines during the first eight days of the acute phase of the measles disease. Nevertheless, further studies including larger cohorts and sera collected during the convalescent phase of the infection are necessary to clarify the role of these mediators in the pathogenicity of MV.

## Part IV

---

### Investigation of MV outbreaks

---

Manuscript of part IV is submitted as:

*Revealing new transmission routes of measles virus epidemics using phosphor- and haemagglutinin sequence analysis.*

Julia R. Kessler, Jacques R. Kremer, Sergey V. Shulga, Nina T. Tikhonova, Sabine Santibanez, Annette Mankertz, Galina V. Semeiko, Elena O. Samoilovich, Jean-Jacques Muyembe Tamfum, Elisabeth Pukuta, Claude P. Muller

Since the introduction of measles vaccination, the global burden of measles disease has continuously decreased. However measles continues to be endemic in many developing countries and to certain extend also in industrialized countries (Wichmann, 2009). Molecular epidemiology of MV has proven to be a very useful tool for monitoring the progress in measles control (Samoilovich et al., 2006). Since 1998 the WHO recommends that the hypervariable 450 nts

encoding the C-terminal 150 amino acids of the MV-NP gene (MV-NP HVR) is the minimal sequence data required for MV genotyping (Kremer et al., 2008). Additionally the complete MV-H sequence should be obtained, if a new genotype is suspected (Shulga et al., 2009). MV genotyping is an important tool of measles surveillance to document chains of transmission, discriminate between imported or indigenous viruses and monitor elimination programs. Only the sequences of the MV-NP HVR are available for most strains obtained from clinical cases. However, with the enhanced control the genetic variability of circulating strains continues to decrease and identical MV-NP HVR sequences have been found for several years in a same region (Xu et al., 1998). Very similar sequence variants were found throughout Europe and beyond. For instance, two main variants of genotype D6, differing by a single nt in their MV-NP HVR, were widely distributed in the WHO European Region in 2005 and 2006 (Bankamp et al., 2008). Thus it becomes increasingly difficult to determine the origin of a virus using only this part of the MV genome.

In this study the sequence variability of MV-P and H genes of strains with identical or very similar MV-NP HVR sequences were investigated. We showed for four different outbreaks in Europe and Africa that phylogenetic analysis of the MV-P/H-pseudo-gene sequences provides an improved picture of MV circulation.

## **1. Results**

### **1.1. Genotype D6: Germany**

Between January and July 2006, 1,749 measles cases have been reported during a measles outbreak in NRW, which was suspected to be caused by a virus imported from the Ukraine. Eleven NP-HVR variants differing by up to three nts, were found among the 125 MV strains, sequenced in the context of this

outbreak (Wichmann, 2009). Among these variants, we investigated the genetic diversity of P and H genes of 13 of these strains with identical NP-HVR sequences (Figure 17-20). Nine of them were collected in April 2006 at the peak of the epidemic and the other four one or two months later. Six strains that were identical in their NP-HVR sequences had each a unique P/H-pseudo-gene sequence, differing by one or two nts from the most common variant (Figure 18). The highest genetic distance of four nts was found between two strains (MVs/BadNeunahr.GER/21.06/1, MVs/Borken.GER/21.06/2) collected towards the end of the outbreak. In the H gene all 13 strains were identical, except for one (MVs/Neunkirchen.GER/17.06/1), with a single point mutation (Figure 20). Thus, the diversity of P/H-pseudo-gene sequences was mainly due to random mutations in the P gene (Figure 19).

## 1.2. Genotype D6: Belarus

Between January and September 2006, 149 measles cases were reported from five different regions in Belarus (Samoilovich et al., 2006); personal communication from Galina Semeiko). A total of five NP-HVR variants, differing by one to three nts, were obtained from 47 MV strains which were sequenced in the context of this outbreak (Kremer et al., 2008). Ten of these strains with identical NP-HVR sequences were analyzed here for their P and H gene diversity (Figure 17-20). The latter were collected between March and September 2006 in three different regions of Belarus (details about regions please see Table 6). Among the 10 strains with identical NP-HVR sequences four and three different P and H gene sequences were found (Figure 19, 20). Six different P/H-pseudo-gene variants could be distinguished (Figure 18).

The strains imported independently from two very distant locations within the Ukraine (MVi/Smorgon.BLR/28.06, epidemiologically linked to Khmel'nitsky; and MVi/Smorgon.BLR/31.06, from a patient returning from the Crimea two weeks before onset of disease) had identical P gene sequences and differed by a single

fixed nt in the H gene (Figure 19, 20). The latter nt was found in several other strains from Smorgon (Grodno Region) and Volozhin (Minsk Region) collected several weeks later. Similarly all four strains from Minsk Region (Molodechno, Vilejka, Volozhin) differed from each other by the same fixed H nt as well as some random mutations in the P gene, suggesting several independent importations into both regions. Indeed MVi/Volozhin.BLR/34.06 (Minsk Region) was epidemiologically linked to Grodno Region. Strain MVi/Minsk.BLR/12.06/3 was suspected to be imported from the Netherlands.

In conclusion, six sequence variants could be distinguished among the 10 MV strains from Belarus (with identical NP-HVR) on the basis of their P/H-pseudo-gene sequences. Although the overall sequence diversity remained low, the fixed H nt accurately reflected the known epidemiological links, while the random mutations of the P gene were less informative.

**Figure 17: (see next page) Phylogenetic tree of D6a strains from Russia and D6b strains from Germany and Belarus displaying MV-NP HVR genes.**

Phylogenetic tree of D6a strains (collected in the Russian Federation (n=31, March 2003 to May 2007)) and D6b strains (collected in Germany (□, n=13, April to June 2006) or Belarus (○, n=10, May to October 2006)). The calculation was based on the 450 nts of the MV-NP HVR. WHO reference strain is indicated with •. Strains with epidemiological link to the Ukraine indicated as ▲; Strain imported from Grodno to Minsk region indicated as ▼. Genetic distances are represented as number of nucleotide differences between strains.



**Figure 17: Phylogenetic tree of D6a strains from Russia and D6b strains from Germany and Belarus displaying MV-NP HVR genes.** Detailed figure legend please see previous page.

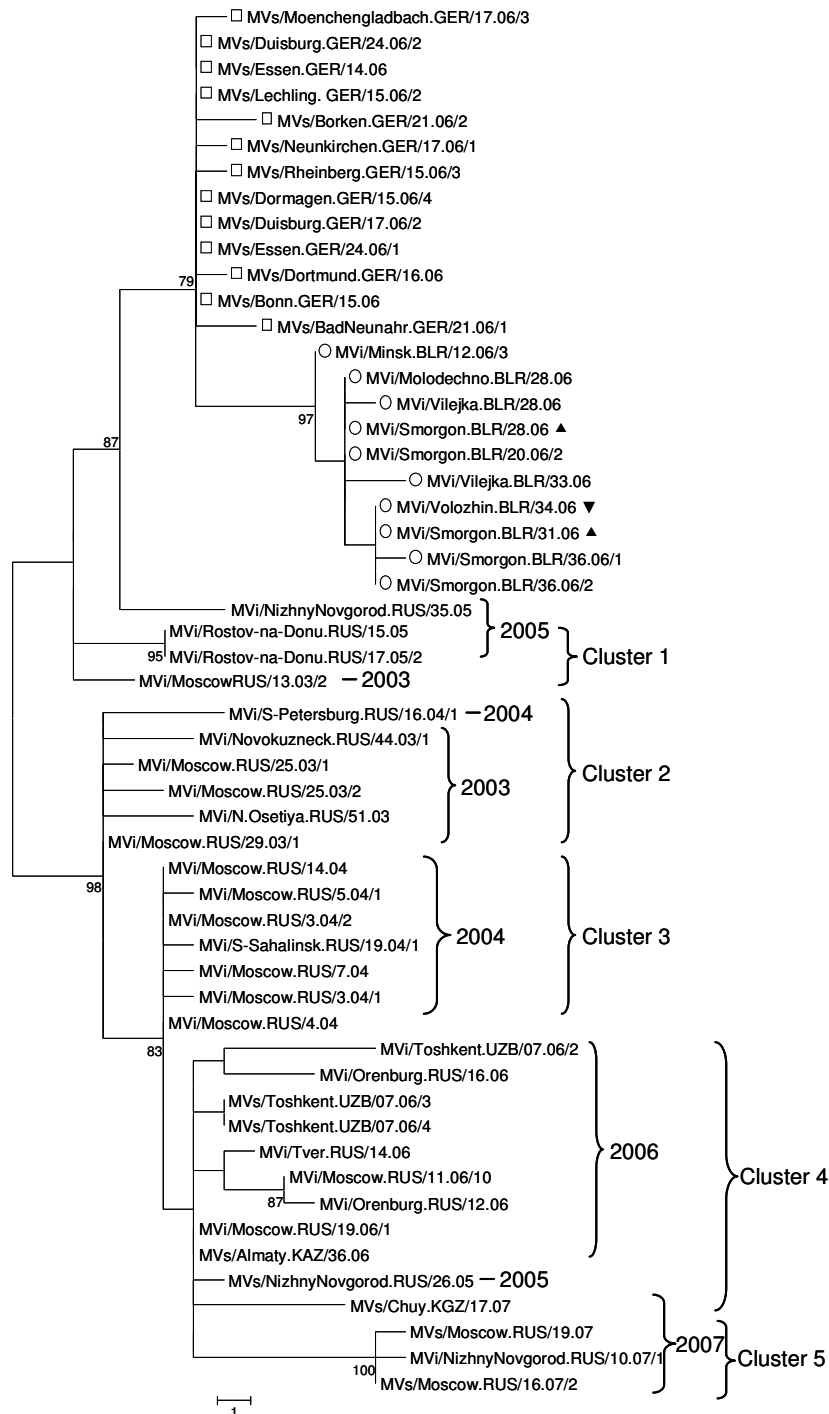


**Figure 18: Phylogenetic tree of D6a strains from Russia and D6b strains from Germany and Belarus displaying MV-P/H-pseudo-genes.**

Phylogenetic tree of D6a and D6b strains based on the 3377 nts of the MV-P/H-pseudo-gene. Strain designating as in Figure 17. Strains with epidemiological link to the Ukraine indicated as ▲; Strain imported from Grodno to Minsk region indicated as ▼. Genetic distances are represented as number of nucleotide differences between strains.

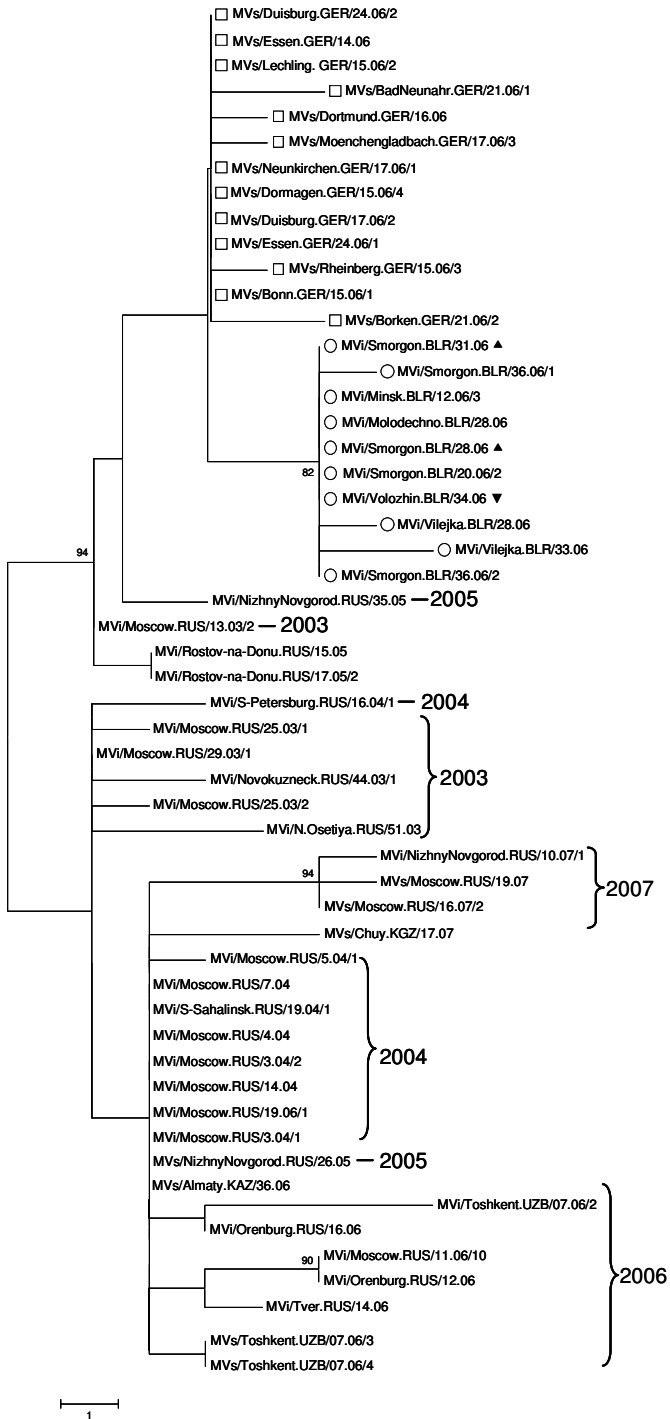


**Figure 19: Phylogenetic tree of D6a strains from Russia and D6b strains from Germany and Belarus displaying MV-P genes.**

Phylogenetic tree of D6a and D6b strains based on the 1524 nts of the MV-P gene. Strain designating as in Figure 17. Strains with epidemiological link to the Ukraine indicated as ▲; Strain imported from Grodno to Minsk region indicated as ▼. Genetic distances are represented as number of nucleotide differences between strains.

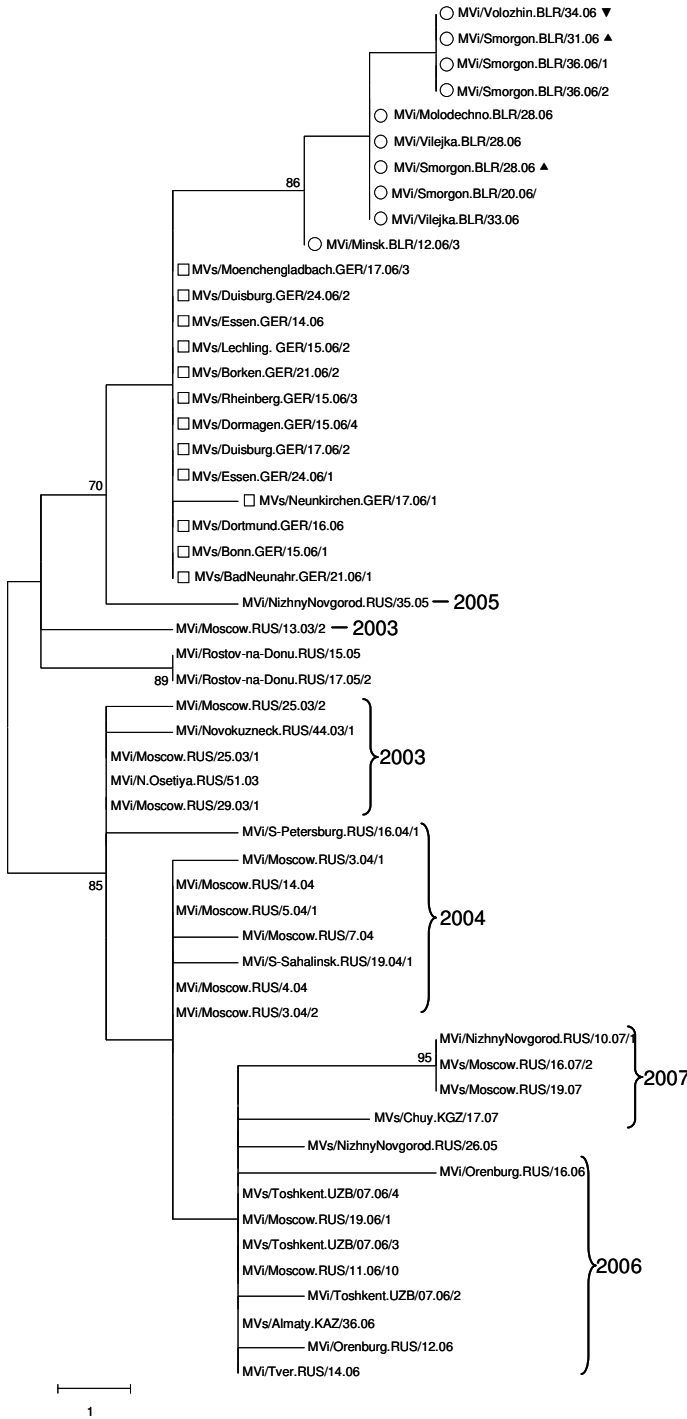


**Figure 20: Phylogenetic tree of D6a strains from Russia and D6b strains from Germany and Belarus displaying MV-H genes.**

Phylogenetic tree of D6a and D6b strains based on the 1854 nts of the MV-H gene. Strain designating as in Figure 17. Strains with epidemiological link to the Ukraine indicated as ▲; Strain imported from Grodno to Minsk region indicated as ▼ The calculation was based on Genetic distances are represented as number of nucleotide differences between strains.

### 1.3. Genotype D6: Russia

In order to monitor the evolution of the P and H gene of MV strains with identical or very similar NP-HVR sequences over a prolonged period, 31 genotype D6 viruses collected during March 2003 until May 2007 in the Russian Federation, and the Newly Independent States (NIS) Uzbekistan, Kazakhstan and Kyrgyzstan, were analyzed. Most of the strains (n=21) collected during these five years, had the same NP-HVR sequence (variant D6a). Eleven strains differed by one or two nts from variant D6a and by up to three nts (0.67%) from each other (Figure 17). The maximal overall genetic distance between all MV sequences reported during the same period from the Russian Federation was four nts (0.89%) in the NP-HVR (Shulga et al., 2009).

In our study, the P/H-pseudo-gene revealed 18 variants among the 21 D6a strains (maximal genetic distance: 20 nts, 0.59%) (Figure 18). Using H gene sequences only of the same strains, 13 variants (maximal genetic distance: 10 nts, 0.54%) could be distinguished. Similarly, 13 different P gene variants were found among the 21 D6a strains (maximal genetic distance: 10 nts, 0.66%) (Figure 19). The maximal genetic distance increased to 11 nts (0.72%) in the P gene when the 11 other MV variants with slightly different NP-HVR sequences were included in the analysis, but did not increase for the H gene.

Thus, phylogenetic dendrograms of P and/or H genes were in contrast to the NP-HVR tree clearly structured. The fused P and H genes formed at least five clusters (Figure 18). Cluster 1 included strains identified in the Russian Federation during 2003 until 2005; cluster 2 included mainly strains from throughout Russia 2003 including Moscow; cluster 3 strains were mostly from Moscow 2004; cluster 4 had mostly 2006 strains from various regions throughout Russia and NIS; and finally cluster 5 incorporated strains collected throughout Russia in 2007. These clusters resulted mainly, but not exclusively from accumulating fixed nt in the H gene.

The three MV strains from Nizhny Novgorod (MVs/NizhnyNovgorod.RUS/26.05, MVi/NizhnyNovgorod.RUS/10.07/1, MVi/NizhnyNovgorod.RUS/35.05) had highly

diverse P and H gene sequences. Interestingly, the latter 2005 strain was relatively closely related to the strain that spread from the Ukrainian outbreak one year later. This strain also showed the highest genetic distance of all strains represented here to the 2007 strain from the same city, suggesting repeated independent importation of MV, rather than continued circulation in Nizhny Novgorod. Similarly the P/H-pseudo-gene variability clearly demonstrated that the strains from Moscow were not directly related or part of a larger outbreak.

Considering the large differences in sequence diversity, strains with identical P and/or H sequences were much more likely to be epidemiologically linked, than strains with identical NP-HVR sequences. For instance, two strains from Rostov (MVi/Rostov-na-Donu.RUS/15.05, MVi/Rostov-na-Donu.RUS/17.05/2) differed by one nt in their NP-HVR, but had identical P and H sequences. MVs/Almaty.KAZ/36.06 and MVi/Moscow.RUS/19.06/1 had identical sequences in all genes, suggesting a direct epidemiological link between measles cases in Moscow and Kazakhstan in 2006. Similarly, two of the three MV strains obtained in Tashkent (Uzbekistan) during the same week of 2006, had identical sequences in all genes, whereas the third one seems to represent a different chain of transmission.

In conclusion, P and H gene sequences structured chains of transmission of strains with virtually identical NP-HVR sequences.

#### **1.4. Genotype B2: Democratic Republic of Congo**

Between 2004 and 2006, a large measles epidemic with more than 36,000 cases occurred in the DR-Congo. Among 45 MV strains (genotype B2) sequenced from this outbreak, mainly three NP-HVR variants (B2KIN-A, B2KIN-B and B2KIN-C) differing by up to two nts, were detected (Kremer et al. 2010 in preparation). From 18 of these viruses including three B2KIN-A, two B2KIN-B and nine B2KIN-C strains, collected between December 2004 and February 2006, the P and H

genes were sequenced (Figure 21, 22). Four additional strains, that differed by a single nt from B2KIN-C were also included.

All strains, except two (MVi/Kinshasa.COD/19.05/15, MVs/Kinshasa.COD/19.05/10), had unique P/H-pseudo-gene sequences (Figure 21b). However, only the three strains from variant B2KIN-A formed a separate cluster in their P/H-pseudo-genes, containing three distinct variants with a maximal genetic distance of seven nts (0.21%). This difference was mostly due to the P gene, with a maximal genetic distance of six nts (0.39%), but also to two H gene variants differing by a single nt (Figure 22a, b). B2KIN-B and B2KIN-C strains did not form distinct clusters in the phylogenetic tree based on P/H-pseudo-gene sequences and genetic distances between B2KIN-C strains were due to substitutions in their P genes (maximal diversity: 11 nts, 0.72%) rather than their H genes (maximal diversity: 4 nts, 0.22%). On the other hand, four strains with different NP-HVR sequences were identical in their P genes (MVs/Kinshasa.COD/41.05/6, MVs/Kinshasa.COD/42.05/3, MVs/Kinshasa.COD/19.05/10, MVi/Kinshasa.COD/19.05/15 and MVs/Bas-Congo.COD/06.06/9).

The earliest available sequence of the 2004-2006 outbreak a B2KIN-A variant (Mvi/Kinshasa.DRC/50.04), differed only by two nts (0.44%) in the NP-HVR from a B2 strain detected in Gabon twenty years earlier ( MVi.Libreville.GAB/84 (R96) [U01994]). Also B2KIN-B and B2KIN-C differed only by one or two nts from the Gabon strains. In contrast, in the P/H-pseudo-gene the B2 strains from DR-Congo differed by 45 and 53 nts (1.33% and 1.57%) from the Gabon strains. Most of the latter mutations (29 to 34) were found in the H gene, whereas their P genes showed less differences (16 to 23).

The pseudogene of the B2KIN-A variants, which were only detected during the early phase of the epidemic in Kinshasa, were genetically more distant (minimal distance 49 nts, 1.45%) from the Gabon strains from 1984, than B2KIN-B and B2KIN-C variants. Therefore, it is unlikely that B2KIN-B and B2KIN-C have evolved from B2KIN-A during the 2004-2006 epidemic in Kinshasa, but rather

represent independent introductions of different genotype B2 variants, during 2005.

The three strains collected during the same week in the province of Bas-Congo (MVs/Bas-Congo.COD/06.06/6, MVs/Bas-Congo.COD/06.06/9, MVs/Bas-Congo.COD/06.06/3), differed by three to five nts from each other. Similarly, between 9 and 14 nts difference was found in the P/H-pseudo-gene sequences of strains MVi/Mbujimayi.COD/06.06/4, MVi/Mbujimayi.COD/06.06/3 and MVi/Mbujimayi.COD/06.06/2, collected in the same week in the province of Kasai-Oriental. These sequence data, as well as their phylogeny (Figure 21b) suggest that measles outbreaks in Bas-Congo and Kasai-Oriental, which occurred during the epidemic peak in Kinshasa, were linked by several independent chains of transmissions with Kinshasa.

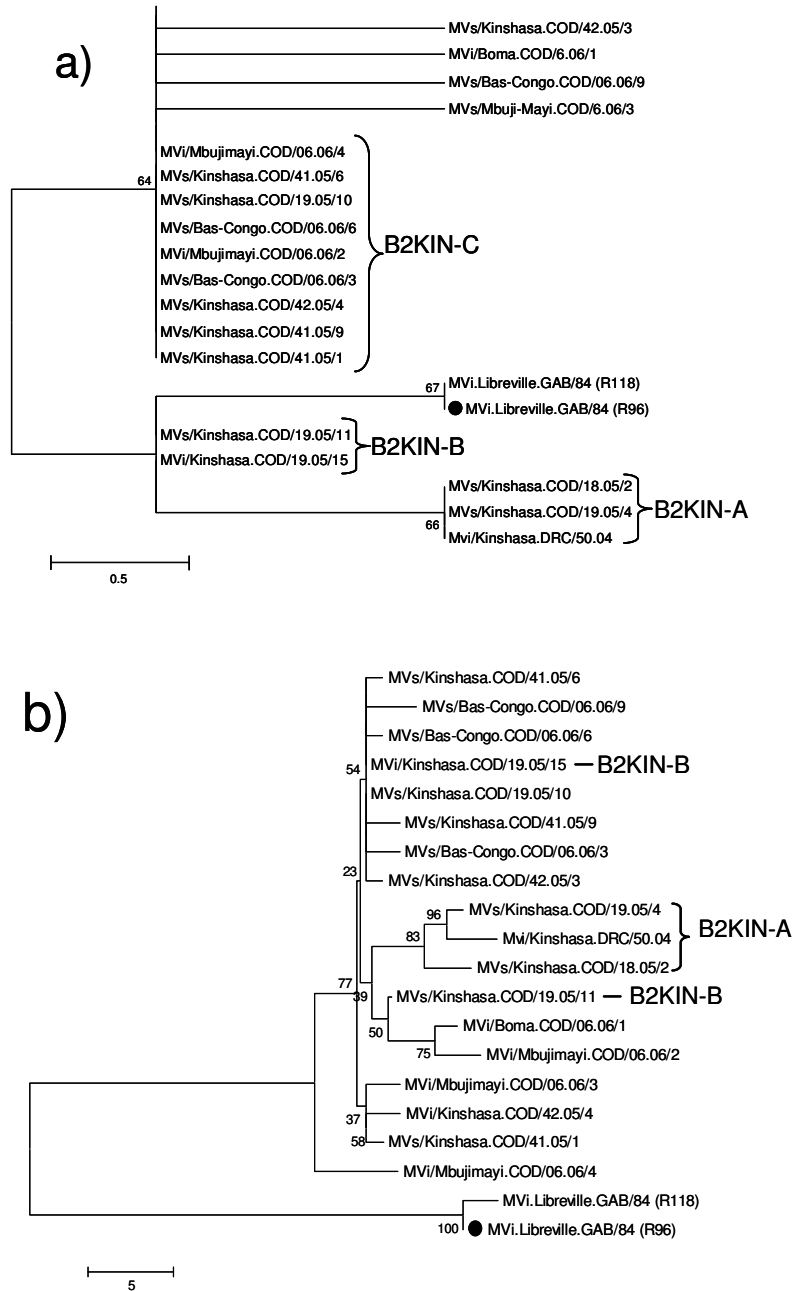


**Figure 21: Phylogenetic trees showing MV-NP HVR and MV-P/H-pseudo-genes of B2 strains collected in the DR-Congo.**

Phylogenetic tree showing B2 strains collected in the DR-Congo (n=18, collected during May 2005 and February 2006). WHO reference strain is indicated by •. The phylogenetic tree was calculated on a) the basis of the 450 nts of the MV-NP HVR or b) on the 3377 nts of the MV-P/H-pseudo-gene. Genetic distances are represented as number of nucleotide differences between strains.

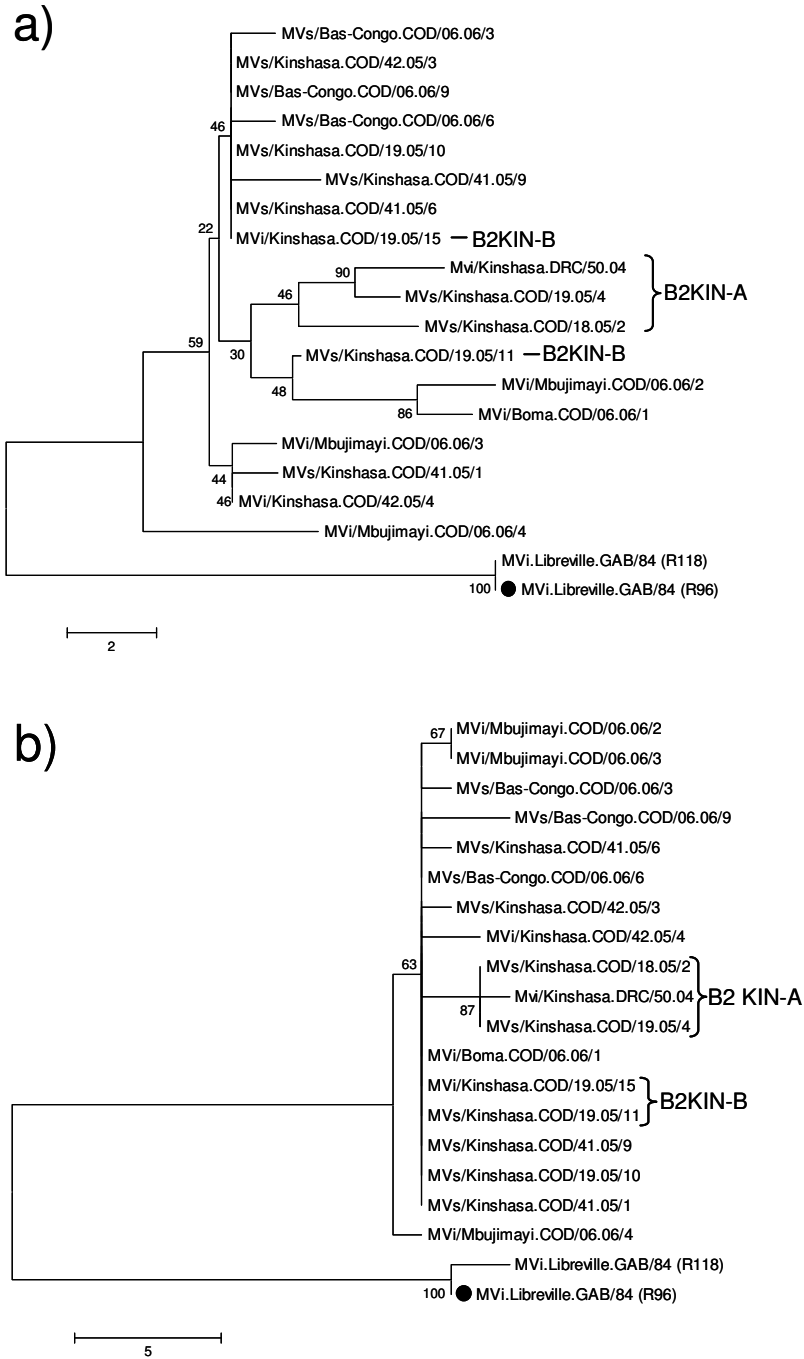


**Figure 22: Phylogenetic trees showing MV-P and H genes of B2 strains collected in the DR-Congo.**

Phylogenetic tree showing B2 strains collected in the DR-Congo (n=18, collected during May 2005 and February 2006). WHO reference strain is indicated by •. The phylogenetic tree was calculated on a) the 1524 nts of the MV-P gene and b) the 1854 nts of the MV-H gene. Genetic distances are represented as number of nucleotide differences between strains.

## 2. Discussion

By extending the sequencing window recommended by WHO for molecular epidemiology of MV from the NP-HVR to included P and H genes, links between outbreaks, and transmission chains became more clearly defined. Without epidemiological data, identical NP-HVR sequences found in Belarus and Germany, may have suggested that strains belong to the same outbreak. However, their P/H-pseudo-gene sequences formed distinct clusters supported by high bootstrap values that clearly identified the cases in both countries as part of two distinct parallel outbreaks. Interestingly the outbreak in Germany showed only a single cluster in the P/H-pseudo-gene, whereas the Belarusian strains both from Grodno and Minsk, showed at least two clusters of pseudo-genes which corresponded to several independent introductions from the Ukraine. Thus the strains from both regions do not correspond to an ongoing transmission, affirming a better measles control in Belarus than suggested by the NP-HVR analysis. Unlike the German strains, the Belarusian pseudo-genes showed an apparent evolution during the 24 weeks of observation, which was mainly due to the fixation of two specific mutations after week 12 and 31 in the H gene, while the P gene added additional variability to the P/H-pseudo-gene. In contrast all German H genes except one were all identical. Also in this case the variability within the single cluster of the pseudo-gene was due to mutations in the P gene. In the NP-HVR the strains from Russia (D6a) and Belarus/Germany (D6b) differed by a single nt with no intermixing. While this is suggestive of 2 parallel outbreaks in both regions, the NP-HVR provided no further insights into transmission pathways. In the P/H-pseudo-genes of the Belarusian/German strains the tree structure suggested a common most recent ancestor with 2003/2005 strains from Russia. Most other strains from Russia formed a clearly separated cluster of their own with high boot strap support. Interestingly the analysis of the pseudo-genes of the Russian strains revealed well defined sub-clusters by calendar years, suggesting that closely related viruses circulated simultaneously in different locations throughout Russia and NIS as a single

epidemiological space and continued to evolve over the years. Thus, the P/H-pseudo-gene permitted a temporal and geographic interpretation of MV circulation. In contrast, the NP-HVR sequences provided no insight into circulation patterns of MV and could be interpreted as belonging to a single major outbreak lasting for several years at the different locations. Especially strains collected in Moscow during five years were all identical in their NP-HVR, suggesting a continuous circulation of MV in the city. However, the P/H pseudo-gene showed that most of the strains in Moscow were more closely related to strains from several other locations during the same years than to earlier or later strains from Moscow. This suggests that every year virus strains have been reintroduced into Moscow from different regions within Russia and NIS with ongoing outbreaks. Interestingly, the phylogenetic structure reflects a molecular evolution of the H gene between 2003 and 2007, with the irreversible fixation of distinct mutations. This was much less evident for the P gene, but the phylogeny of the constructed P/H-pseudo-genes confirms this evolution.

Recently three distinct variants of NP-HVR genotype B2 (B2KIN-A/B/C) were found in DR-Congo (Kremer et al. 2010 in preparation). However, using their P/H-pseudo-genes only strains from variant B2KIN-A formed a distinct cluster, supported by bootstrap values in the H gene. Thus, our findings suggest circulation of variant B2KIN-A in Kinshasa and multiple independent importations of B2KIN-B and B2KIN-C into Kinshasa. The most surprising finding in DR-Congo was that strains collected during this outbreak showed only a very low genetic distance (maximum two nts) in their NP-HVR, compared to strains collected more than 20 years before in Gabon. In contrast, they displayed a very high genetic diversity in their P/H-pseudo-genes (> 45 nts) compared to these strains. Interestingly 2/3 of this variability was contributed by the H gene.

The NP-HVR provides most bar-coding information per sequence length (12%) (Xu et al., 1998). Nevertheless, the P and H genes (and most other MV genes) also have a considerable sequence diversity (5.5% and 6.1% (Bankamp et al., 2008), which as we showed here can be exploited to follow up on viruses with reduced genetic diversity.

However, the above examples suggest some striking differences between the molecular evolution of the P and the H gene. While mutations in the H gene seem to have a high tendency to become fixed in the viral genome, mutations in the P gene seem to be more variable. As a result, mutations in the H gene tend to form distinct clusters, whereas P gene mutations only add variability to these clusters. This was very obvious in the Belarus and the Russian strains, where several more or less well time-defined clusters evolved from each other. The German H genes showed only one mutation and only a single cluster in the P/H pseudo-gene. This evolutionary pattern was particularly obvious, when a recent B2 strain from DR-Congo was compared to a 24 years old sequence from Gabon, where the H gene and the P gene showed a strong and a weaker evolutionary drift, while the NP-HVR showed none over the 24 years period. Recently it has been shown that especially the MV-P open reading frame has a high structural flexibility and a high acceptance for non-synonymous point mutations (Gerlier & Valentin, 2009). Likewise, it has been assumed that gradual mutations in the MV-H gene are rather induced by random drift than selective amino acid changes driven by the immune system (WHO, 2008). Since we did not find a mutation in any of the sites currently recognized as having important biological and immunological functions our results support the latter assumption (Moss, 2009).

However, the MV-NP HVR only represents 450 nts of the whole 1578 nts (~29%) of the MV-NP gene, whereas the MV-P and H genes were completely sequenced. Analyzing the evolution rate of the whole MV-NP gene would perhaps be an alternative to sequence the latter genes in addition, but this needs to be further investigated. We demonstrated that viruses with identical MV-NP HVR are very likely to differ in their MV-P and MV-H sequences and links between outbreaks and transmission chains became more clearly defined.

## **Chapter IV**

---

## **Conclusions and Perspectives**

---

The current study describes the genetic and phenotypic characterisation of various MV strains from all over the world. Beside the genetic classification of variants circulating during different measles outbreaks, the main focus of the project was the interaction of strains with the innate immune response *in vitro* and *in vivo*.

The innate immunity is critical to control viral infections during the development of the adaptive immune response. Alpha and beta interferons (IFN-alpha/beta) are key cytokines in the early host reaction to viral infections. Therefore phenotypic differences between MV strains, relating to IFN-alpha/beta induction and signalling, may influence virus spread and severity of disease. We showed here for the first time that various MV strains belonging to different genotypes interfere differently with the early immune response. Surprisingly we found that among all wt strains a large variability exists regarding their replication fitness, sensitivity to type I IFN and ability to induce other cytokines of the innate response. For the first time we also verified the existence of diRNA in MV wt strains *in vitro*. These subgenomic RNAs are an important confounding parameter in passaged wt viruses, which must be carefully assessed in all *in vitro* studies. Thus, using a large panel of wt strains our observations reconcile earlier reports that wt strains are more sensitive to IFN-alpha than vaccine strains (WHO, 2009a), with those reporting the opposite (Riddell et al., 2005). Considering that also vaccine strains differ in their sensitivity to type I IFN, previous results probably reflect differences between individual strains, rather than differences between attenuated and wt viruses in general.

MV infection results in multiple effects on the host cell. Our quantitative proteomic approach and subsequently performed bioinformatics analyses revealed that the investigated MV strains differently induced alterations in the cellular host proteome. Thus, a global overview of the host cell response to different MV strains was achieved, underlining our previous findings on phenotypic differences among MV wt strains.

Recently Mubarak et al. (Rota et al., 2009) suggested differences in the level of pathogenicity among various wt strains, since they found variations in clinical

parameters, MV replication and antibody responses in macaques infected with two different wt strains (genotype C2 or B3). In our sensitivity study these strains also behaved differently. The C2 strain in our study was one of the most sensitive wt strains to IFN, whereas the B3 strain was the least sensitive one to IFN-alpha treatment.

Since our *in vitro* findings support the latter *in vivo* observations, we compared the immune response in humans infected with those two different wt strains. Likewise, we found variations in the cytokine response from patients infected either with genotype B3 or C2. Thus, our findings underline the hypothesis of differences in pathogenicity among various wt strains, but further *in vivo* investigations are necessary.

Until now little is known about the complex interactions between MV and the host cell. Only around 20 interactions between cellular and virus encoded proteins have been identified. Recent findings like the induction of IFN-beta by the interaction of RIG-I with MV transcripts or the inhibition of the JAK/STAT signalling pathway by the non-structural proteins of MV are just small pieces of the large molecular puzzle underlying the virus interplay with the innate immune response. Details of protein partnerships supporting an optimal virus life cycle, like intracellular trafficking of viral proteins, assembly and budding of the virion, remain largely a black box.

Despite the availability of cost-effective and safe measles vaccines for more than 45 years, measles still kills more children than any other vaccine-preventable disease. In 2008 more than 160,000 measles related deaths were estimated worldwide - nearly 450 deaths every day or 18 deaths every hour. Most of these cases (>95%) occurred in low-income countries with weak health infrastructures and areas of political conflicts. In particular large cities in Africa and Asia with high-density slum areas comprise the fuel for huge measles epidemics. In these areas measles control is extremely hindered due to high population density, complicating vaccination campaigns and poor health care systems, resulting still in large numbers of measles susceptibles. In areas of political conflict the

maintenance of routine high vaccination coverage is difficult and devastating measles outbreaks frequently occur in refugee populations. Especially regions from South-East Asia, including populous countries like Indonesia, Bangladesh and India (the country with the highest number of measles related deaths – in 2008 three out of four children who died from measles lived in India) may jeopardize the goal of global measles elimination. Nowadays also the ease of global travel and cross-border population movements alleviate the re-importation of measles into areas where the disease was already eliminated.

MV genotyping is an important tool of measles surveillance to document chains of transmission, discriminate between imported or indigenous viruses and monitor elimination programs. However, with the enhanced control the genetic variability of circulating strains continues to decrease and identical MV-NP HVR sequences, which are routinely used for MV genotyping, have been found for several years in a same region. Very similar sequence variants were found throughout Europe and beyond. Thus it becomes increasingly difficult to determine the origin of a virus using only this part of the MV genome for the genetic characterization. We showed here for four different outbreaks in Europe and Africa that phylogenetic analysis of the MV-P/H-pseudo-gene sequences in addition to NP-HVR, provides a more refined picture of MV circulation. By extending the sequencing window recommended by the WHO for molecular epidemiology of MV, links between outbreaks and transmission chains became more clearly defined. Identical NP-HVR sequences found in Belarus and Germany in 2006, may have suggested that strains belong to the same outbreak. However, the P/H-pseudo-gene sequences clearly identified the cases in both countries as part of two distinct outbreaks. Among the samples collected throughout Russia 2003 to 2007 the P/H-pseudo-gene provides more insights into the time course and geography of strains indicating rather the circulation and importation of independent variants, than a single major outbreak lasting for several years, like suggested by the identical NP-HVR sequences.

Also in the DR-Congo our findings suggests an independent evolution of variants and multiple independent importations into to country. Although the overall

genetic variability of the WHO reference strains is lower in P and H genes, viruses with identical NP-HVR are very likely to differ in the latter sequences and links between outbreaks and transmission chains became more clearly defined.

Although the results presented here elaborated clearly phenotypic differences among circulating MV wt strains, they only scratch the surface of the complicated interaction of different MV strains with the human antiviral response. Since we found variations in the replication fitness of different strains, future experiments should investigate the binding and fusion ability and the polymerase activity of various strains, as well as the transcription gradient of different viral genes. Using the 2D-DIGE technology, detailed analysis of changes in the host cell proteome following MV infection, provides new cellular interaction partners of MV proteins. Likewise, this approach could identify cellular factors regulating the transcription and replication process of the virus.

Genetic characterization of wt strains is an important tool to study transmission chains and is an essential component of the WHO measles laboratory surveillance. Exploiting the genetic variability of the MV-P and H genes, we revealed transmission chains and provided a more refined picture of MV circulation than using MV-NP HVR sequence information only. However, since the MV-NP HVR only represents 450 nts of the whole 1578 nts (~29%) of the MV-NP gene, whereas the MV-P and H genes were completely sequenced, analyzing the evolution rate of the whole MV-NP gene, would perhaps be an alternative to sequence the latter genes in addition, but this need to be further investigated. This approach will help to improve measles surveillance, to document chains of transmission, discriminate between imported or indigenous viruses and monitor elimination programs in case identical MV-NP HVR sequences provide no insight into circulation patterns of the virus.

---

## References

---

1. Alkhatib, G. & Briedis, D. J. (1986). The predicted primary structure of the measles virus hemagglutinin. *Virology* **150**, 479-90.
2. Andersen, J., VanScoy, S., Cheng, T. F., Gomez, D. & Reich, N. C. (2008). IRF-3-dependent and augmented target genes during viral infection. *Genes Immun* **9**, 168-75.
3. Auwaerter, P. G., Rota, P. A., Elkins, W. R., Adams, R. J., DeLozier, T., Shi, Y., Bellini, W. J., Murphy, B. R. & Griffin, D. E. (1999). Measles virus infection in rhesus macaques: altered immune responses and comparison of the virulence of six different virus strains. *J Infect Dis* **180**, 950-8.
4. Bankamp, B., Horikami, S. M., Thompson, P. D., Huber, M., Billeter, M. & Moyer, S. A. (1996). Domains of the measles virus N protein required for binding to P protein and self-assembly. *Virology* **216**, 272-7.
5. Bankamp, B., Lopareva, E. N., Kremer, J. R., Tian, Y., Clemens, M. S., Patel, R., Fowlkes, A. L., Kessler, J. R., Muller, C. P., Bellini, W. J. & Rota, P. A. (2008). Genetic variability and mRNA editing frequencies of the phosphoprotein genes of wild-type measles viruses. *Virus Res* **135**, 298-306.
6. Barrett, A. D. & Dimmock, N. J. (1986). Defective interfering viruses and infections of animals. *Curr Top Microbiol Immunol* **128**, 55-84.
7. Bellini, W. J., Englund, G., Rozenblatt, S., Arnheiter, H. & Richardson, C. D. (1985). Measles virus P gene codes for two proteins. *J Virol* **53**, 908-19.
8. Berghall, H., Wallen, C., Hyypia, T. & Vainionpaa, R. (2004). Role of cytoskeleton components in measles virus replication. *Arch Virol* **149**, 891-901.
9. Billing, A. M., Fack, F., Turner, J. D. & Muller, C. P. (2010). Cortisol is a potent modulator of lipopolysaccharide-induced interferon signaling in macrophages. *Innate Immun*.
10. Black, F. L. (1989). Measles active and passive immunity in a worldwide perspective. *Prog Med Virol* **36**, 1-33.

11. Black, F. L. & Rosen, L. (1962). Patterns of measles antibodies in residents of Tahiti and their stability in the absence of re-exposure. *J Immunol* **88**, 725-31.
12. Bohn, W., Rutter, G., Hohenberg, H., Mannweiler, K. & Nobis, P. (1986). Involvement of actin filaments in budding of measles virus: studies on cytoskeletons of infected cells. *Virology* **149**, 91-106.
13. Bourhis, J. M., Receveur-Brechot, V., Oglesbee, M., Zhang, X., Buccellato, M., Darbon, H., Canard, B., Finet, S. & Longhi, S. (2005). The intrinsically disordered C-terminal domain of the measles virus nucleoprotein interacts with the C-terminal domain of the phosphoprotein via two distinct sites and remains predominantly unfolded. *Protein Sci* **14**, 1975-92.
14. Caignard, G., Bourai, M., Jacob, Y., Tangy, F. & Vidalain, P. O. (2009). Inhibition of IFN-alpha/beta signaling by two discrete peptides within measles virus V protein that specifically bind STAT1 and STAT2. *Virology* **383**, 112-20.
15. Cantin, A. M., Paquette, B., Richter, M. & Larivee, P. (2000). Albumin-mediated regulation of cellular glutathione and nuclear factor kappa B activation. *Am J Respir Crit Care Med* **162**, 1539-46.
16. Cattaneo, R., Kaelin, K., Baczko, K. & Billeter, M. A. (1989). Measles virus editing provides an additional cysteine-rich protein. *Cell* **56**, 759-64.
17. Cattaneo, R., Rebmann, G., Baczko, K., ter Meulen, V. & Billeter, M. A. (1987). Altered ratios of measles virus transcripts in diseased human brains. *Virology* **160**, 523-6.
18. Chernoff, A. E., Granowitz, E. V., Shapiro, L., Vannier, E., Lonnemann, G., Angel, J. B., Kennedy, J. S., Rabson, A. R., Wolff, S. M. & Dinarello, C. A. (1995). A randomized, controlled trial of IL-10 in humans. Inhibition of inflammatory cytokine production and immune responses. *J Immunol* **154**, 5492-9.
19. Childs, K., Stock, N., Ross, C., Andrejeva, J., Hilton, L., Skinner, M., Randall, R. & Goodbourn, S. (2007). mda-5, but not RIG-I, is a common target for paramyxovirus V proteins. *Virology* **359**, 190-200.
20. Clements, C., Evans, G., Dittman, S. & Reeler, A. (1992). The epidemiology of measles. *Q J Med* **(2-3)**, 285-91.
21. Cudmore, S., Reckmann, I. & Way, M. (1997). Viral manipulations of the actin cytoskeleton. *Trends Microbiol* **5**, 142-8.
22. Curran, J., Boeck, R., Lin-Marq, N., Lupas, A. & Kolakofsky, D. (1995). Paramyxovirus phosphoproteins form homotrimers as determined by an epitope dilution assay, via predicted coiled coils. *Virology* **214**, 139-49.
23. Cutts, F. T., Grabowsky, M. & Markowitz, L. E. (1995). The effect of dose and strain of live attenuated measles vaccines on serological responses in young infants. *Biologicals* **23**, 95-106.
24. de Swart, R. L., Yuksel, S. & Osterhaus, A. D. (2005). Relative contributions of measles virus hemagglutinin- and fusion protein-specific serum antibodies to virus neutralization. *J Virol* **79**, 11547-51.

25. de Witte, L., Abt, M., Schneider-Schaulies, S., van Kooyk, Y. & Geijtenbeek, T. B. (2006). Measles virus targets DC-SIGN to enhance dendritic cell infection. *J Virol* **80**, 3477-86.
26. Devaux, P. & Cattaneo, R. (2004). Measles virus phosphoprotein gene products: conformational flexibility of the P/V protein amino-terminal domain and C protein infectivity factor function. *J Virol* **78**, 11632-40.
27. Doi, Y., Kurita, M., Matsumoto, M., Kondo, T., Noda, T., Tsukita, S., Tsukita, S. & Seya, T. (1998). Moesin is not a receptor for measles virus entry into mouse embryonic stem cells. *J Virol* **72**, 1586-92.
28. Duke, T. & Mgone, C. S. (2003). Measles: not just another viral exanthem. *Lancet* **361**, 763-73.
29. Ebihara, N., Yamagami, S., Chen, L., Tokura, T., Iwatsu, M., Ushio, H. & Murakami, A. (2007). Expression and function of toll-like receptor-3 and -9 in human corneal myofibroblasts. *Invest Ophthalmol Vis Sci* **48**, 3069-76.
30. El Mubarak, H. S., Yuksel, S., van Amerongen, G., Mulder, P. G., Mukhtar, M. M., Osterhaus, A. D. & de Swart, R. L. (2007). Infection of cynomolgus macaques (*Macaca fascicularis*) and rhesus macaques (*Macaca mulatta*) with different wild-type measles viruses. *J Gen Virol* **88**, 2028-34.
31. Emeny, J. M. & Morgan, M. J. (1979). Regulation of the interferon system: evidence that Vero cells have a genetic defect in interferon production. *J Gen Virol* **43**, 247-52.
32. Enami, M., Kohama, T. & Sugiura, A. (1989). A measles virus subgenomic RNA: structure and generation mechanism. *Virology* **171**, 427-33.
33. Enders, J. F. & Peebles, T. C. (1954). Propagation in tissue cultures of cytopathogenic agents from patients with measles. *Proc Soc Exp Biol Med* **86**, 277-86.
34. Fontana, J. M., Bankamp, B., Bellini, W. J. & Rota, P. A. (2008). Regulation of interferon signaling by the C and V proteins from attenuated and wild-type strains of measles virus. *Virology* **374**, 71-81.
35. Fujii, N., Yokosawa, N. & Shirakawa, S. (1999). Suppression of interferon response gene expression in cells persistently infected with mumps virus, and restoration from its suppression by treatment with ribavirin. *Virus Res* **65**, 175-85.
36. Gerlier, D., Loveland, B., Varior-Krishnan, G., Thorley, B., McKenzie, I. F. & Roubourdin-Combe, C. (1994). Measles virus receptor properties are shared by several CD46 isoforms differing in extracellular regions and cytoplasmic tails. *J Gen Virol* **75** (Pt 9), 2163-71.
37. Gerlier, D. & Valentin, H. (2009). Measles virus interaction with host cells and impact on innate immunity. *Curr Top Microbiol Immunol* **329**, 163-91.
38. Graves, M., Griffin, D. E., Johnson, R. T., Hirsch, R. L., de Soriano, I. L., Roedenbeck, S. & Vaisberg, A. (1984). Development of antibody to measles virus polypeptides during complicated and uncomplicated measles virus infections. *J Virol* **49**, 409-12.
39. Griffin, D. E. (1995). Immune responses during measles virus infection. *Curr Top Microbiol Immunol* **191**, 117-34.

40. Griffin, D. E. (2007). Measles Virus. *Fields Virology Fifth Edition*.
41. Hall, T. (1999). BioEdit: a user-friendly biological sequence alignment editor and analysis program for Windows 95/98/NT. *Nucl Acid Symp Ser* **41**:95–98.
42. Haller, O., Staeheli, P. & Kochs, G. (2007). Interferon-induced Mx proteins in antiviral host defense. *Biochimie* **89**, 812-8.
43. Haller, O., Staeheli, P. & Kochs, G. (2009). Protective role of interferon-induced Mx GTPases against influenza viruses. *Rev Sci Tech* **28**, 219-31.
44. Haspolat, S., Anlar, B., Kose, G., Coskun, M. & Yegin, O. (2001). Interleukin-1beta, interleukin-1 receptor antagonist levels in patients with subacute sclerosing panencephalitis and the effects of different treatment protocols. *J Child Neurol* **16**, 417-20.
45. Hastings, R. H., Folkesson, H. G. & Matthay, M. A. (2004). Mechanisms of alveolar protein clearance in the intact lung. *Am J Physiol Lung Cell Mol Physiol* **286**, L679-89.
46. Helin, E., Vainionpaa, R., Hyypia, T., Julkunen, I. & Matikainen, S. (2001). Measles virus activates NF-kappa B and STAT transcription factors and production of IFN-alpha/beta and IL-6 in the human lung epithelial cell line A549. *Virology* **290**, 1-10.
47. Herbein, G. & O'Brien, W. A. (2000). Tumor necrosis factor (TNF)-alpha and TNF receptors in viral pathogenesis. *Proc Soc Exp Biol Med* **223**, 241-57.
48. Hirano, A., Ayata, M., Wang, A. H. & Wong, T. C. (1993). Functional analysis of matrix proteins expressed from cloned genes of measles virus variants that cause subacute sclerosing panencephalitis reveals a common defect in nucleocapsid binding. *J Virol* **67**, 1848-53.
49. Hirsch, R. L., Griffin, D. E., Johnson, R. T., Cooper, S. J., Lindo de Soriano, I., Roedenbeck, S. & Vaisberg, A. (1984). Cellular immune responses during complicated and uncomplicated measles virus infections of man. *Clin Immunol Immunopathol* **31**, 1-12.
50. Horikami, S. M., Smallwood, S., Bankamp, B. & Moyer, S. A. (1994). An amino-proximal domain of the L protein binds to the P protein in the measles virus RNA polymerase complex. *Virology* **205**, 540-5.
51. Hu, A., Kovamees, J. & Norrby, E. (1994). Intracellular processing and antigenic maturation of measles virus hemagglutinin protein. *Arch Virol* **136**, 239-53.
52. Hubschen, J. M., Kremer, J. R., De Landtsheer, S. & Muller, C. P. (2008). A multiplex TaqMan PCR assay for the detection of measles and rubella virus. *J Virol Methods* **149**, 246-50.
53. Ichiyama, T., Siba, P., Suarkia, D., Reeder, J., Takasu, T., Miki, K., Maeba, S. & Furukawa, S. (2006). Analysis of serum and cerebrospinal fluid cytokine levels in subacute sclerosing panencephalitis in Papua New Guinea. *Cytokine* **33**, 17-20.
54. Indoh, T., Yokota, S., Okabayashi, T., Yokosawa, N. & Fujii, N. (2007). Suppression of NF-kappaB and AP-1 activation in monocytic cells persistently infected with measles virus. *Virology* **361**, 294-303.

55. Katz, S. L. (2009). John F. Enders and measles virus vaccine--a reminiscence. *Curr Top Microbiol Immunol* **329**, 3-11.
56. Katz, S. L., Enders, J. F. & Holloway, A. (1960). Studies on an attenuated measles-virus vaccine. II. Clinical, virologic and immunologic effects of vaccine in institutionalized children. *N Engl J Med* **263**, 159-61.
57. Kenis, G., Teunissen, C., De Jongh, R., Bosmans, E., Steinbusch, H. & Maes, M. (2002). Stability of interleukin 6, soluble interleukin 6 receptor, interleukin 10 and CC16 in human serum. *Cytokine* **19**, 228-35.
58. Kremer, J. R., Brown, K. E., Jin, L., Santibanez, S., Shulga, S. V., Aboudy, Y., Demchyshyna, I. V., Djemileva, S., Echevarria, J. E., Featherstone, D. F., Hukic, M., Johansen, K., Litwinska, B., Lopareva, E., Lupulescu, E., Mentis, A., Mihneva, Z., Mosquera, M. M., Muscat, M., Naumova, M. A., Nedeljkovic, J., Nekrasova, L. S., Magurano, F., Fortuna, C., de Andrade, H. R., Richard, J. L., Robo, A., Rota, P. A., Samoilovich, E. O., Sarv, I., Semeiko, G. V., Shugayev, N., Utegenova, E. S., van Binnendijk, R., Vinner, L., Waku-Kouomou, D., Wild, T. F., Brown, D. W., Mankertz, A., Muller, C. P. & Mulders, M. N. (2008). High genetic diversity of measles virus, World Health Organization European Region, 2005-2006. *Emerg Infect Dis* **14**, 107-14.
59. Kremer, J. R., Nguyen, G. H., Shulga, S. V., Nguyen, P. H., Nguyen, U. T., Tikhonova, N. T. & Muller, C. P. (2007). Genotyping of recent measles virus strains from Russia and Vietnam by nucleotide-specific multiplex PCR. *J Med Virol* **79**, 987-94.
60. Kumar, S., Tamura, K. & Nei, M. (2004). MEGA3: Integrated software for Molecular Evolutionary Genetics Analysis and sequence alignment. *Brief Bioinform* **5**, 150-63.
61. Lee, S. O., Cho, K., Cho, S., Kim, I., Oh, C. & Ahn, K. (2010). Protein disulphide isomerase is required for signal peptide peptidase-mediated protein degradation. *Embo J* **29**, 363-75.
62. Liao, S., Bao, X., Liu, T., Lai, S., Li, K., Garofalo, R. P. & Casola, A. (2008). Role of retinoic acid inducible gene-I in human metapneumovirus-induced cellular signalling. *J Gen Virol* **89**, 1978-86.
63. Liston, P. & Briedis, D. J. (1995). Ribosomal frameshifting during translation of measles virus P protein mRNA is capable of directing synthesis of a unique protein. *J Virol* **69**, 6742-50.
64. Longhi, S. (2009). Nucleocapsid structure and function. *Curr Top Microbiol Immunol* **329**, 103-28.
65. Lund, G. A., Tyrrell, D. L., Bradley, R. D. & Scraba, D. G. (1984). The molecular length of measles virus RNA and the structural organization of measles nucleocapsids. *J Gen Virol* **65** (Pt 9), 1535-42.
66. Maggio, M., Guralnik, J. M., Longo, D. L. & Ferrucci, L. (2006). Interleukin-6 in aging and chronic disease: a magnificent pathway. *J Gerontol A Biol Sci Med Sci* **61**, 575-84.
67. Makela, M. J., Salmi, A. A., Norrby, E. & Wild, T. F. (1989). Monoclonal antibodies against measles virus haemagglutinin react with synthetic peptides. *Scand J Immunol* **30**, 225-31.

68. Makhortova, N. R., Askovich, P., Patterson, C. E., Gechman, L. A., Gerard, N. P. & Rall, G. F. (2007). Neurokinin-1 enables measles virus trans-synaptic spread in neurons. *Virology* **362**, 235-44.
69. Malvoisin, E. & Wild, F. (1990). Contribution of measles virus fusion protein in protective immunity: anti-F monoclonal antibodies neutralize virus infectivity and protect mice against challenge. *J Virol* **64**, 5160-2.
70. Manchester, M., Eto, D. S. & Oldstone, M. B. (1999). Characterization of the inflammatory response during acute measles encephalitis in NSE-CD46 transgenic mice. *J Neuroimmunol* **96**, 207-17.
71. Marcus, P. I. & Sekellick, M. J. (1977). Defective interfering particles with covalently linked [+/-]RNA induce interferon. *Nature* **266**, 815-9.
72. Marie, J. C., Kehren, J., Trescol-Biemont, M. C., Evlashev, A., Valentin, H., Walzer, T., Tedone, R., Loveland, B., Nicolas, J. F., Roubourdin-Combe, C. & Horvat, B. (2001). Mechanism of measles virus-induced suppression of inflammatory immune responses. *Immunity* **14**, 69-79.
73. McChesney, M. B., Fujinami, R. S., Lerche, N. W., Marx, P. A. & Oldstone, M. B. (1989). Virus-induced immunosuppression: infection of peripheral blood mononuclear cells and suppression of immunoglobulin synthesis during natural measles virus infection of rhesus monkeys. *J Infect Dis* **159**, 757-60.
74. McNeill, W. (1976). *Plagues and Peoples*. Anchor Press/Doubleday.
75. Moriuchi, H., Moriuchi, M. & Fauci, A. S. (1997). Nuclear factor-kappa B potently up-regulates the promoter activity of RANTES, a chemokine that blocks HIV infection. *J Immunol* **158**, 3483-91.
76. Moss, W. J. (2009). Measles control and the prospect of eradication. *Curr Top Microbiol Immunol* **330**, 173-89.
77. Moss, W. J. & Griffin, D. E. (2006). Global measles elimination. *Nat Rev Microbiol* **4**, 900-8.
78. Moss, W. J., Ryon, J. J., Monze, M. & Griffin, D. E. (2002). Differential regulation of interleukin (IL)-4, IL-5, and IL-10 during measles in Zambian children. *J Infect Dis* **186**, 879-87.
79. Moyer, S. A., Baker, S. C. & Horikami, S. M. (1990). Host cell proteins required for measles virus reproduction. *J Gen Virol* **71** (Pt 4), 775-83.
80. Munday, D., Emmott, E., Surtees, R., Lardeau, C. H., Wu, W., Duprex, W. P., Dove, B. K., Barr, J. N. & Hiscox, J. A. Quantitative proteomic analysis of A549 cells infected with human respiratory syncytial virus. *Mol Cell Proteomics*.
81. Nakatsu, Y., Takeda, M., Ohno, S., Shirogane, Y., Iwasaki, M. & Yanagi, Y. (2008). Measles virus circumvents the host interferon response by different actions of the C and V proteins. *J Virol* **82**, 8296-306.
82. Nandy, R., Handzel, T., Zaneidou, M., Biey, J., Coady, R. Z., Perry, R., Strebel, P. & Cairns, L. (2006). Case-fatality rate during a measles outbreak in eastern Niger in 2003. *Clin Infect Dis* **42**, 322-8.
83. Nanche, D. (2009). Human immunology of measles virus infection. *Curr Top Microbiol Immunol* **330**, 151-71.

84. Naniche, D., Varior-Krishnan, G., Cervoni, F., Wild, T. F., Rossi, B., Roubourdin-Combe, C. & Gerlier, D. (1993). Human membrane cofactor protein (CD46) acts as a cellular receptor for measles virus. *J Virol* **67**, 6025-32.
85. Naniche, D., Yeh, A., Eto, D., Manchester, M., Friedman, R. M. & Oldstone, M. B. (2000). Evasion of host defenses by measles virus: wild-type measles virus infection interferes with induction of Alpha/Beta interferon production. *J Virol* **74**, 7478-84.
86. Navaratnarajah, C. K., Leonard, V. H. & Cattaneo, R. (2009). Measles virus glycoprotein complex assembly, receptor attachment, and cell entry. *Curr Top Microbiol Immunol* **329**, 59-76.
87. Norrby, E., Kovamees, J., Blixenkrone-Moller, M., Sharma, B. & Orvell, C. (1992). Humanized animal viruses with special reference to the primate adaptation of morbillivirus. *Vet Microbiol* **33**, 275-86.
88. Norrby, E., Orvell, C., Vandvik, B. & Cherry, J. D. (1981). Antibodies against measles virus polypeptides in different disease conditions. *Infect Immun* **34**, 718-24.
89. Ohno, S., Ono, N., Takeda, M., Takeuchi, K. & Yanagi, Y. (2004). Dissection of measles virus V protein in relation to its ability to block alpha/beta interferon signal transduction. *J Gen Virol* **85**, 2991-9.
90. Ono, N., Tatsuo, H., Hidaka, Y., Aoki, T., Minagawa, H. & Yanagi, Y. (2001). Measles viruses on throat swabs from measles patients use signaling lymphocytic activation molecule (CDw150) but not CD46 as a cellular receptor. *J Virol* **75**, 4399-401.
91. Opal, S. M., Wherry, J. C. & Grint, P. (1998). Interleukin-10: potential benefits and possible risks in clinical infectious diseases. *Clin Infect Dis* **27**, 1497-507.
92. Orenstein, W. A., Papania, M. J. & Wharton, M. E. (2004). Measles elimination in the United States. *J Infect Dis* **189 Suppl 1**, S1-3.
93. Ozato, K., Tailor, P. & Kubota, T. (2007). The interferon regulatory factor family in host defense: mechanism of action. *J Biol Chem* **282**, 20065-9.
94. Palosaari, H., Parisien, J. P., Rodriguez, J. J., Ulane, C. M. & Horvath, C. M. (2003). STAT protein interference and suppression of cytokine signal transduction by measles virus V protein. *J Virol* **77**, 7635-44.
95. Panum, P. (1938). Observations made during the epidemic of measles on the Faroe Islands in the year 1846. *Medical Classics* **3**, 829-886.
96. Papania, M. J. & Orenstein, W. A. (2004). Defining and assessing measles elimination goals. *J Infect Dis* **189 Suppl 1**, S23-6.
97. Partidos, C. D., Stanley, C. M. & Steward, M. W. (1991). Immune responses in mice following immunization with chimeric synthetic peptides representing B and T cell epitopes of measles virus proteins. *J Gen Virol* **72 (Pt 6)**, 1293-9.
98. Pfaller, C. K. & Conzelmann, K. K. (2008). Measles virus V protein is a decoy substrate for I $\kappa$ B kinase alpha and prevents Toll-like receptor 7/9-mediated interferon induction. *J Virol* **82**, 12365-73.

99. Plemper, R. K. & Snyder, J. P. (2009). Measles control--can measles virus inhibitors make a difference? *Curr Opin Investig Drugs* **10**, 811-20.
100. Plumet, S., Duprex, W. P. & Gerlier, D. (2005). Dynamics of viral RNA synthesis during measles virus infection. *J Virol* **79**, 6900-8.
101. Plumet, S., Herschke, F., Bourhis, J. M., Valentin, H., Longhi, S. & Gerlier, D. (2007). Cytosolic 5'-triphosphate ended viral leader transcript of measles virus as activator of the RIG I-mediated interferon response. *PLoS ONE* **2**, e279.
102. Poeck, H., Bscheider, M., Gross, O., Finger, K., Roth, S., Rebsamen, M., Hanneschlager, N., Schlee, M., Rothenfusser, S., Barchet, W., Kato, H., Akira, S., Inoue, S., Endres, S., Peschel, C., Hartmann, G., Hornung, V. & Ruland, J. (2010). Recognition of RNA virus by RIG-I results in activation of CARD9 and inflammasome signaling for interleukin 1 beta production. *Nat Immunol* **11**, 63-9.
103. Reutter, G. L., Cortese-Grogan, C., Wilson, J. & Moyer, S. A. (2001). Mutations in the measles virus C protein that up regulate viral RNA synthesis. *Virology* **285**, 100-9.
104. Rhazes, A. (1748). Treatise on the Smallpox and Measles. *J Brindley*.
105. Riddell, M. A., Rota, J. S. & Rota, P. A. (2005). Review of the temporal and geographical distribution of measles virus genotypes in the prevaccine and postvaccine eras. *Viol J* **2**, 87.
106. Riley-Vargas, R. C., Gill, D. B., Kemper, C., Liszewski, M. K. & Atkinson, J. P. (2004). CD46: expanding beyond complement regulation. *Trends Immunol* **25**, 496-503.
107. Rima, B. K., Earle, J. A., Baczko, K., ter Meulen, V., Liebert, U. G., Carstens, C., Carabana, J., Caballero, M., Celma, M. L. & Fernandez-Munoz, R. (1997). Sequence divergence of measles virus haemagglutinin during natural evolution and adaptation to cell culture. *J Gen Virol* **78** (Pt 1), 97-106.
108. Rota, P. A. & Bellini, W. J. (2003). Update on the global distribution of genotypes of wild type measles viruses. *J Infect Dis* **187** Suppl 1, S270-6.
109. Rota, P. A., Featherstone, D. A. & Bellini, W. J. (2009). Molecular epidemiology of measles virus. *Curr Top Microbiol Immunol* **330**, 129-50.
110. Roux, L., Simon, A. E. & Holland, J. J. (1991). Effects of defective interfering viruses on virus replication and pathogenesis in vitro and in vivo. *Adv Virus Res* **40**, 181-211.
111. Sadler, A. J. & Williams, B. R. (2008). Interferon-inducible antiviral effectors. *Nat Rev Immunol* **8**, 559-68.
112. Saitou, N. & Nei, M. (1987). The neighbor-joining method: a new method for reconstructing phylogenetic trees. *Mol Biol Evol* **4**, 406-25.
113. Samoilovich, E., Yermalovich, M., Semeiko, G., Svirchevskaya, E., Rimzha, M. & Titov, L. (2006). Outbreak of measles in Belarus, January-June 2006. *Eurosurveillance*, <http://www.eurosurveillance.org/ViewArticle.aspx?ArticleId=3011>.

114. Santibanez, S., Tischer, A., Heider, A., Siedler, A. & Hengel, H. (2002). Rapid replacement of endemic measles virus genotypes. *J Gen Virol* **83**, 2699-708.
115. Santos, C. X., Stolf, B. S., Takemoto, P. V., Amanso, A. M., Lopes, L. R., Souza, E. B., Goto, H. & Laurindo, F. R. (2009). Protein disulfide isomerase (PDI) associates with NADPH oxidase and is required for phagocytosis of *Leishmania chagasi* promastigotes by macrophages. *J Leukoc Biol* **86**, 989-98.
116. Saruhan-Direskeneli, G., Gurses, C., Demirbilek, V., Yentur, S. P., Yilmaz, G., Onal, E., Yapici, Z., Yalcinkaya, C., Cokar, O., Akman-Demir, G. & Gokyigit, A. (2005). Elevated interleukin-12 and CXCL10 in subacute sclerosing panencephalitis. *Cytokine* **32**, 104-10.
117. Sato, H., Kobune, F., Ami, Y., Yoneda, M. & Kai, C. (2008). Immune responses against measles virus in cynomolgus monkeys. *Comp Immunol Microbiol Infect Dis* **31**, 25-35.
118. Sato, H., Miura, R. & Kai, C. (2005). Measles virus infection induces interleukin-8 release in human pulmonary epithelial cells. *Comp Immunol Microbiol Infect Dis* **28**, 311-20.
119. Sayos, J., Wu, C., Morra, M., Wang, N., Zhang, X., Allen, D., van Schaik, S., Notarangelo, L., Geha, R., Roncarolo, M. G., Oettgen, H., De Vries, J. E., Aversa, G. & Terhorst, C. (1998). The X-linked lymphoproliferative-disease gene product SAP regulates signals induced through the co-receptor SLAM. *Nature* **395**, 462-9.
120. Schneider-Schaulies, J., Schneider-Schaulies, S. & Ter Meulen, V. (1993). Differential induction of cytokines by primary and persistent measles virus infections in human glial cells. *Virology* **195**, 219-28.
121. Schneider-Schaulies, S. & ter Meulen, V. (2002). Measles virus and immunomodulation: molecular bases and perspectives. *Expert Rev Mol Med* **4**, 1-18.
122. Schote, A. B., Turner, J. D., Schiltz, J. & Muller, C. P. (2007). Nuclear receptors in human immune cells: expression and correlations. *Mol Immunol* **44**, 1436-45.
123. Shaffer, J. A., Bellini, W. J. & Rota, P. A. (2003). The C protein of measles virus inhibits the type I interferon response. *Virology* **315**, 389-97.
124. Shakhov, A. N., Collart, M. A., Vassalli, P., Nedospasov, S. A. & Jongeneel, C. V. (1990). Kappa B-type enhancers are involved in lipopolysaccharide-mediated transcriptional activation of the tumor necrosis factor alpha gene in primary macrophages. *J Exp Med* **171**, 35-47.
125. Shingai, M., Ebihara, T., Begum, N. A., Kato, A., Honma, T., Matsumoto, K., Saito, H., Ogura, H., Matsumoto, M. & Seya, T. (2007). Differential type I IFN-inducing abilities of wild-type versus vaccine strains of measles virus. *J Immunol* **179**, 6123-33.
126. Shlapatska, L. M., Mikhalap, S. V., Berdova, A. G., Zelensky, O. M., Yun, T. J., Nichols, K. E., Clark, E. A. & Sidorenko, S. P. (2001). CD150 association with either the SH2-containing inositol phosphatase or the

- SH2-containing protein tyrosine phosphatase is regulated by the adaptor protein SH2D1A. *J Immunol* **166**, 5480-7.
127. Shulga, S. V., Rota, P. A., Kremer, J. R., Naumova, M. A., Muller, C. P., Tikhonova, N. T., Lopareva, E. N., Mamaeva, T. A., Tsvirkun, O. V., Mulders, M. N., Lipskaya, G. Y. & Gerasimova, A. G. (2009). Genetic variability of wild-type measles viruses, circulating in the Russian Federation during the implementation of the National Measles Elimination Program, 2003-2007. *Clin Microbiol Infect* **15**, 528-37.
  128. Sidhu, M. S., Crowley, J., Lowenthal, A., Karcher, D., Menonna, J., Cook, S., Udem, S. & Dowling, P. (1994). Defective measles virus in human subacute sclerosing panencephalitis brain. *Virology* **202**, 631-41.
  129. Sieling, P. A., Abrams, J. S., Yamamura, M., Salgame, P., Bloom, B. R., Rea, T. H. & Modlin, R. L. (1993). Immunosuppressive roles for IL-10 and IL-4 in human infection. In vitro modulation of T cell responses in leprosy. *J Immunol* **150**, 5501-10.
  130. Stephenson, J. R. & ter Meulen, V. (1979). Antigenic relationships between measles and canine distemper viruses: comparison of immune response in animals and humans to individual virus-specific polypeptides. *Proc Natl Acad Sci U S A* **76**, 6601-5.
  131. Strebel, P., Cochi, S., Grabowsky, M., Bilous, J., Hersh, B. S., Okwo-Bele, J. M., Hoekstra, E., Wright, P. & Katz, S. (2003). The unfinished measles immunization agenda. *J Infect Dis* **187 Suppl 1**, S1-7.
  132. Takeda, M., Ohno, S., Seki, F., Nakatsu, Y., Tahara, M. & Yanagi, Y. (2005). Long untranslated regions of the measles virus M and F genes control virus replication and cytopathogenicity. *J Virol* **79**, 14346-54.
  133. Takeda, M., Sakaguchi, T., Li, Y., Kobune, F., Kato, A. & Nagai, Y. (1999). The genome nucleotide sequence of a contemporary wild strain of measles virus and its comparison with the classical Edmonston strain genome. *Virology* **256**, 340-50.
  134. Takeuchi, K., Kadota, S. I., Takeda, M., Miyajima, N. & Nagata, K. (2003a). Measles virus V protein blocks interferon (IFN)-alpha/beta but not IFN-gamma signaling by inhibiting STAT1 and STAT2 phosphorylation. *FEBS Lett* **545**, 177-82.
  135. Takeuchi, K., Miyajima, N., Nagata, N., Takeda, M. & Tashiro, M. (2003b). Wild-type measles virus induces large syncytium formation in primary human small airway epithelial cells by a SLAM(CD150)-independent mechanism. *Virus Res* **94**, 11-6.
  136. Tamashiro, V. G., Perez, H. H. & Griffin, D. E. (1987). Prospective study of the magnitude and duration of changes in tuberculin reactivity during uncomplicated and complicated measles. *Pediatr Infect Dis J* **6**, 451-4.
  137. Tamura, K., Dudley, J., Nei, M. & Kumar, S. (2007). MEGA4: Molecular Evolutionary Genetics Analysis (MEGA) software version 4.0. *Mol Biol Evol* **24**, 1596-9.
  138. Tatsuo, H., Ono, N., Tanaka, K. & Yanagi, Y. (2000). SLAM (CDw150) is a cellular receptor for measles virus. *Nature* **406**, 893-7.

139. tenOever, B. R., Servant, M. J., Grandvaux, N., Lin, R. & Hiscott, J. (2002). Recognition of the measles virus nucleocapsid as a mechanism of IRF-3 activation. *J Virol* **76**, 3659-69.
140. Thavasu, P. W., Longhurst, S., Joel, S. P., Slevin, M. L. & Balkwill, F. R. (1992). Measuring cytokine levels in blood. Importance of anticoagulants, processing, and storage conditions. *J Immunol Methods* **153**, 115-24.
141. Thompson, J. D., Higgins, D. G. & Gibson, T. J. (1994). CLUSTAL W: improving the sensitivity of progressive multiple sequence alignment through sequence weighting, position-specific gap penalties and weight matrix choice. *Nucleic Acids Res* **22**, 4673-80.
142. Unlu, M., Morgan, M. E. & Minden, J. S. (1997). Difference gel electrophoresis: a single gel method for detecting changes in protein extracts. *Electrophoresis* **18**, 2071-7.
143. van Diepen, A., Brand, H. K., Sama, I., Lambooy, L. H., van den Heuvel, L. P., van der Well, L., Huynen, M., Osterhaus, A. D., Andeweg, A. C. & Hermans, P. W. (2010). Quantitative proteome profiling of respiratory virus-infected lung epithelial cells. *J Proteomics* **73**, 1680-93.
144. Vincent, S., Gerlier, D. & Manie, S. N. (2000). Measles virus assembly within membrane rafts. *J Virol* **74**, 9911-5.
145. Wakefield, A. J., Murch, S. H., Anthony, A., Linnell, J., Casson, D. M., Malik, M., Berelowitz, M., Dhillon, A. P., Thomson, M. A., Harvey, P., Valentine, A., Davies, S. E. & Walker-Smith, J. A. (1998). Ileal-lymphoid-nodular hyperplasia, non-specific colitis, and pervasive developmental disorder in children. *Lancet* **351**, 637-41.
146. Wang, F., Gao, X., Barrett, J. W., Shao, Q., Bartee, E., Mohamed, M. R., Rahman, M., Werden, S., Irvine, T., Cao, J., Dekaban, G. A. & McFadden, G. (2008). RIG-I mediates the co-induction of tumor necrosis factor and type I interferon elicited by myxoma virus in primary human macrophages. *PLoS Pathog* **4**, e1000099.
147. Wang, N., Satoskar, A., Faubion, W., Howie, D., Okamoto, S., Feske, S., Gullo, C., Clarke, K., Sosa, M. R., Sharpe, A. H. & Terhorst, C. (2004). The cell surface receptor SLAM controls T cell and macrophage functions. *J Exp Med* **199**, 1255-64.
148. Wang, T., Campbell, R. V., Yi, M. K., Lemon, S. M. & Weinman, S. A. (2009). Role of Hepatitis C virus core protein in viral-induced mitochondrial dysfunction. *J Viral Hepat.*
149. Weiss, R. (1992). Measles battle loses potent weapon. *Science* **258**, 546-7.
150. WHO (1999). WHO Guidelines for Epidemic Preparedness and Response to Measles Outbreaks. *WHO/CDS/CSR/ISR/99.1*.
151. WHO (2007). Manual for the laboratory diagnosis of measles and rubella virus infection. *WHO/IVB/07.01*.
152. WHO (2008). Measles, Fact sheet. <http://www.who.int/mediacentre/factsheets/fs286/en/index.html>.
153. WHO (2009a). 450 deaths a day is still too many - stalled momentum puts millions more children at risk.

- [http://www.who.int/mediacentre/news/releases/2009/measles\\_mdg\\_20091203/en/index.html](http://www.who.int/mediacentre/news/releases/2009/measles_mdg_20091203/en/index.html).
154. WHO (2009b). WHO vaccine-preventable diseases: monitoring system - 2009 global summary. *WHO/IVB/2009*.
  155. WHO & UNICEF (2001). Measles mortality reduction and regional elimination strategic plan 2001-2005.
  156. Wichmann, S., Sagebiel, Hellenbrand, Santibanez, Mankertz, Vogt, van Treeck, Krause (2009). Further efforts needed to achieve measles elimination in Germany: results of an outbreak investigation. *Bull World Health Organ* 2009 **87**, 108-115.
  157. Wickremasinghe, M. I., Thomas, L. H., O'Kane, C. M., Uddin, J. & Friedland, J. S. (2004). Transcriptional mechanisms regulating alveolar epithelial cell-specific CCL5 secretion in pulmonary tuberculosis. *J Biol Chem* **279**, 27199-210.
  158. Wild, T. F. & Buckland, R. (1997). Inhibition of measles virus infection and fusion with peptides corresponding to the leucine zipper region of the fusion protein. *J Gen Virol* **78 (Pt 1)**, 107-11.
  159. Wileman, T. (2007). Aggresomes and pericentriolar sites of virus assembly: cellular defense or viral design? *Annu Rev Microbiol* **61**, 149-67.
  160. Wu, W., Booth, J. L., Duggan, E. S., Wu, S., Patel, K. B., Coggeshall, K. M. & Metcalf, J. P. (2010). Innate immune response to H3N2 and H1N1 influenza virus infection in a human lung organ culture model. *Virology* **396**, 178-88.
  161. Xiao, B. G., Mousa, A., Kivisakk, P., Seiger, A., Bakhiet, M. & Link, H. (1998). Induction of beta-family chemokines mRNA in human embryonic astrocytes by inflammatory cytokines and measles virus protein. *J Neurocytol* **27**, 575-80.
  162. Xu, W., Tamin, A., Rota, J. S., Zhang, L., Bellini, W. J. & Rota, P. A. (1998). New genetic group of measles virus isolated in the People's Republic of China. *Virus Res* **54**, 147-56.
  163. Yanagi, Y., Ono, N., Tatsuo, H., Hashimoto, K. & Minagawa, H. (2002). Measles virus receptor SLAM (CD150). *Virology* **299**, 155-61.
  164. Yasumura, Y. & Kawakita, M. (1963). The research for the SV40 by means of tissue culture technique. *Nippon Rinsho* **21**, 1201-1219.
  165. Yokota, S., Saito, H., Kubota, T., Yokosawa, N., Amano, K. & Fujii, N. (2003). Measles virus suppresses interferon-alpha signaling pathway: suppression of Jak1 phosphorylation and association of viral accessory proteins, C and V, with interferon-alpha receptor complex. *Virology* **306**, 135-46.
  166. Zhang, Y., Ding, Z., Wang, H., Li, L., Pang, Y., Brown, K. E., Xu, S., Zhu, Z., Rota, P. A., Featherstone, D. & Xu, W. (2010). New measles virus genotype associated with outbreak, China. *Emerg Infect Dis* **16**, 943-7.
  167. Zhu, M., John, S., Berg, M. & Leonard, W. J. (1999). Functional association of Nmi with Stat5 and Stat1 in IL-2- and IFNgamma-mediated signaling. *Cell* **96**, 121-30.

168. Zoellner, H., Hofler, M., Beckmann, R., Hufnagl, P., Vanyek, E., Bielek, E., Wojta, J., Fabry, A., Lockie, S. & Binder, B. R. (1996). Serum albumin is a specific inhibitor of apoptosis in human endothelial cells. *J Cell Sci* **109** (Pt **10**), 2571-80.

---

## Annexes

---

### 1. Conference Participations

2010 Initiator and coordinator of the 2010 founded “BioLux.Network” in Bio-Healthcare in Luxembourg

J. R. Kessler: Representative of the Institute of Immunology at the CRP-Santé introduction day (Oral presentation)

2009 J. R. Kessler: Defective interfering RNA in measles wild type strains and the interaction with the early immune response; ESCV winter meeting; Amsterdam, Netherlands, 2009 (Oral presentation)

Participation at the meeting of the Regional Reference Laboratories of the WHO European Regional Measles and Rubella Laboratory Network, in Luxembourg, 2009

J. R. Kessler: Defective interfering RNA in measles wild type strains and the interaction with the early immune response; Scientific symposium: “50<sup>th</sup> doctoral student at the Institute of

- Immunology; Luxembourg, Luxembourg, 2009 (Oral presentation)
- J. R. Kessler: Interplay of Measles Virus with the innate immunity; Gordon Research Conference Viruses & Cells; Barga, Italy, 2009 (Poster presentation)
- 2008 J. R. Kessler: Aspects of viral escape mechanism from the innate immunity; Leipzig; Germany, 2009 (Invited lecture)
- J. R. Kessler: Measles Virus and Type I Interferon; Saar-Lor-Lux workshop on Virus research held in Remich, Luxembourg, 2008 (Oral presentation)
- J. R. Kessler: Interplay of Measles Virus with the innate immunity; Immunobiology of viral infections/ Society of virology; Deidesheim, Germany, 2008 (Oral presentation)
- J. R. Kessler: Interplay of Measles Virus with the innate immunity; Annual meeting of the "Arbeitskreis klinische Virologie"; Zeilitzheim, Germany, 2008 (Oral presentation)
- 2007 J. R. Kessler: MV proliferation on IFN- $\alpha$  stimulated Vero/hSLAM cells; Saar-Lor-Lux workshop on Virus research in Homburg/Saar, Germany, 2007 (Oral presentation)
- 2006 Participation at the International Conference on Proteomics: "Bridging the Gap Between Gene expression and Biological Function" in Luxembourg, 2006

Participation at the Saar-Lor-Lux workshop on Virus research in Nancy, France, 2006

## 2. Publications

- 2010 J. R. Kessler, J. R. Kremer, C. P. Muller. *Interplay of measles virus with early induced cytokines reveals different wild type phenotypes*. Submitted June, 2010.
- 2009 F. Fack, J. R. Kessler, P. Pirrotte, J. R. Kremer, D. Revets, W. Ammerlaan, C. P. Muller. *Detection of differentially modified pathogen proteins by Western Blot after 2D- gel electrophoreses and identification by Maldi-Tof-Tof*. Proteomics and Genomics of BSL 3 pathogens. COST B28. Wiley 2009
- 2008 Bankamp B, Lopareva EN, Kremer JR, Tian Y, Clemens MS, Patel R, Fowlkes AL, Kessler JR, Muller CP, Bellini WJ, Rota PA. *Genetic variability and mRNA editing frequencies of the phosphoprotein genes of wild-type measles viruses*. Virus Res. 2008 Aug;135(2):298-306

---

## Acknowledgements

---

I would like to thank Prof. Claude P. Muller for offering me the opportunity to do this work as a member of his team in the Institute of Immunology of the Centre de la Recherche Public de la Santé in Luxembourg and for his persistent scientific guidance and continuous confidence during the last years.

Especially I would like to gratefully acknowledge the enthusiastic supervision of Dr. Jacques Kremer. His invaluable expertise, inspiration, guidance and critical manuscript reading were greatly appreciated.

I also want to thank all the past and present colleagues of the Institute, especially my former officemates Nancy Gerloff and Dr. Monique Jacoby for great discussions, their invaluable friendship and support during all these years.

Also, Simone, Aurélie, Judith, Mario, Emilie, Tom, Carole, Ulla, Claire, Fred, Fabienne, Laetitia, Wim, Patrick, Sophie, Stéphanie, Jon, Nathalie, Anna, Iris, Chantal, Dominique, Lei, Vitor, Anja, Sara, Sebastien, Linda, Konstantin, Slavena, Victor and Oliver deserve my sincerest gratitude. Thank you for being a cheerful team and for your assistance in both scientific and non-scientific purposes.

Thanks also to all my friends, who made life during and after work so enjoyable.

For their financial support, I would like to thank the Fonds National de la Recherche, the Aides à la Formation Recherche, the Centre de Recherche Public de la Santé and the Ministère de la Culture, de l'Enseignement Supérieur et de la Recherche



Finally, I am forever indebted to my parents and my sister for having been with me all my life, for their understanding, endless patience and encouragement when it was most required.

*Julia*